CENTRIFUGAL TESTING OF MODEL PILES AND PILE GROUPS

VOL. III CENTRIFUGE TESTS IN CLAY

U.S. Department of Transportation
Federal Highway Administration

Research, Development, and Technology

Turner-Fairbank Highway Research Center
6300 Georgetown Pike
McLean, Virginia 22101

Report No.
FHWA/RD-84/004

Final Report
November 1984

FOREWORD

This report presents a detailed description of a research study on the use of geotechnical centrifuge to test model piles and pile groups in clay. Information presented will be of use to other investigators using the centrifuge as a research or engineering design tool. Results presented will be of interest to engineers designing pile foundations in clay.

The project was conducted for the Federal Highway Administration, Office of Engineering and Highway Operations Research and Development, Washington, D.C., under contract DTFH61-81-R-00034, "Centrifuge Testing of Model Piles and Pile Groups."

Richard E. Hay, Director
Office of Engineering
and Highway Operations
Research and Development

NOTICE

Technical Report Documentation Page

1. Report No.	2. Government Accession No.	3. Recipient's Catalog No.
FHWA/RD-84/004	PB85 247724/AS	

4. Title and Subtitle	5. Report Date
CENTRIFUGAL TESTING OF MODEL PILES AND PILE GROUPS VOL. III, CENTRIFUGAL TESTS IN CLAY	November 1984
	6. Performing Organization Code
	8. Performing Organization Report No.
7. Author(s) Ko, H-Y.; Atkinson, R.H.; Goble, G.G.	
9. Performing Organization Name and Address Atkinson-Noland & Associates, Inc. 2619 Spruce Street Boulder, Colorado 80302	10. Work Unit No. (TRAIS) FCP 35P1-132
	11. Contract or Grant No. DTFH 61-81-R-00034
12. Sponsoring Agency Name and Address Offices of Research & Development Federal Highway Administration U.S. Department of Transportation Washington, D.C. 20590	13. Type of Report and Period Covered Final Report June 1981 - June 1984
	14. Sponsoring Agency Code CME/0123

15. Supplementary Notes

FHWA Contract Manager: Carl D. Ealy, (HNR-30)

16. Abstract

This volume is a detailed report of a research program conducted to evaluate the feasibility of centrifute tests on model piles and pile groups in clay using the geotechnical centrifuge. The report describes the preparation of the clay samples, details of the model piles, methods of pile placement, centrifuge details and operation, and test procedures. Results are presented and analyzed. Conclusions are presented on the verification of the similitude relations, sensitivity of capacity to shear strength, load transfer relations, and pile group efficiencies.

Other reports developed in this study are FHWA/RD-84/002, Vol. I, Executive Summary, and FHWA/RD-84/003, Vol. II, Centrifuge Tests in Sand.

Dr. R.H. Atkinson, Atkinson-Noland & Associates served as project director. Prof. H-Y. Ko and G.G. Goble served as principal investigators. Mr. F. Harrison conducted the test program in clay. All experimental work was conducted using the geotechnical centrifuge of the Department of Civil, Environmental, and Architectural Engineering, University of Colorado, Boulder, Colorado.

17. Key Words	18. Distribution Statement
Piles, Pile Groups, Clay, Model Tests, Centrifuge	No restrictions. This document is available to the public through the National Technical Information Service, Springfield, VA 22161.

19. Security Classif. (of this report)	20. Security Classif. (of this page)	21. No. of Pages	22. Price
Unclassified	Unclassified	131	

METRIC CONVERSION FACTORS

APPROXIMATE CONVERSIONS FROM METRIC MEASURES

SYMBOL	WHEN YOU KNOW	MULTIPLY BY	TO FIND	SYMBOL
LENGTH				
in	inches	2.5	centimeters	cm
ft	feet	30	centimeters	cm
yd	yards	0.9	meters	m
mi	miles	1.6	kilometers	km
AREA				
in^2	square inches	6.5	square centimeters	cm^2
ft^2	square feet	0.09	square meters	m^2
yd^2	square yards	0.6	square meters	m^2
mi^2	square miles	2.6	square kilometers	km^2
	acres	0.4	hectares	ha
MASS (weight)				
oz	ounces	28	grams	g
lb	pounds	0.45	kilograms	kg
	short tons(2000lb)	0.9	tonnes	t
VOLUME				
tsp	teaspoons	5	milliliters	ml
tbsp	tablespoons	15	milliliters	ml
fl oz	fluid ounces	30	milliliters	ml
c	cups	0.24	liters	l
pt	pints	0.47	liters	l
qt	quarts	0.95	liters	l
gal	gallons	3.8	liters	l
ft^3	cubic feet	0.03	cubic meters	m^3
yd^3	cubic yards	0.76	cubic meters	m^3
TEMPERATURE (exact)				
°F	Fahrenheit temperature	5/9 (after subtracting 32)	Celsius temperature	°C

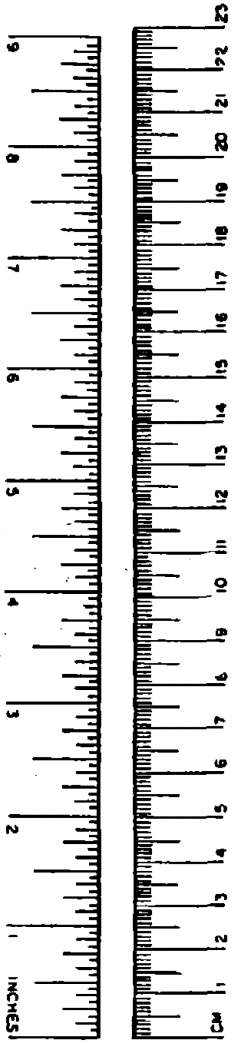

APPROXIMATE CONVERSIONS FROM METRIC MEASURES

SYMBOL	WHEN YOU KNOW	MULTIPLY BY	TO FIND	SYMBOL
LENGTH				
mm	millimeters	0.04	inches	in
cm	centimeters	0.4	inches	in
m	meters	3.3	feet	ft
m	meters	1.1	yards	yd
km	kilometers	0.6	miles	mi
AREA				
cm^2	square centimeters	0.16	square inches	in^2
m^2	square meters	1.2	square yards	yd^2
km^2	square kilometers	0.4	square miles	mi^2
ha	hectares(10,000m^2)	2.5	acres	
MASS (weight)				
g	grams	0.035	ounces	oz
kg	kilograms	2.2	pounds	lb
t	tonnes (1000kg)	1.1	short tons	
VOLUME				
ml	milliliters	8.03	fluid ounces	fl oz
l	liters	2.1	pints	pt
l	liters	1.06	quarts	qt
l	liters	0.26	gallons	gal
m^3	cubic meters	36	cubic feet	ft^3
m^3	cubic meters	1.3	cubic yards	yd^3
TEMPERATURE (exact)				
°C	Celsius temperature	9/5 (then add 32)	Fahrenheit temperature	°F

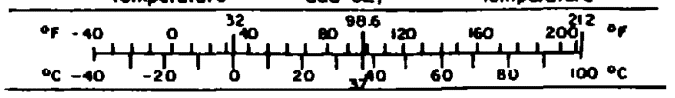

TABLE OF CONTENTS

		Page
LIST OF TABLES		v
LIST OF FIGURES		vi
CHAPTER 1.	INTRODUCTION	1
CHAPTER 2.	HISTORY AND CONCEPTS OF GEOTECHNICAL MODELING	3
	2.1 Theories of Similitude	3
	2.2 Pile Modeling at 1 g	6
	2.3 The Centrifuge in Geotechnical Modeling	6
CHAPTER 3.	DISCUSSION OF PROTOTYPE	8
	3.1 Introduction	8
	3.2 Test Site	8
	3.3 Piles and Instrumentation	8
	3.4 Test Program	12
CHAPTER 4.	TEST EQUIPMENT	15
	4.1 Centrifuge	15
	4.1.1 General Description	15
	4.1.2 Drive and Control System	15
	4.1.3 Arms	15
	4.1.4 Slip Rings	20
	4.1.5 Limitations	20
	4.1.6 Container	20
	4.1.7 Vane Shear Apparatus	22
	4.1.8 Model Piles	22
	4.1.9 Driving and Loading Apparatus	26
	4.2 Instrumentation	29
	4.2.1 Load Cells	29
	4.2.2 Displacement Measurement	29
	4.2.3 Pore Pressure Transducers	29
	4.2.4 Instrumentation of Model Piles	32
	4.3 Data Acquisition	32
	4.3.1 Analog	32
	4.3.2 Digital	32
CHAPTER 5.	SPECIMEN PREPARATION AND TEST PROCEDURE	37
	5.1 Discussion of Preparation Technique	37
	5.2 Discussion of Test Sequence	40

TABLE OF CONTENTS (continued)

		Page
CHAPTER 6.	TEST PROGRAM AND RESULTS	44
	6.1 Discussion of Test Program	44
	6.1.1 Goals of Program	44
	6.1.2 Format of Program	44
	6.2 Discussion of Results	46
	6.2.1 Determination of Undrained Shear Strength	46
	6.2.2 S_u vs. Single Pile Capacity	46
	6.2.3 Group Capacities and Group Factors	48
	6.2.4 Load Transfer Data	48
	6.2.5 Load-Displacement Characteristics	52
	6.2.6 Lateral Load Behavior	52
	6.2.7 Modeling of Models	58
CHAPTER 7.	ANALYSIS	59
	7.1 The Use of Model Tests in Developing Analytical Techniques	59
	7.2 Axial Behavior	59
	7.2.1 Determination of F-Z and Q-Z Curves	60
	7.2.2 Results	61
CHAPTER 8.	CONCLUSION	67
	8.1 Summary of Work Performed	67
	8.2 Problems Encountered	67
	8.3 Recommendations for Future Research	68
REFERENCES		69
APPENDIX 1		72
APPENDIX 2		90
APPENDIX 3		106

LIST OF TABLES

Table		Page
1.	Scaling Factors for Various Quantities	5
2.	Centrifuge Specifications	16
3.	Dimensions of Model Piles	26
4.	Geotechnical Properties of Georgia Kaolin	38
5.	Summary of Testing Program	45
6.	Group Test Data	50
7.	Ultimate Loads for Single Pile Tests	107

LIST OF FIGURES

Figure		Page
1.	Measurements of undrained shear strength, prototype (O'Neill et al., 1980) (1 ksf - 47.9 kPa; 1 ft = 0.305 m)	9
2.	Interpreted S_u profile (1 ksf = 47.9 kPa; 1 ft = 0.305 m)	10
3.	Plan view of test site (O'Neill et al., 1980) (1 ft = 0.305 m)	11
4.	Pile instrumentation (O'Neill et al., 1980) (1 ft = 0.305 m)	13
5.	Site instrumentation (O'Neill et al., 1980) (1 ft = 0.305 m)	14
6.	Centrifuge drive system	17
7.	Centrifuge control panel	18
8.	Centrifuge arms	19
9.	Exploded view of soil container (1 in = 2.54 cm)	21
10.	Vane shear apparatus, including motor	23
11.	Close up of vane, showing instrumentation	24
12.	Driving and loading apparatus	28
13.	Axial load test configuration	30
14.	Lateral load test configuration	31
15.	1/50th scale pile halves showing strain gauge station positions	33
16.	Wheatstone bridge configuration for measurement of axial load	34
17.	Wheatstone bridge configuration for measurement of bending moment	35
18.	Desired undrained shear profile (1 ksf = 47.9 kPa; 1 ft = 0.305 m)	41
19.	S_u profiles for initial tests (1 ksf = 47.9 kPa; 1 ft = 0.305 m)	47
20.	S_u vs. single pile capacity (1 ksf = 47.9 kPa; 1 kip = 4.45 KN)	49
21.	Typical load transfer curve (1 kip = 4.45 KN; 1 ft = 0.305 m)	51
22.	Load-transfer curves from model and prototype (1 kip = 4.45 KN; 1 ft = 0.305 m)	53
23.	Load-deflection curves, single piles (1 kip = 4.45 KN; 1 in = 2.54 cm)	54
24.	Load-deflection curves, group (1 kip = 4.45 KN; 1 in = 2.54 cm)	55
25.	Lateral load-displacement curves, (1 kip = 4.45 KN; 1 in = 2.54 cm)	56
26.	Moment vs. depth curve, from model test (1 ft-kip = 1.36 m-KN; 1 ft = 0.305 m)	57
27.	Unit skin friction vs. deflection, pile head (1 psi = 6.9 kPa; 1 in = 2.54 cm)	62

LIST OF FIGURES (continued)

Figure		Page
28.	Unit skin friction vs. deflection, pile tip (1 psi = 6.9 kPa; 1 in = 2.54 cm)	63
29.	Tip load vs. deflection (1 kip = 4.45 KN; 1 in. = 2.54 cm)	64
30.	Single pile load-displacement as predicted by PILGP1 (1 kip = 4.45 KN; 1 in = 2.54 cm)	65
31.	Pile group load-displacement as predicted by PILGP1 (1 kip = 4.45 KN; 1 in = 2.54 cm)	66
32.	Test 1, S_u profile (1 ksf = 47.9 kPa; 1 ft = 0.305 m)	73
33.	Test 2, S_u profile (1 ksf = 47.9 kPa; 1 ft = 0.305 m)	74
34.	Test 3, S_u profile (1 ksf = 47.9 kPa; 1 ft = 0.305 m)	75
35.	Test 4, S_u profile (1 ksf = 47.9 kPa; 1 ft = 0.305 m)	76
36.	Test 5, S_u profile (1 ksf = 47.9 kPa; 1 ft = 0.305 m)	77
37.	Test 6, S_u profile (1 ksf = 47.9 kPa; 1 ft = 0.305 m)	78
38.	Test 7, S_u profile (1 ksf = 47.9 kPa; 1 ft = 0.305 m)	79
39.	Test 8, S_u profile (1 ksf = 47.9 kPa; 1 ft = 0.305 m)	80
40.	Test 12, S_u profile (1 ksf = 47.9 kPa, 1 ft = 0.305 m)	81
41.	Test 13, S_u profile (1 ksf = 47.9 kPa; 1 ft = 0.305 m)	82
42.	Test 15, S_u profile (1 ksf = 47.9 kPa; 1 ft = 0.305 m)	83
43.	Test 16, S_u profile (1 ksf = 47.9 kPa; 1 ft = 0.305 m)	84
44.	Test 17, S_u profile (1 ksf = 47.9 kPa; 1 ft = 0.305 m)	85
45.	Test 18, S_u profile (1 ksf = 47.9 kPa; 1 ft = 0.305 m)	86
46.	Test 20, S_u profile (1 ksf = 47.9 kPa; 1 ft = 0.305 m)	87
47.	Test 21, S_u profile (1 ksf = 47.9 kPa; 1 ft = 0.305 m)	88
48.	Test 22, S_u profile (1 ksf = 47.9 kPa; 1 ft = 0.305 m)	89
49.	Test 3, load transfer curve (1 kip = 4.45 KN; 1 ft = 0.305 m)	91
50.	Test 4a, load transfer curve (1 kip = 4.45 KN; 1 ft = 0.305 m)	92
51.	Test 4b, load transfer curve (1 kip = 4.45 KN; 1 ft = 0.305 m)	93
52.	Test 5, load transfer curve (1 kip = 4.45 KN; 1 ft = 0.305 m)	94
53.	Test 6, load transfer curve (1 kip = 4.45 KN; 1 ft = 0.305 m)	95
54.	Test 13, load transfer curve (1 kip = 4.45 KN; 1 ft = 0.305 m)	96
55.	Test 15, load transfer curve (1 kip = 4.45 KN; 1 ft = 0.305 m)	97
56.	Test 16, load transfer curve (1 kip = 4.45 KN; 1 ft = 0.305 m)	98

LIST OF FIGURES (continued)

Figure		Page
57.	Test 17, load transfer curve (1 kip = 4.45 KN; 1 ft = 0.305 m)	99
58.	Test 20, load transfer curve (1 kip = 4.45 KN; 1 ft = 0.305 m)	100
59.	Test 22, load transfer curve (1 kip = 4.45 KN; 1 ft = 0.305 m)	101
60.	Prototype, load transfer curve (1 kip = 4.45 KN; 1 ft = 0.305 m)	102
61.	Test 17, group load transfer curves (1 kip = 4.45 KN; 1 ft = 0.305 m)	103
62.	Test 22, group load transfer curves (1 kip = 4.45 KN; 1 ft = 0.305 m)	104
63.	Prototype, group load transfer curves (1 kip = 4.45 KN; 1 ft = 0.305 m)	105
64.	Test 3, load-displacement curve (1 kip = 4.45 KN; 1 in = 2.54 cm)	108
65.	Test 4, load=displacement curve (1 kip = 4.45 KN; 1 in = 2.54 cm)	109
66.	Test 5, load-displacement curve (1 kip = 4.45 KN; 1 in = 2.54 cm)	110
67.	Test 6, load-displacement curve (1 kip = 4.45 KN; 1 in = 2.54 cm)	111
68.	Test 15, load-displacement curve (1 kip = 4.45 KN; 1 in = 2.54 cm)	112
69.	Test 16, load-displacement curve (1 kip = 4.45 KN; 1 in = 2.54 cm)	113
70.	Test 18, load-displacement curve (1 kip = 4.45 KN; 1 in = 2.54 cm)	114
71.	Test 20, load-displacement curve (1 kip = 4.45 KN; 1 in = 2.54 cm)	115
72.	Test 21, load-displacement curve (1 kip = 4.45 KN; 1 in = 2.54 cm)	116
73.	Test 22, load-displacement curve (1 kip = 4.45 KN; 1 in = 2.54 cm)	117
74.	Prototype, load displacement curve (1 kip = 4.45 KN; 1 in = 2.54 cm)	118
75.	Test 18, group load-displacement curve (1 kip = 4.45 KN; 1 in = 2.54 cm)	119
76.	Test 21, group load-displacement curve (1 kip = 4.45 KN; 1 in = 2.54 cm)	

LIST OF FIGURES (continued)

Figure		Page
77.	Test 22, group load-displacement curve (1 kip = 4.45 KN; 1 in = 2.54 cm)	121
78.	Prototype, group load-displacement curve (1 kip = 4.45 KN; 1 in = 2.54 cm)	122

CHAPTER 1. INTRODUCTION

Pile foundations have long been used to support structures, particularly in areas with poor soil conditions. Despite this long history of usage, the behavior of pile foundations remains a subject of great uncertainty. Analytical techniques of predicting pile behavior have advanced significantly in recent decades, but uncertainty still exists to the extent that full scale load tests are often still required on today's construction sites to verify the adequacy of the installed foundation.

This uncertainty results from several factors. The most apparent, and one common to most geotechnical problems, is the great variability inherent in soil deposits. It is often difficult for the engineer to know what he is dealing with. Sampling techniques also contribute to uncertainty, causing errors in the determination of properties used to predict behavior. It can also be safely stated that the actual mechanics of pile behavior are not well understood, a fact substantiated by the vastly different computational techniques that have been used. Finally, there is a significant lack of data on the performance of pile foundations. It is with this that this report is concerned.

This lack of data can be attributed to the high cost of performing full scale tests and to the lack of availability of suitable test locations. Even when a suitable location can be found, only a certain number of tests can be performed, often under very limited conditions.

These shortcomings associated with full scale testing suggest the possibility of using small scale models. Some scale model tests have been performed under normal gravity (one g) conditions, but the application of these types of tests are somewhat limited because the stress field in a model tested under earth's gravity is not similar to that in a full scale prototype. The alternative is to conduct scale model tests under an artificial gravity induced by a geotechnical centrifuge. The centrifugal acceleration produced by the rotating centrifuge can produce the artificial gravity field necessary to reproduce the gravity-induced stress conditions of

a full-scale pile load test. Thus, through the use of the centrifuge, numerous pile load tests can be performed under a variety of conditions at a fraction of the cost of full scale tests.

The research described by this report consisted of a series of single pile and pile group axial and lateral load tests carried out in the centrifuge at the University of Colorado. These tests were scale models of a full scale load test performed on single piles and pile groups on the campus of the University of Houston (O'Neill et al., 1980). The intent is to demonstrate the value of centrifugal modeling of pile foundations, by proving that the obtained field results can be duplicated in the laboratory.

This report will first give an outline of the pertinent similitude relationships and a brief history of the use of the centrifuge in geotechnical engineering. Then a description will be given of the full scale pile load tests that this research undertook to model.

A wide variety of equipment and instrumentation was employed during the course of this project. This is described in detail in Chapter 3.

Following this description of equipment, the method of specimen preparation is explained and a discussion is provided of the procedure carried out in testing a specimen. The testing program is then outlined and the results of this program are given. Among the data obtained are load-displacement curves, load transfer functions, and ultimate pile capacity vs. undrained shear strength.

In the analysis, the data obtained are examined in order to verify the concepts of similitude. This is done by comparison with the prototype data, as well as within the test program, through a concept called modeling of models (this concept is explained in Chapter 2). Comparison is also made with several available analytical techniques.

CHAPTER 2. HISTORY AND CONCEPTS OF GEOTECHNICAL MODELING

2.1 Theories of Similitude

In geotechnical engineering, physical modeling involves development of a model system that accurately depicts the behavior of a full scale system, hereafter referred to as the prototype. In order to do this, the requirements of similitude must be satisfied. Two systems are said to be physically similar when a unique relationship between all points of the two systems can be determined and when the physical quantities have a constant relationship at corresponding points (Fumagalli, 1973).

The basic similitude relationship is given by equation 2.1, which is derived from the Buckingham Pi theory (Rocha, 1957; Fumagalli, 1973; Kim, 1980). Here y is a property of the prototype, y' is the corresponding model property, and Ω is a scaling factor determined from the funadmental properties of the two systems.

$$y = y'\Omega \tag{2.1}$$

For the work described by this report, the scaling relationships for three independent quantities, from which all other quantities are derived, are required. They are length, stress, and time; and their scaling factors are depicted in equations 2.2, 2.3, and 2.4. It should be noted that these scaling factors must be accurate for derived quantities.

$$L = L'\lambda \tag{2.2}$$

$$\sigma = \sigma'\varepsilon \tag{2.3}$$

$$t = t'\tau \tag{2.4}$$

For example, the specific case of strains, as demonstrated by equation 2.5.

$$\frac{\varepsilon}{\varepsilon'} = \frac{\Delta L/L}{\Delta L'/L'} = \frac{L'\Delta L}{\Delta L'L} = \frac{L'\Delta L\lambda}{\lambda\ \Delta L'L'} = 1 \tag{2.5}$$

This requirement can be met easily if the prototype material is used in the model. Two assumptions are involved here, however. The first is that the grain size of the prototype materials is small enough to be considered a continuum even at the model scale. This assumption is reasonable for clays, silts, and some sands if the geometric scaling factor, λ, is not overly large. For very large values of λ, say in the neighborhood of 200, problems may be encountered in using many sands as model materials. This is not a problem in the case of the work described by this report, as the material in question is clay.

The other assumption that must be considered is that body forces are insignificant enough to be negligible. This is clearly not reasonable in most geotechnical problems. If we are required to achieve similarity of body forces, then equation 2.6 must be satisfied,

$$\frac{\gamma'}{\gamma} = \lambda \tag{2.6}$$

where γ' and γ are the specific weights of the model and prototype, respectively. If the same material is to be used, this can only be accomplished by inducing a higher gravity in the model than that of the prototype. This can only be practically achieved with the use of a centrifuge.

Since the prototype exists under earth's normal gravitational acceleration g (32 ft/sec^2 or 9.81 m/sec^2), the gravitational acceleration to which the model must be subjected to satisfy equation 2.6 is given by equation 2.7.

$$a = \lambda g \tag{2.7}$$

The centrifugal (radial) acceleration generated by a centrifuge of radius r spinning at a constant angular velocity w is given in equation 2.8, which is a well-known law of physics.

$$a = w^2 r \tag{2.8}$$

Hence, the angular velocity required for a model with a geometric scaling factor λ and centrifuge of radius r is given in equation 2.9, which is

obtained by substituting equation 2.7 into 2.8 and solving for w.

$$w = \sqrt{\frac{\lambda \cdot g}{r}} \qquad (2.9)$$

The scaling relationship for time (τ) is more difficult to determine. Roscoe (1968) and Croce (1982) have used separate methods and found that $\tau = \lambda^2$ for pore pressure dissipation problems, given the criteria already established. The scaling relationships for the three independent quantities as well as derived quantities significant to this report are summarized in Table 1.

Table 1. Scaling Factors for Various Quantities.

Length	λ
Stress	1
Time	λ^2
Strain	1
Force	λ^2
Area	λ^2
Volume	λ^3
Specific Weight	$1/\lambda$
Gravitational Acceleration	$1/\lambda$
Mass Density	1
Mass	λ^3

A limitation of the centrifugal method that should be pointed out is that the gravity of the model is not constant with depth, but linearly increasing with radius as is apparent from equation 2.8. Hence the lower portions of the model are subjected to a higher level of gravity than are the upper portions. This effect can be minimized by performing high gravity tests on a centrifuge with a larger radius. In this manner the same average centrifugal acceleration can be achieved, with less variation over the depth of the model.

Despite this limitation, centrifugal modeling is the only practical method of modeling most geotechnical problems that adhere to the principles of similitude.

2.2 Pile Modeling at 1 g

Various investigators have studied pile group behavior through one g models (Whitaker, 1957; Saffery and Tate, 1961; and Sowers et al., 1961). These were largely qualitative tests designed to determine the influence of spacing on group effect. Results from these investigations generally do not compare well with measured field data, indicating group factors lower than should be expected (Vesic, 1977).

The chief objection to such studies is that scaling relationships between these tests and a prototype may not exist (Rocha, 1957) as is discussed in the previous section. Hence, the data produced by one g tests may be of value in a qualitative sense, but it has little or no quantitative value since the model cannot positively be related to a prototype.

2.3 The Centrifuge in Geotechnical Modeling

The first recorded uses of the centrifuge to model geotechnical systems were in the 1930's. It was used in the U.S. to study mining structures (Bucky, 1931, 1935, 1938) and in the Soviet Union to study foundation deformations (Pokrovsky and Fedorov, 1936). The technique was not widely accepted in the U.S. or Western Europe at that time. The work by Pokrovsky and Fedorov, however, fostered widespread use of the geotechnical centrifuge in the Soviet Union, where it has remained in use up to the present time.

In the late 1960's, the centrifuge saw a resurgence in popularity with western researchers. Cambridge University completed its first centrifuge at this time and began extensive research into soil mechanics problems (Roscoe, 1968). Geotechnical centrifuges were soon in operation in Japan (Mikasa and Takada, 1973) and in the U.S. They have been employed to study a variety of geotechnical problems too numerous to mention here. An excellent discussion of centrifuge testing is provided by Schofield in his 20th Rankine Lecture (1980).

Research specifically involving behavior of pile foundations has begun fairly recently. Scott (1979) performed research on single piles in silt subjected to cyclic lateral loads at the California Institute of Technology. Scott's results were internally consistent and demonstrated the feasibility of conducting pile load tests centrifugally. The lack of good comparison with the prototype which would verify the similitude relationships is the only shortcoming.

Axially loaded piles in sand were investigated by Hougnon (1980) at the University of Colorado. Although this was largely a feasibility study, some useful data regarding the effect of taper and soil density on bearing capacity was obtained. Problems encountered with uniform sample preparation and the loading apparatus limited the effectiveness of this program.

CHAPTER 3. DISCUSSION OF PROTOTYPE

3.1 Introduction

As stated in the introduction (Chapter 1), the research described by this report was performed to model a full scale pile load test performed on an instrumented 9-pile group and accompanying reference piles. This test program was carried out on the campus of the University of Houston, Houston, Texas. This chapter provides a brief discussion of this prototype test. Particular emphasis is placed on those aspects of the prototype which required special attention in modeling.

3.2 Test Site

The two principal geologic formations at the test site are the Beaumont formation, to a depth of 26 ft (8 m), and the Montgomery formation, below 26 ft. Both deposits consist of fairly stiff clay interspersed with sand seams. Both deposits have been desiccated and are therefore somewhat over-consolidated (O'Neill et al., 1980).

It was decided that the variation of undrained shear strength with depth should be the primary consideration in the modeling of this test site. Measurement of this quantity proved difficult, however, as the various methods used did not necessarily agree (see Figure 1). It was decided to use an interpretation of this data that led to a good prediction of the actual behavior exhibited by the test piles. This interpreted profile is provided in Figure 2. The chosen method for reproducing this profile in the laboratory is discussed in Chapter 5.

3.3 Piles and Instrumentation

The test piles employed were steel pipe piles, 10.75 in (273 mm) in outside diameter, with a 0.365 in (9.27 mm) wall thickness. They were closed at the bottom by a steel boot plate. Both reference (single) piles and the 9-pile group were driven to depths of 43 ft (13 m). Spacing in the pile group was nominally 33 in (.85 m) on centers. Figure 3 is a plan view of the test site, with the test piles being numbered 1 through 11. The reference piles, numbers 1 and 11, were tested as single piles.

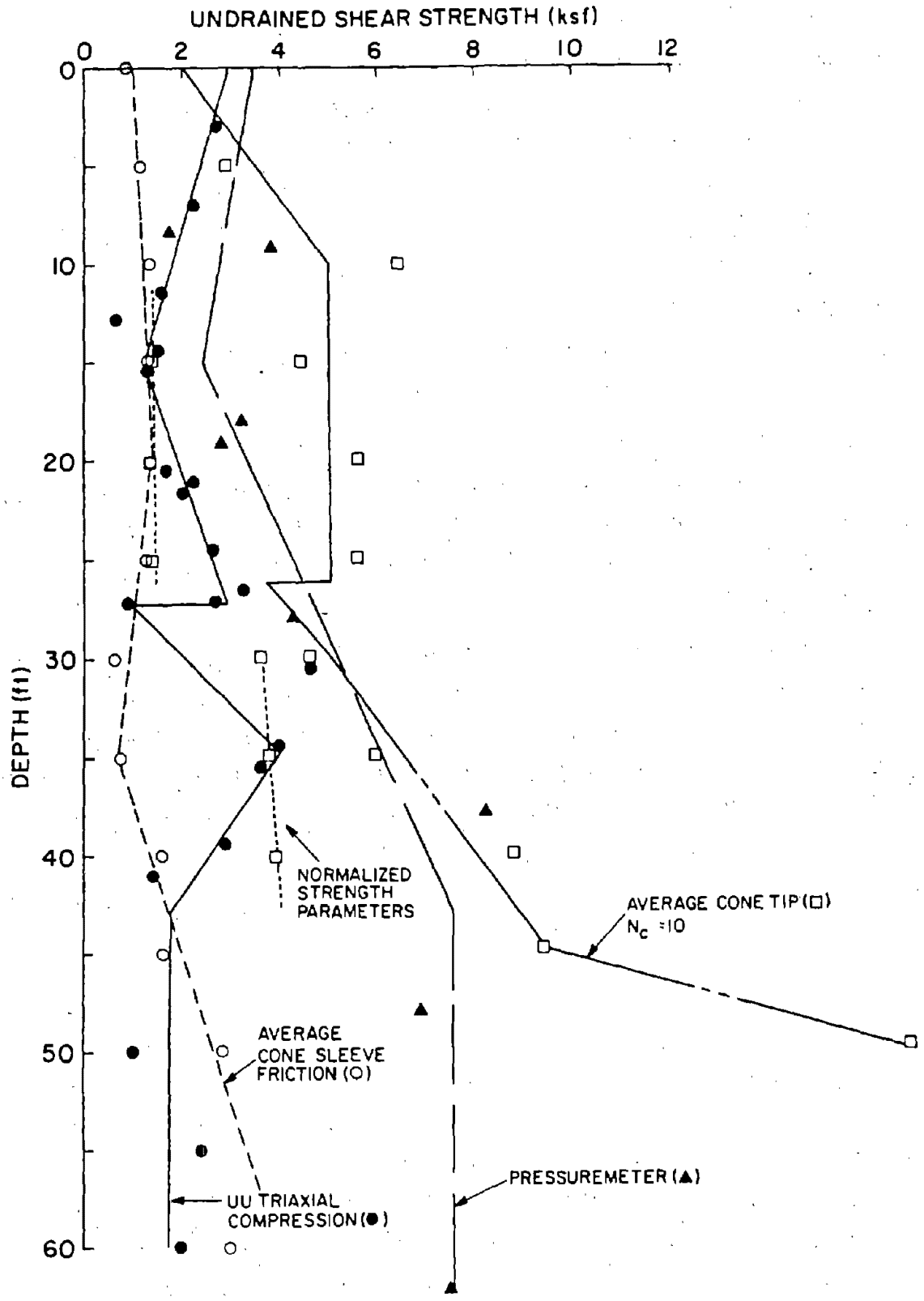

Figure 1. Measurements of undrained shear strength, prototype (O'Neill et al., 1980) (1 ksf = 47.9 kPa; 1 ft = 0.305 m)

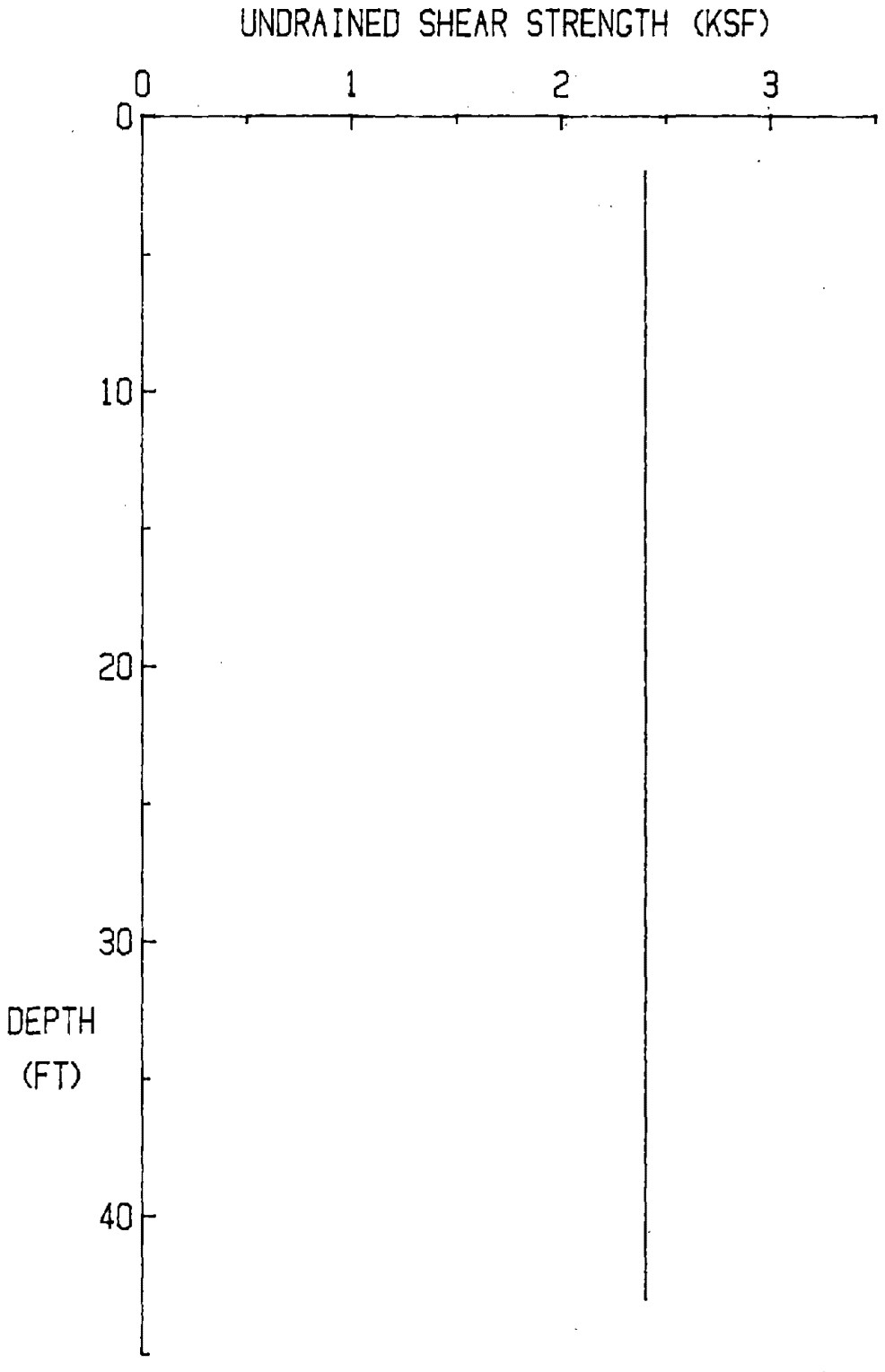

Figure 2. Interpreted S_u profile (1 **ksf** = 47.9 **kPa;** 1 ft = 0.305 m)

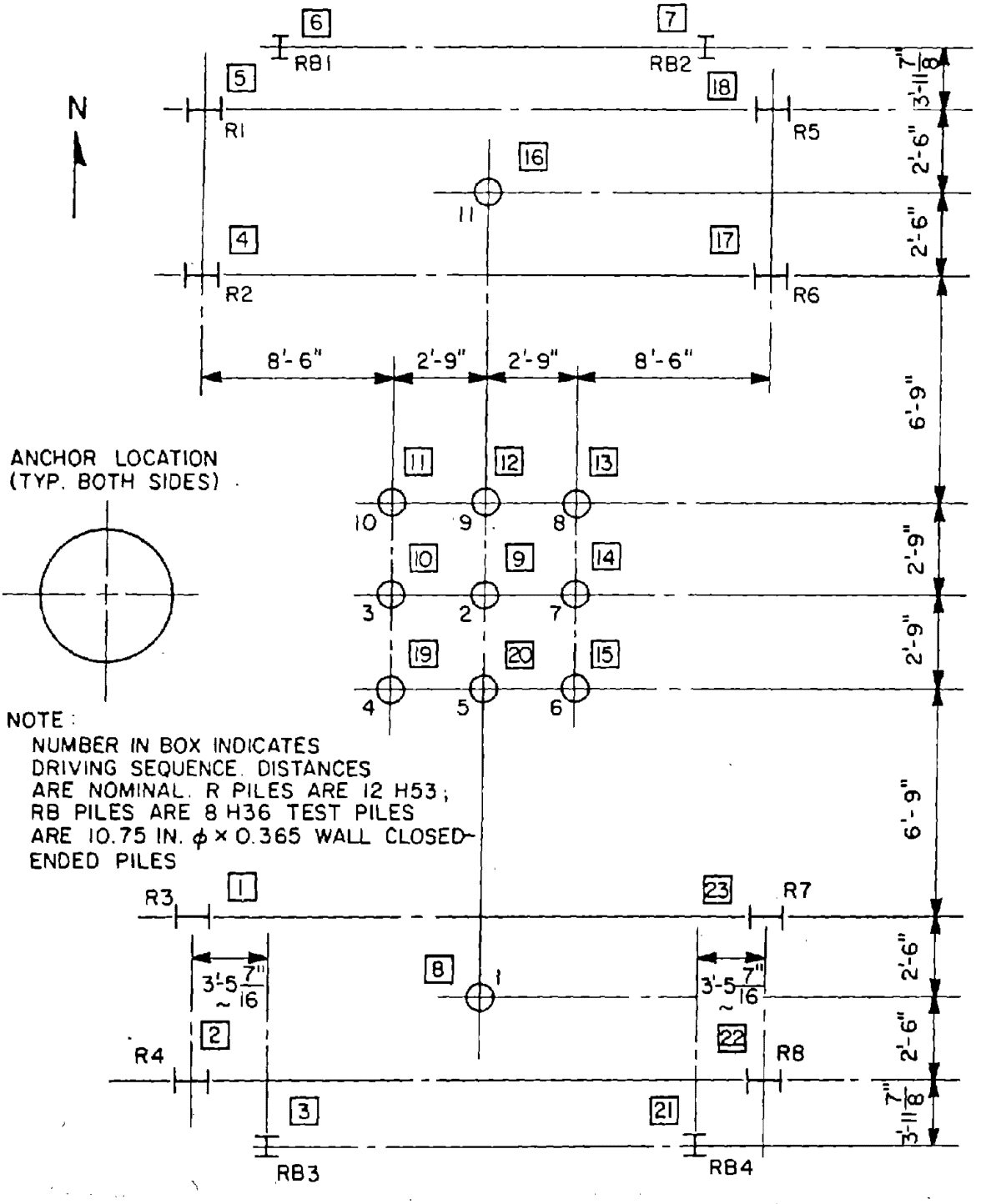

Figure 3. Plan view of test site (O'Neill et al., 1980)
(1 ft = 0.305 m)

The types and locations of pile instrumentation are provided in Figure 4. Of particular interest are the strain gauge stations, which were used to measure load transfer through the length of the pile. This type of instrumentation was provided in the model. All other types of pile instrumentation were not feasible (due to the small size of the model piles) or of no value (since the model piles were pushed, rather than driven).

Types and locations of soil instrumentation are provided in Figure 5. Of interest are the locations of the various piezometers.

3.4 Test Program

Both the single piles and the 9-pile group were loaded by hydraulic jacks. All tests were conducted over approximately an 8-hour period, with one hour between each load increment application. Instruments were read 5, 30, and 55 minutes after each load application.

The 9-pile group was tested to failure 20, 82, and 110 days after driving. Single pile tests were performed approximately 5 days prior to each of these group tests.

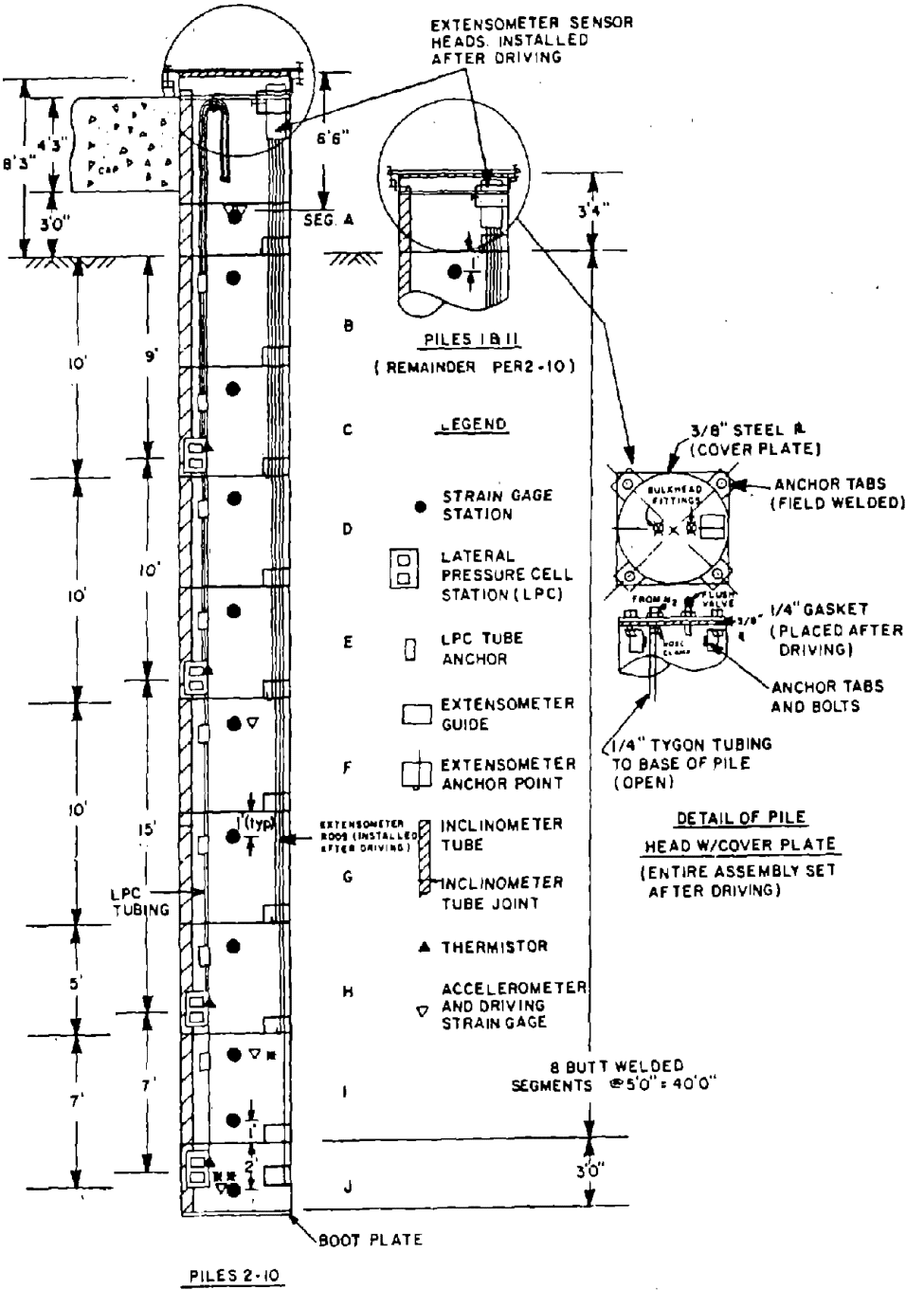

Figure 4. Pile instrumentation (O'Neill et al., 1980)
(1 ft = 0.305 m)

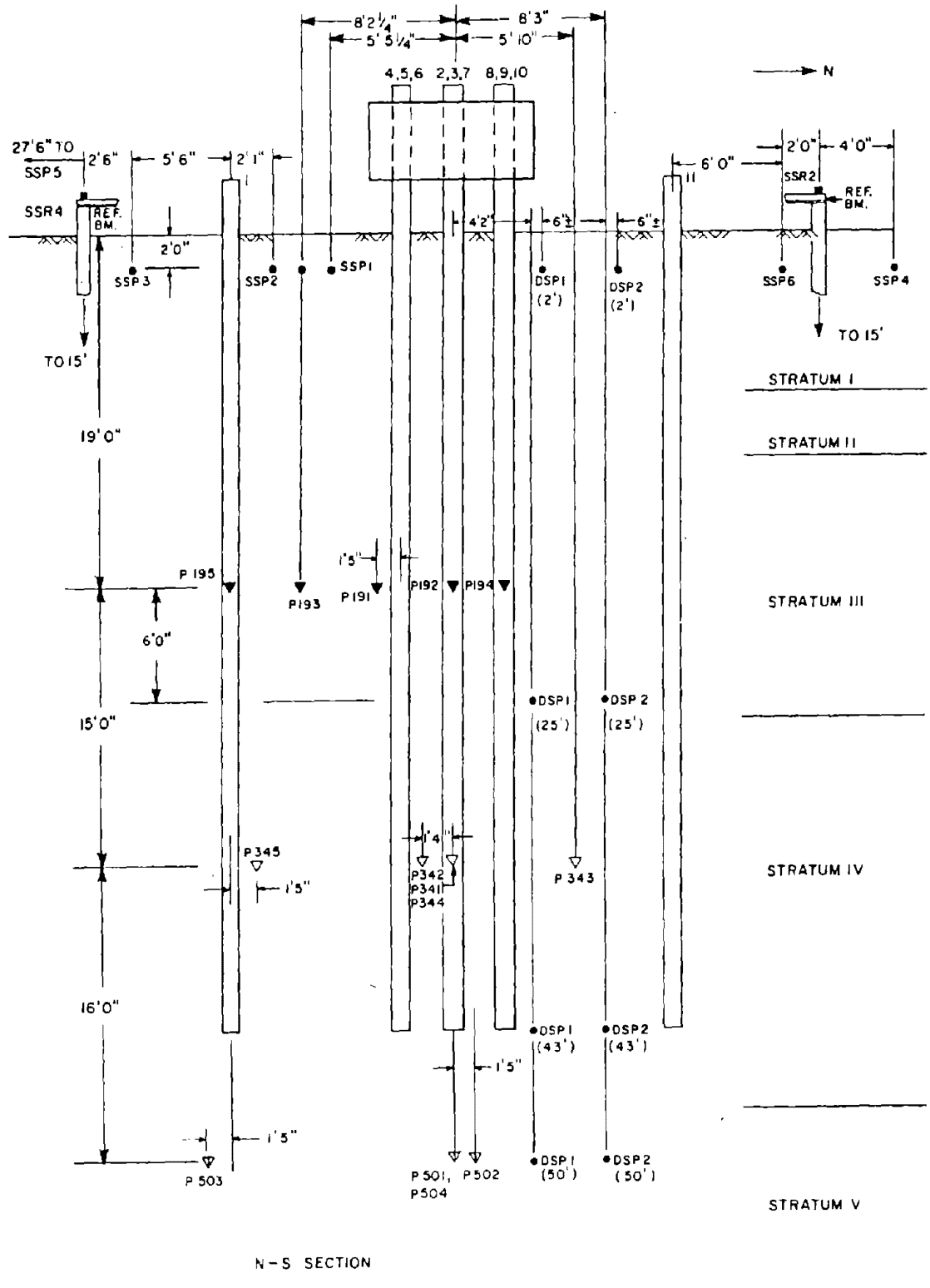

Figure 5. Site instrumentation (O'Neill et al., 1980)
(1 ft = 0.305 m)

CHAPTER 4. TEST EQUIPMENT

4.1 Centrifuge

4.1.1 General Description

The University of Colorado centrifuge is a Genesco G-Accelerator Model 1230-5, capable of generating angular velocities as high as 470 rpm. Its rated payload capacity is 10 g-tons; that is to say, for example, that it can spin a 200 lb (890 kN) package at a centrifugal acceleration of 100 g. The major components of the centrifuge are the arms and baskets, which are encased in a 9-foot (2.76 m) diameter, 3-foot (.92 m) high steel cylinder; the drive pump; and the controls. The drive pump and controls are mounted separately. The University of Colorado centrifuge has been in operation since 1978. Specifications are given in Table 2.

4.1.2 Drive and Control System

The centrifuge is driven by a hydraulic system (Figure 6) with oil being used as the hydraulic fluid. The oil is pressurized by a 2500 psi (17.2 MPa) centrifugal pump, which is powered by a 25 hp electric motor. Flow of oil to the drive system is regulated by an adjustable valve. This provides the means for controlling centrifuge speed. A solenoid valve is also present which can be closed in the event of an emergency to provide a quick shut-down of the system.

Centrifuge operation is controlled from a panel adjacent to the drive system (Figure 7). This control panel consists of a toggle switch and start-stop buttons for the electric motor, a toggle switch for the solenoid valve, a crank wheel that operates the speed control valve, and a tachometer. Also mounted are the terminals for the electric slip rings, 115 volt AC outlets, and a circuit breaker for the entire system.

4.1.3 Arms

The configuration of the centrifuge arms and baskets can be seen in Figure 8. The arms are made of structural aluminum and rotate about the axis in the center of the containment cylinder. The baskets at the ends of the arms have floor areas 17.5 in x 18 in (.45 m x .46 m). The pivot points are 11.5 in (.29 m) above the basket floor. These pivot points allow a

Table 2. Centrifuge Specifications.

Type	Genesco G-Accelerator
Model	1230-5
Maximum RPM	470
Size	3 ft (.92 m) x 9 ft (2.77 m) dia.
Pump Capacity	2500 psi (17.2 MPa)
Motor	25 hp
Electrical Slip Rings	5 amp/110 v.
Hydraulic Slip Rings	3000 psi (20.7 MPa)
Package Size	17.5" x 18"x 11.5" (.40 m x .45 m x .3 m)

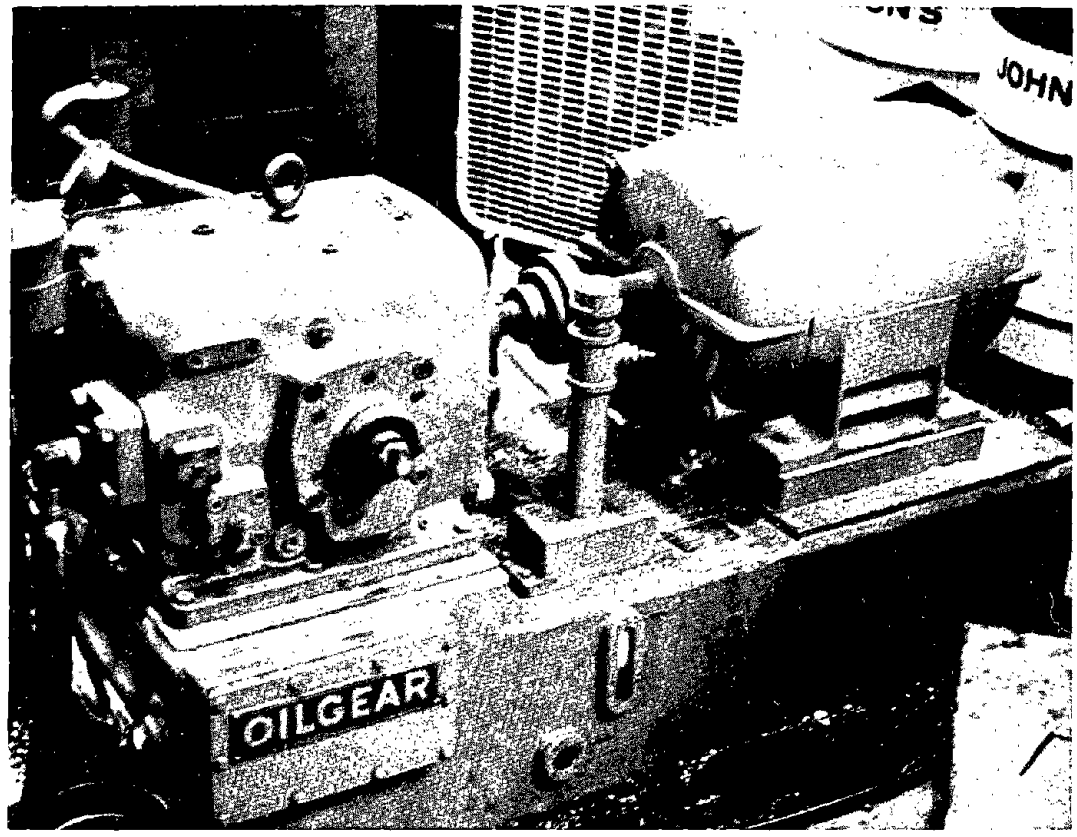

Figure 6. Centrifuge drive system.

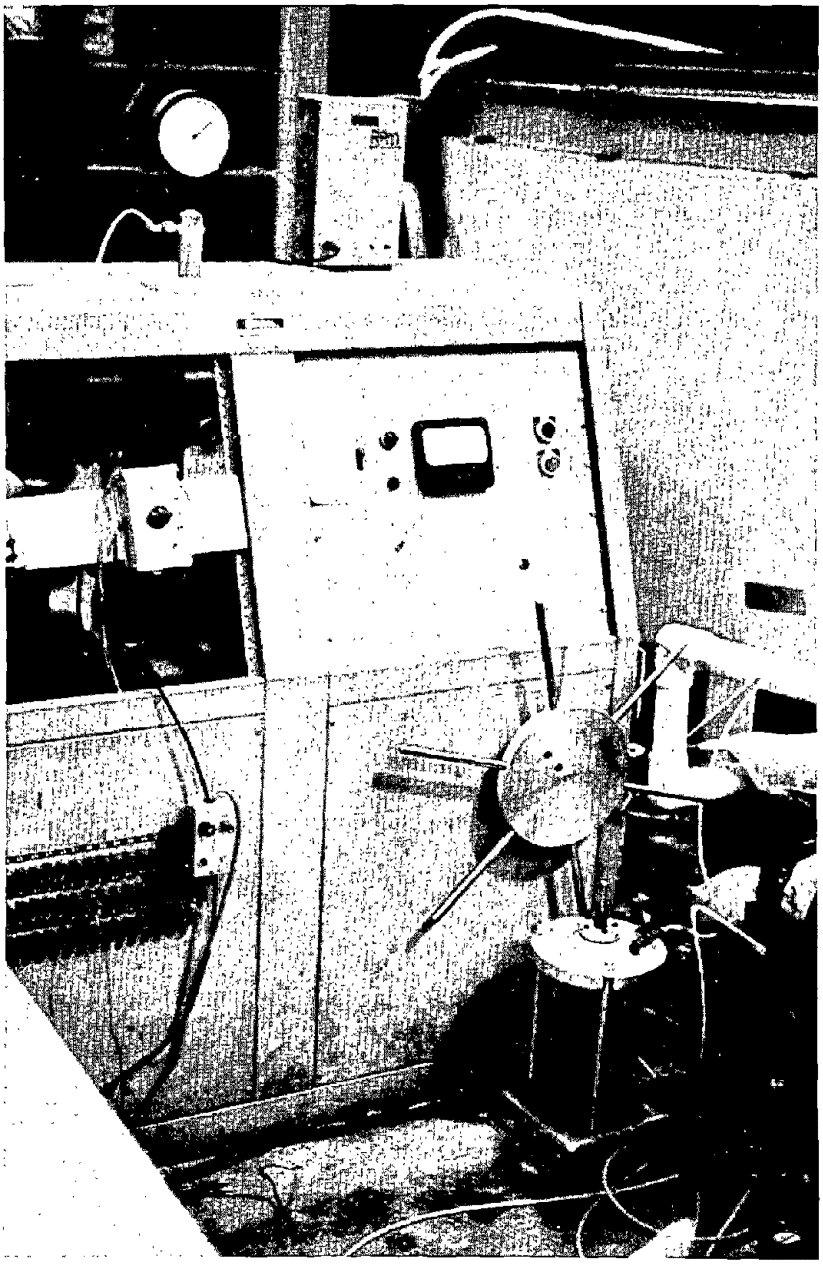

Figure 7. Centrifuge control panel.

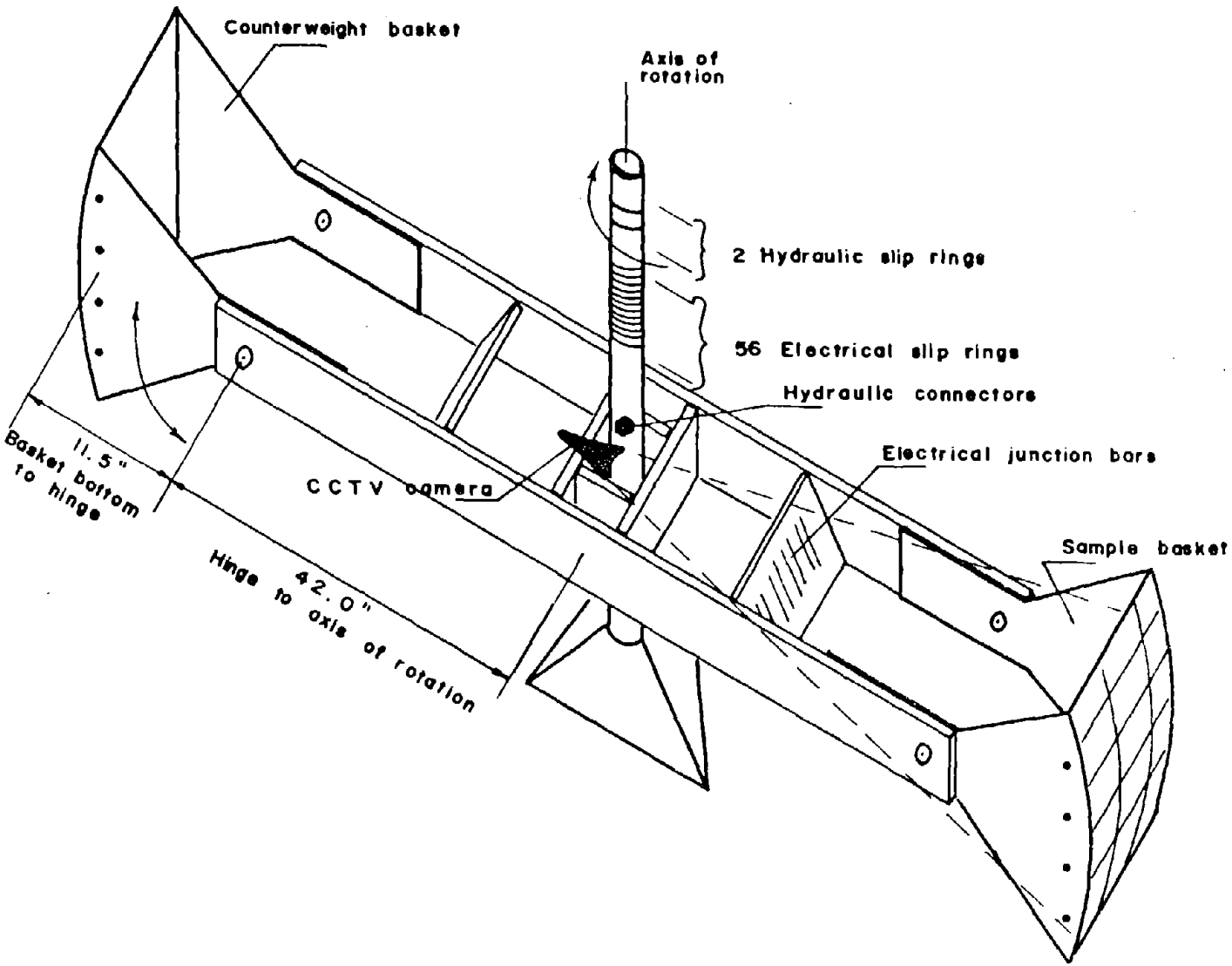

Figure 8. Centrifuge arms.

specimen mounted in the basket to swing up and out, keeping the resultant of centrifugal acceleration and gravity acting perpendicular to the model ground line at all times. The identical baskets allow two tests to be performed at once, but normally only one is performed, and the other basket is weighted to balance the centrifugal forces felt by the centrifuge axis.

4.1.4 Slip Rings

Fifty-six electrical slip rings are mounted on an extension of the centrifuge axis. These slip rings are used to transfer electrical power to various devices inside the centrifuge, and to carry signals from instrumentation on the test package back out to the operator.

A pair of fluid slip rings rated at 3000 psi (20.7 MPa) are also mounted on the axis. These can be utilized to pass hydraulic pressure to equipment inside the centrifuge.

4.1.5 Limitations

A significant limitation for all centrifugal modeling is brought about by the fact that centrifugal force varies directly with the radius of rotation. Hence, the gravity felt by any model increases with depth of the model. This is especially true of smaller centrifuges such as that at the University of Colorado. For example, consider a model pile 10 in (.25 m) in length with its center of mass at a radius of 48 in (1.22 m) spun to 50 g. The centrifugal acceleration at the pile top is only 44.8 g, while that at the tip is 55.2 g.

Other limitations already mentioned include those on package size, speed, and payload capacity.

4.1.6 Container

The soil container for this project had to serve two purposes. First, specimens were prepared by consolidation at 1 g, so the container had to function essentially as a one-dimensional consolidometer. Second, the container had to hold the equipment necessary to perform in-flight testing in the centrifuge.

An exploded drawing of the container is given in Figure 9. To consolidate specimens, load was applied through the piston which was free to move

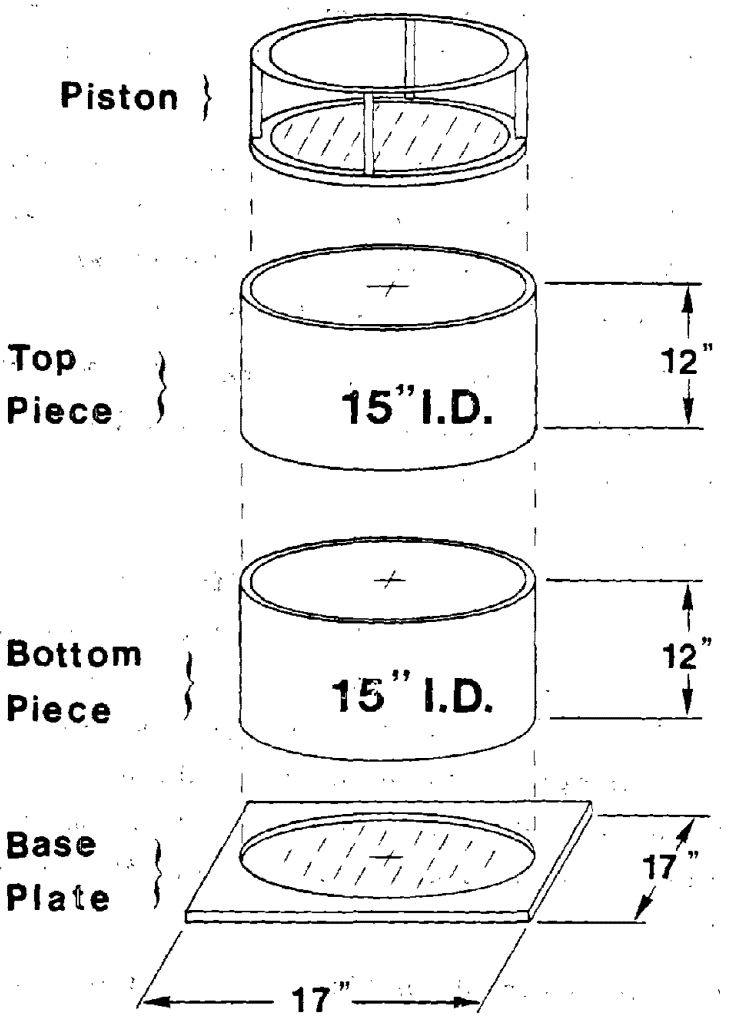

Figure 9. Exploded view of soil container (1 in. = 2.54 cm).

through the full length of the top piece. Top drainage was provided through the piston, and bottom drainage was provided through the base plate, by sand layers. Migration of fines was prevented by layers of filter paper between the specimen and sand layers. O-ring seals were employed to prevent leakage between the top and bottom pieces and between the bottom piece and the base plate.

After consolidation, the top piece was removed, and only the base plate and the bottom piece were installed in the centrifuge. Drilled and tapped holes were provided on the bottom piece to attach necessary equipment. Aluminum was chosen for all parts because of its light weight.

4.1.7 Vane Shear Apparatus

Vane shear tests were performed on the specimen while in-flight to determine the undrained shear strength. The apparatus employed in this procedure is shown in Figure 10. The vane was inserted in the specimen at one g. At the desired gravity level (in-flight), torsion was applied to the vane by the electric motor. Torsional stress was measured in the shaft of the vane through the use of the strain gauges shown in Figure 11. The output of the strain gauges was amplified within the centrifuge, read on a digital voltmeter, and recorded. The amount of torque applied could then be ascertained, based on the calibration of the apparatus. The apparatus was calibrated (applied torque vs. voltage) with the torsional spring of a Wickham-Farrance laboratory vane. The undrained shear strength of the soil could then be easily computed from the torque required to produce failure (Sowers, 1979).

4.1.8 Model Piles

As previously stated, the prototype piles were steel pipe piles embedded 42 ft (12.8 m), with outside diameters of 10.75 in. (27.3 cm). The first step in modeling this system is to achieve geometric similarity. For example, consider a 1/70th scale model. The length of the model can be determined by equation :

$$L_p = L_m \lambda \qquad (2.1)$$

$$\lambda = 70$$

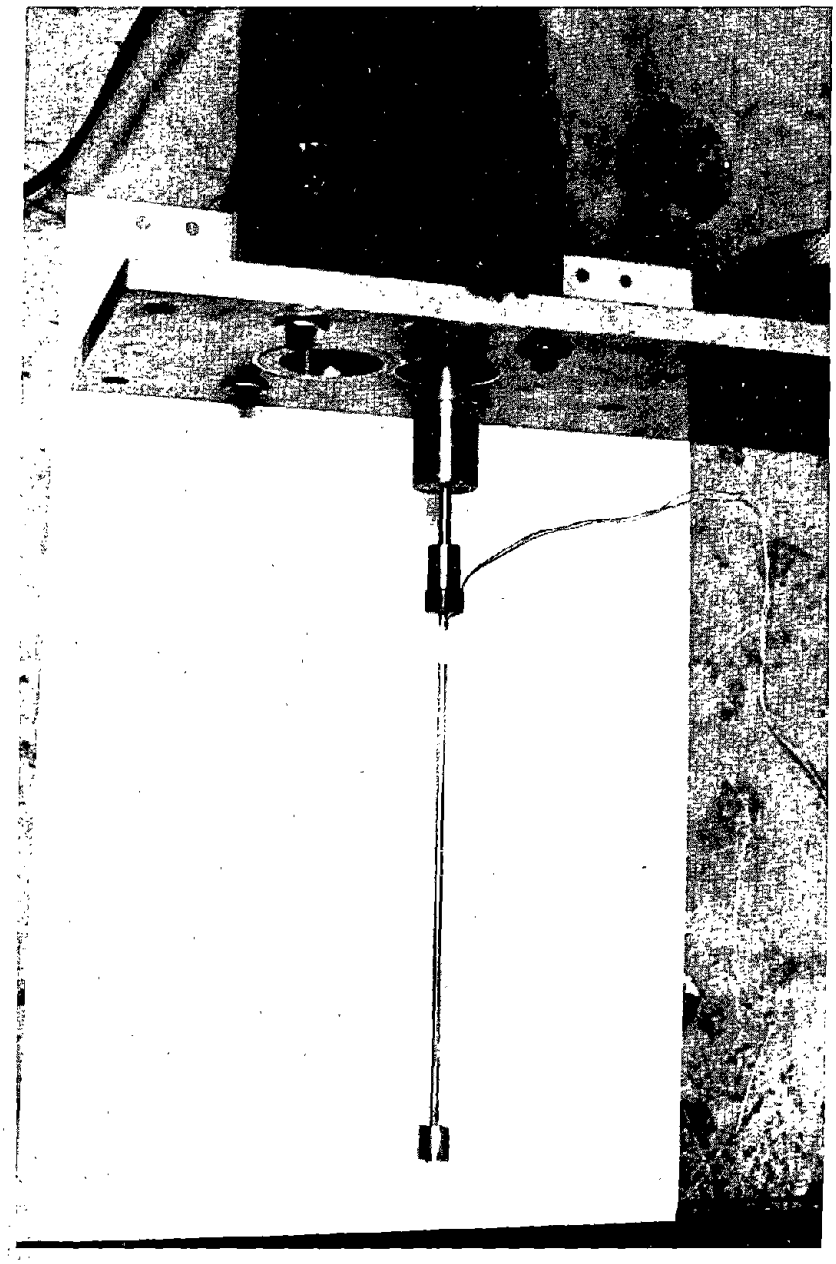

Figure 10. Vane shear apparatus, including motor.

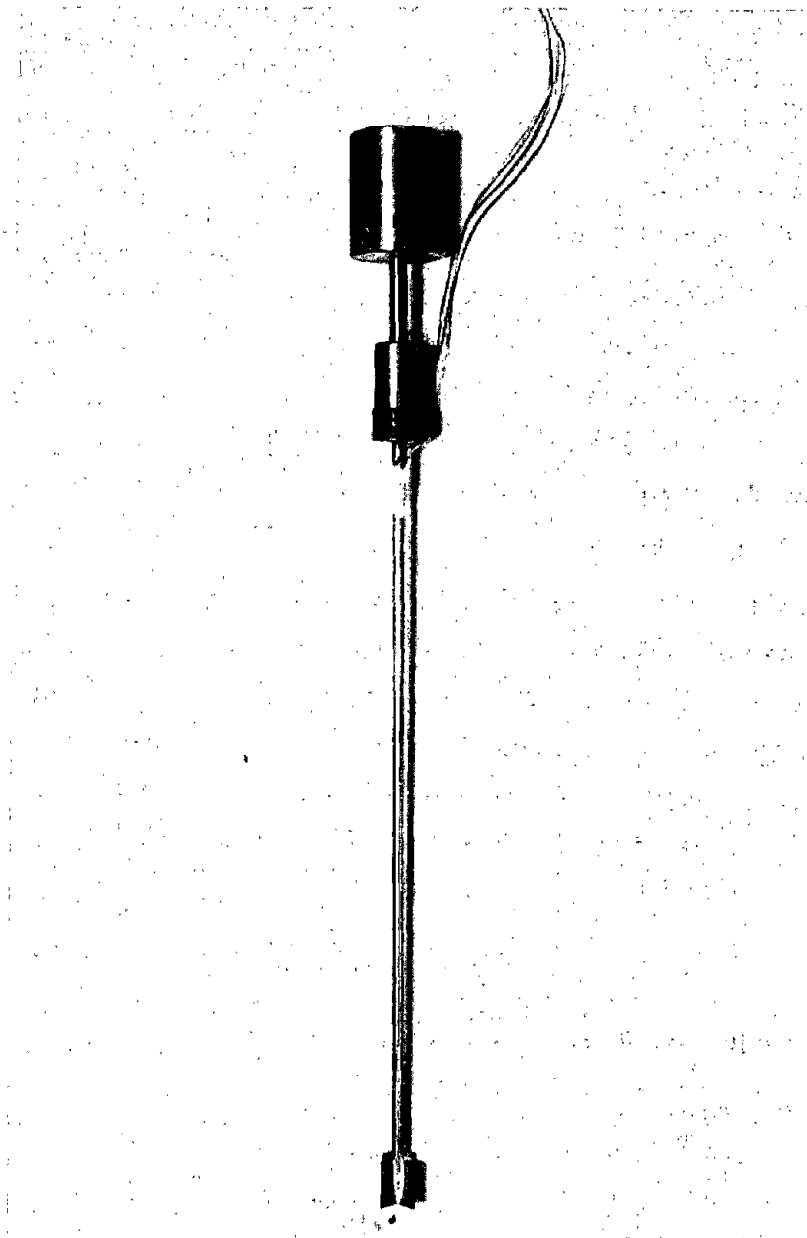

Figure 11. Close up of vane, showing instrumentation.

and $L_p = 42$ ft

so $L_m = \frac{42}{70} = 0.6$ ft

or 7.2 in

The same method yields an outside diameter of 0.154 in (.39 cm). The dimensions of 1/45th and 1/100th scale models are given in Table 3.

It is also necessary to model the material properties of the prototype. If the model and prototype are constructed of the same material, merely duplicating the inside diameter, and thus the wall thickness, as described above is sufficient. However, if a different material is to be used in the model, the inside diameter of the model need be adjusted so that similarity of the material properties exists.

In this case, using steel in the model at 1/70th scale would have necessitated a model wall thickness of 0.005 in (.013 cm). It was feared that this would prove too delicate to work with, so it was decided that the model piles should be constructed of aluminum. Using the product of the elastic modulus (or Young's modulus) and the moment of inertia as the critical property, the required wall thickness of the model can be determined as follows:

$$(EI)_p = (30 \times 10^6 \text{ psi})(160.73 \text{ in}^4)$$
$$= 4.82 \times 10^9 \text{ lb-in}^2,$$

and using equation 2-1 and Table 1,

$$(EI)_m = \frac{4.82 \times 10^9}{(70)^4}$$
$$= 201 \text{ lb-in}^2.$$

Since aluminum was used in the model,

$$E_m = 10 \times 10^6 \text{ psi}$$

so $$I_m = 2.01 \times 10^{-5} \text{ in}^4.$$

For an annular cross section,

$$I = \frac{\pi}{4}\left[\left(\frac{OD}{2}\right)^4 - \left(\frac{OD}{2} - t\right)^4\right] \qquad (4.1)$$

Table 3. Dimensions of Model Piles.

Nominal scale	50	70	100
Actual scale	45	70	107
Length (in)	5.5	8.0	11.0
Embedded length (in)	5.1	7.5	10.25
Outside diameter (in)	.240	.154	.100
Inside diameter (in)	.156	.94	.066

Conversion factor: 1 in = 2.54 cm

where OD is the outside diameter and t is the wall thickness.
Given the outside diameter of 0.154 in , Equation 4-1 can be solved:

$$t = 0.025 \text{ in}$$

$$ID = 0.104 \text{ in}$$

The relevant dimensions and properties of the 1/45th and 1/100th scale models are given in Table 3.

It should be noted that this approach models the lateral stiffness (for bending) of the pile and not the axial stiffness. Hence, some accuracy in modeling axial load transfer is lost. (The axial stiffness is approximately 20% high.) Emphasis was placed on the lateral stiffness as it is much more important to lateral behavior than axial stiffness is to axial behavior. This is due to the ratio of pile stiffness to the stiffness of the adjacent soil being very high.

The model piles were machined from stock aluminum rods. First the rods were turned down to the desired outside diameter on a lathe. They were then waxed into a groove of this size and half of the rod cut away. A radius cutter was used to machine the desired inside diameter of the half pile remaining. Finally, keyed slots were machined into the contact surface to allow secure epoxying to the other pile half. The piles were made in two halves to allow installation of strain gauges throughout their lengths. An exception was the 100 g piles, which were too small to have internal strain gauges.

4.1.9 Driving and Loading Apparatus

The driving and loading of the piles were performed in-flight with the same apparatus. This apparatus is shown in Figure 12. Air pressure applied through the hydraulic slip rings to the top of the Bellofram cylinder caused downward motion of the piston. Water pressure was used (also supplied through the hydraulic slip rings) beneath the piston to hold it in position when not in use and to cause upward motion when desired. Water was used because its mass density is sufficient to generate enough pressure under gravity to counteract the self-weight of the piston, and thus hold the piston in a given

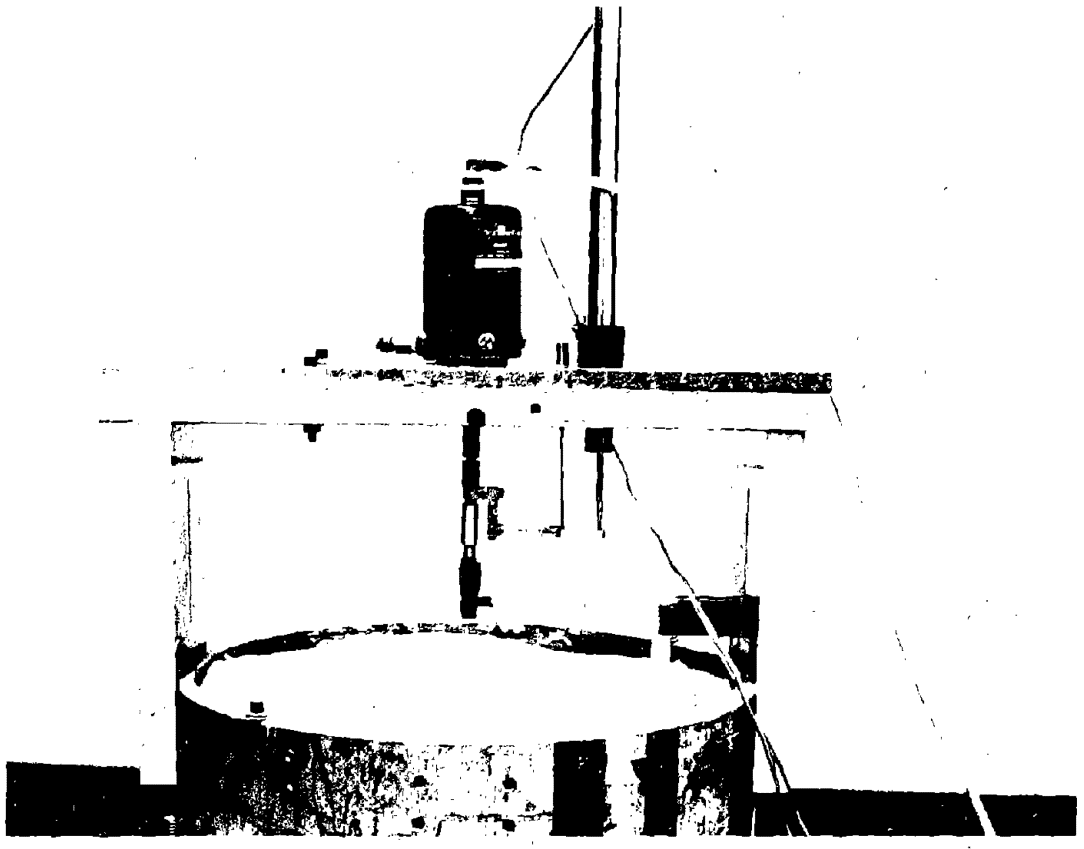

Figure 12. Driving and loading apparatus.

position with a minimum of applied pressure. The Bellofram system was chosen because it allowed movement of the piston with a minimum of friction.

Lateral loads were applied with a similar but smaller Bellofram cylinder, this one single acting. Air pressure applied to the bottom of the cylinder caused upward movement of the piston which applied tension to a small cable. This cable was routed through a pulley in such a way that a horizontal load was applied to the pile top (or the pile cap in the case of group tests).

4.2 Instrumentation

4.2.1 Load Cells

Both axial and lateral loads were measured by load cells instrumented with 350 Ω strain gauges wired in full Wheatstone bridges. Both circuits were powered by 5-volt power supplies and the outputs were amplified inside the centrifuge.

The axial load cell was a machined hollow aluminum cylinder that threaded onto the piston rod of the loading apparatus. It could then contact the pile top (or pile cap).

The lateral load cell was a stainless steel ring, attached in a gap in the loading cable in such a way that tension in the cable induced elongation in the ring.

4.2.2 Displacement Measurement

Displacements during driving and loading of model piles were measured by Linear Variable Differential Transformers (LVDT's). Two types were used: one with a 5-in (12.7 cm) range for installation, and a smaller, more sensitive one with a ½-in (1.27 cm) range for displacements during the load test (both axial and lateral). Configurations for both of these types of tests can be seen in Figures 13 and 14. All LVDT's were calibrated with dial gauges.

4.2.3 Pore Pressure Transducers

During early stages of testing pore pressure transducers were utilized in an attempt to monitor the effect of centrifuging on pore water pressure

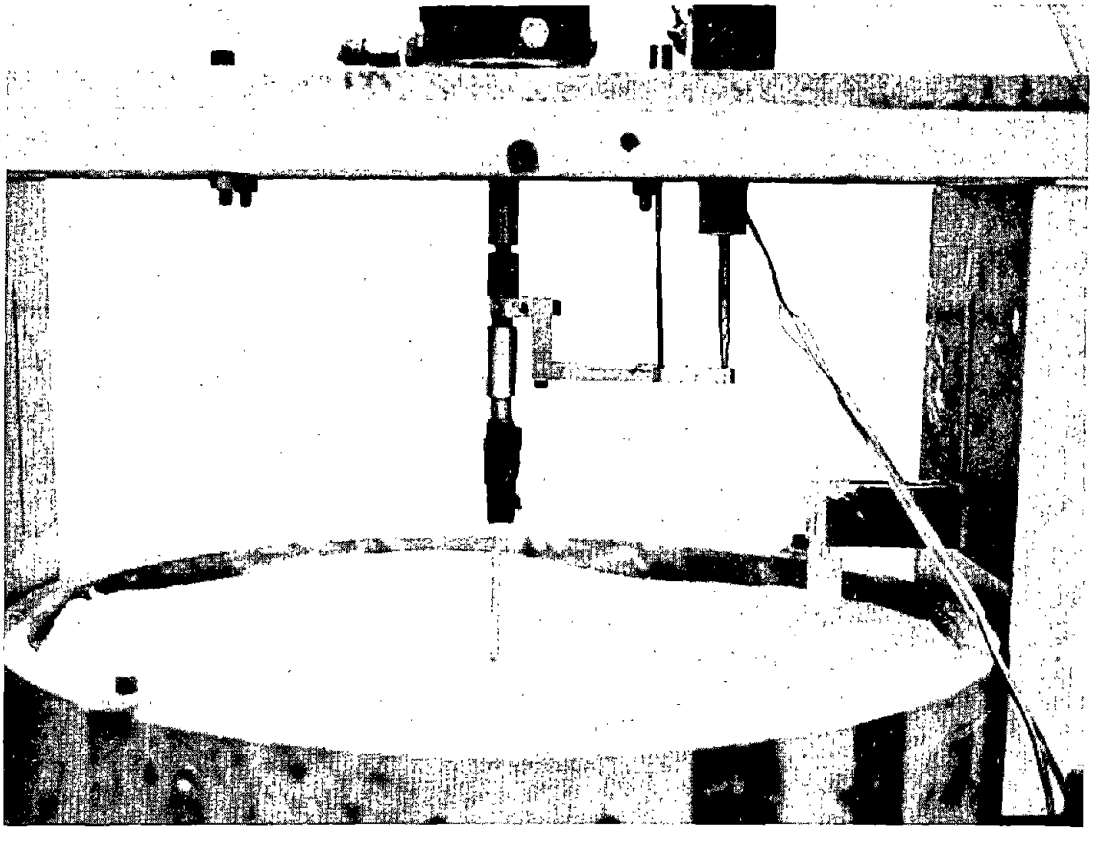

Figure 13. Axial load test configuration.

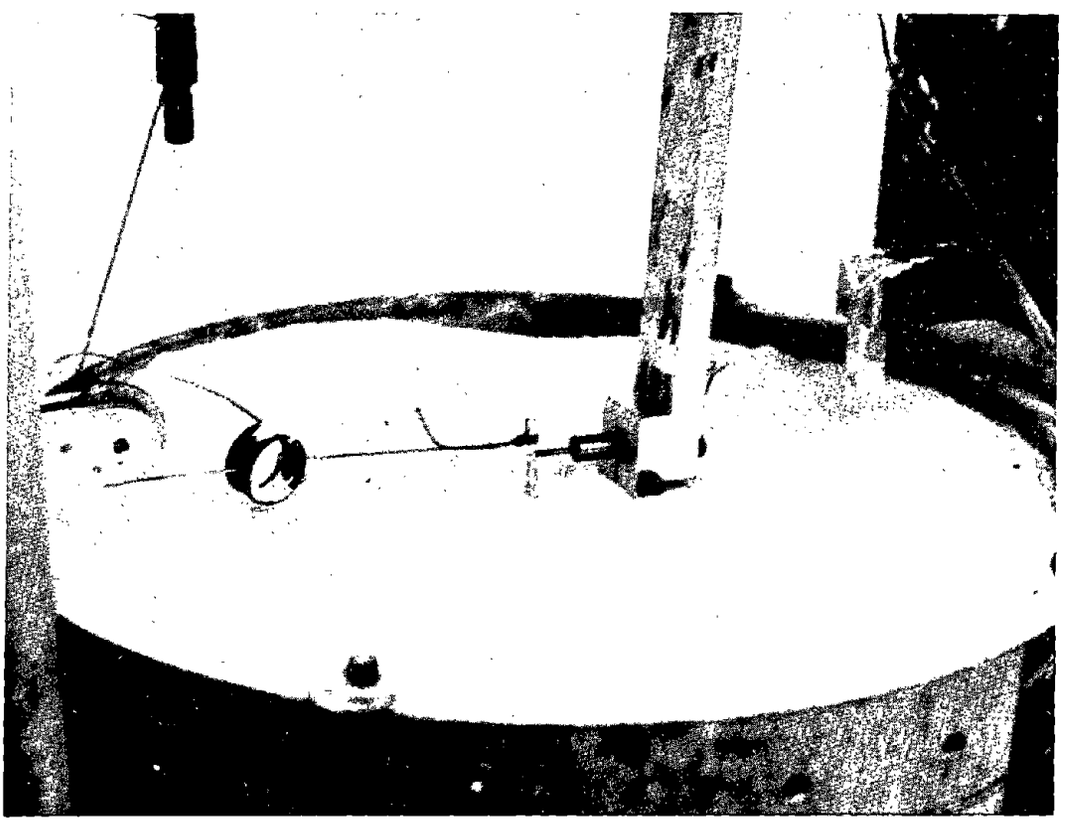

Figure 14. Lateral load test configuration.

in the specimen. These attempts were largely unsuccessful due to a loss of saturation in the piezometer tubes inserted into the specimen. This is attributed to the fact that 100 percent saturation was not insured in the specimen.

4.2.4 Instrumentation of Model Piles

Model piles were manufactured in two halves to allow installation of strain gauges. The purpose of this instrumentation was to read axial load throughout the length of the pile during axial tests, and bending moment throughout the pile during lateral tests. This was accomplished with 120 Ω strain gauges installed in a half-bridge configuration at 5 evenly spaced stations in the pile (see Figure 15).

A signal conditioning unit with 32-channel capacity amplified the outputs and provided balancing capability. Switches located on the centrifuge control panel were used to alter the positions of the two dummy gauges in the Wheatstone bridge, allowing measurement of axial force and bending moment (Figures 16 and 17). The instrumented piles were calibrated for both axial forces and bending moment with dead weights. Axial load calibration also was checked with the axial load cell.

4.3 Data Acquisition

4.3.1 Analog

Analog recording of data was accomplished with several of the x-y recorders and strip-chart recorders available at the University of Colorado Civil Engineering Laboratory. The x-y recorders were used to obtain load-displacement curves for pile load tests. The strip-chart recorders were used to monitor signals from the instrumented piles as the tests were in progress.

4.3.2 Digital

A Hewlitt Packard 9825 B data acquisition system was used to obtain a digital record of test data. This system as employed had a 20-channel capacity and was used only to record signals from the instrumented piles (under axial or lateral loads). Load-displacement could not be recorded with this system due to a variable resistor used to zero the LVDT output. This

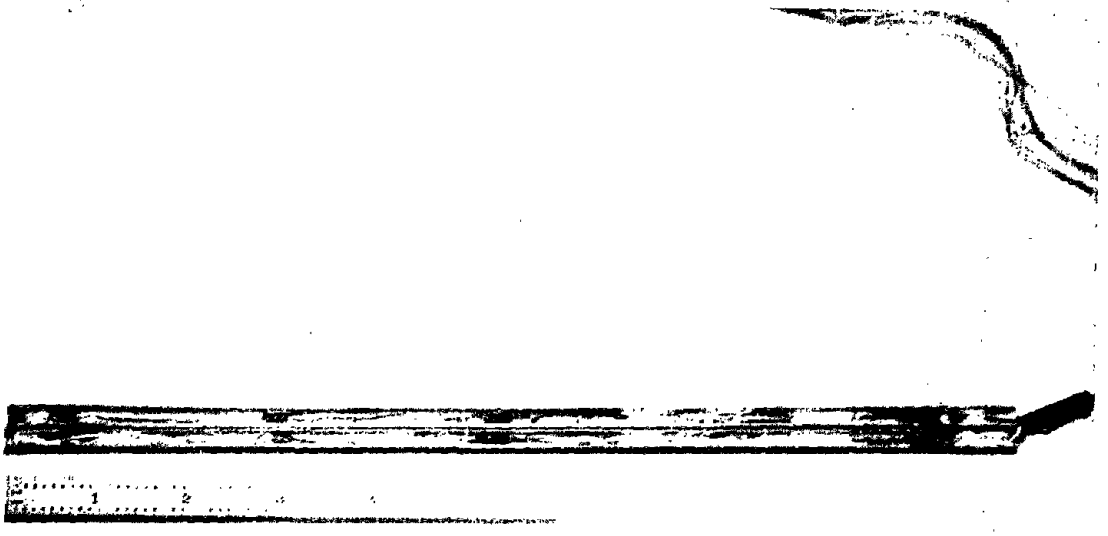

Figure 15. 1/50th scale pile halves showing strain gauge station positions.

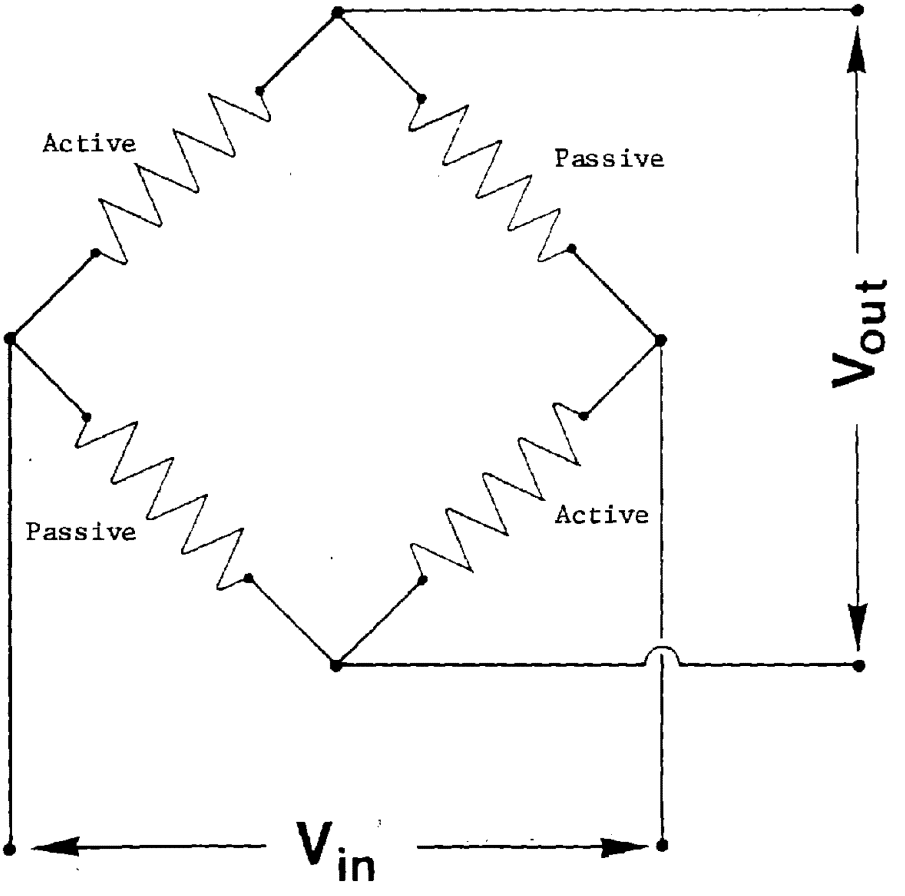

Figure 16. Wheatstone bridge configuration for measurement of axial load.

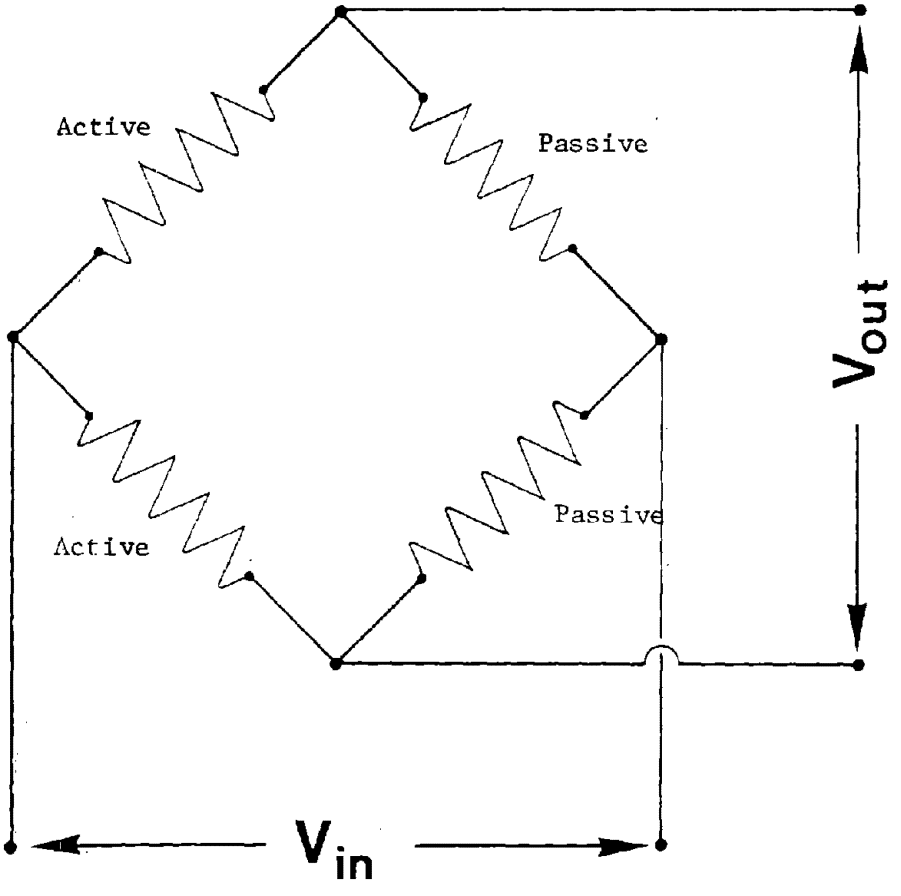

Figure 17. Wheatstone bridge configuration for measurement of bending moment.

component apparently was not compatible with the HP system, causing it to misread the input signals.

The system was operated at its maximum rate of 400 data points per second, so any given channel was read 20 times per second. The data was permanently stored on magnetic tapes from which it could be retrieved for plotting or other manipulation. A variety of plotting software was available and used with this system.

CHAPTER 5. SPECIMEN PREPARATION AND TEST PROCEDURE

5.1 Discussion of Preparation Technique

The first step in arriving at a preparation technique for the model was that of choosing a soil. Samples of Beaumont clay from the full size pile group test were not available. The decision was made to use Georgia kaolin, a dry kaolin commercially produced in powder form for use in the ceramic industry. This decision was based on two facts, the first being that this material is readily obtainable in large quantities at moderate cost. Second, and most importantly, this material has been used extensively in the geotechnical laboratories at the University of Colorado. Therefore, measurements of consolidation properties, permeability, specific gravity, and Atterberg properties had already been performed, and the data was available for use. Geotechnical properties of Georgia kaolin appear in Table 4.

Several methods were considered as a possible means of reproducing the desired undrained shear strength profile discussed in Chapter 3 and shown in Figure 2. The greater portion of testing was to be performed at 70 g, so this environment was given primary consideration in choosing a preparation technique. Hence any analysis performed was done for the 70 g case and then adapted to fit other gravitational levels as necessary.

Initially, consideration was given to preparation by centrifuging the specimen until consolidation under its own weight produced the desired shear strength. Using Equation 5.1, which was developed by Skempton (1957), a relationship between undrained shear strength (S_u) and effective overburden stress (σ_v') could be estimated. σ_v' at a given point is given by the product of γ', height of soil above that point, and the gravity level if the plastic index (PI) was known.

$$\frac{S_u}{\sigma_{v'}} = 0.11 + 0.0037\ PI \qquad (5.1)$$

It should be mentioned that this only applies to a normally consolidated clay. This relationship quickly showed that preparation by centrifuging under self weight was not feasible as an acceleration of over 400 g would be required.

Table 4. Geotechnical Properties of Georgia Kaolin.

Liquid Limit	45
Plastic Limit	25
Plastic Index	20
Specific Gravity	2.60
Activity	0.31
κ/λ	0.25

Consideration was then given to preparation by centrifuging with a surcharge load above the specimen. Equation 5.1 remains the means by which this concept was evaluated. Given an acceleration of 70 g, it was found that almost 4 feet of overburden was required to produce a profile in the neighborhood of that desired. This much space was not available in the centrifuge, and the extra weight would have exceeded payload capacity of the available centrifuge.

The only feasible method which remained was consolidation under an applied stress at one g, henceforth referred to as static preparation. This method involves a more complex stress history, one in which the specimen is subjected to and consolidated under a static one g stress much greater in magnitude than that induced by self weight while in-flight at 70 g in the centrifuge. Hence, a state of overconsolidation can be said to exist in the specimen when testing of the model piles takes place. This fact makes determination of the necessary preconsolidation stress difficult in that Equation 5.1 no longer directly applies. As a means to estimate the preconsolidation stress required to produce the desired undrained shear strength at a given point in the soil profile, Equation 5.2 was used in conjunction with Equation 5.1.

$$\frac{S_{uB}}{S_{uA}} = \left[\frac{1}{OCR}\left(\frac{2K_{oB}}{1 + 2K_{oA}}\right)\right]^{\kappa/\lambda} \tag{5.2}$$

where S_{uB} = undrained shear strength in overconsolidated state
S_{uA} = undrained shear strength in normally consolidated state
OCR = overconsolidation ratio
K_{oB} = coefficient of earth pressure at rest, overconsolidated
K_{oA} = coefficient of earth pressure at rest, normally consolidated
κ = slope of swelling curve, e vs. log p
λ = slope of virgin compression curve, e vs. log p

This equation, which relates S_u for any stress state to S_u for the normally consolidated condition for that soil, was developed by Atkinson and Bransby (1978) and is based on the critical state approach to soil behavior.

With these two equations the strength in a normally consolidated condition (under static pressure) can be predicted using Equation 5.1. When this static pressure is relieved and the specimen is centrifuged, a substantially different (lower) stress exists in the specimen, which causes a reduction in the S_u. This reduction can then be predicted at various points in the soil profile by Equation 5.2.

The preliminary investigation as outlined above predicted that a preconsolidation stress of 16 ksf (766 kPa) was necessary to produce an undrained shear strength profile at 70 g as illustrated in Figure 18. This prediction was checked by the SHANSEP (Stress History and Normalized Soil Engineering Properties) approach (Ladd and Foott, 1974; Mayne, 1980), and was found to be in reasonable agreement. Required consolidation stresses at 50 g and 100 g were predicted to be 15 percent high and lower, respectively.

Specimens were mixed at a water content of 60 percent and then consolidated statically in the container described in Chapter 4 using several load steps over a four-day period to reach the desired level. Finally, specimens were centrifuged for a period of 7 hours at 70 g. This time period was required to achieve equilibrium of pore pressure (steady state) in the specimen under centrifugal loading. The seven-hour period was arrived at by observations of surface deflections measured by LVDT's and proximeter probes during the initial 3 tests. Steady state was assumed to exist when indicated on a deflection vs. log time plot as suggested by Lambe (1954).

Actual measured shear strengths will be discussed fully in Chapter 6, but were generally in the neighborhood of that desired. The variations encountered are attributed to unexpected variations in soil properties between various shipments of kaolin and inconsistencies in degree of consolidation reached.

5.2 Discussion of Test Sequence

It was necessary to perform a number of tests on each specimen. Involved in all tests were one or more (as many as six) vane shear tests and one or more pile load tests, both axial and lateral. Between various tests, it was necessary to stop the centrifuge to set up for the upcoming test, which might involve repositioning equipment, installing and testing equipment,

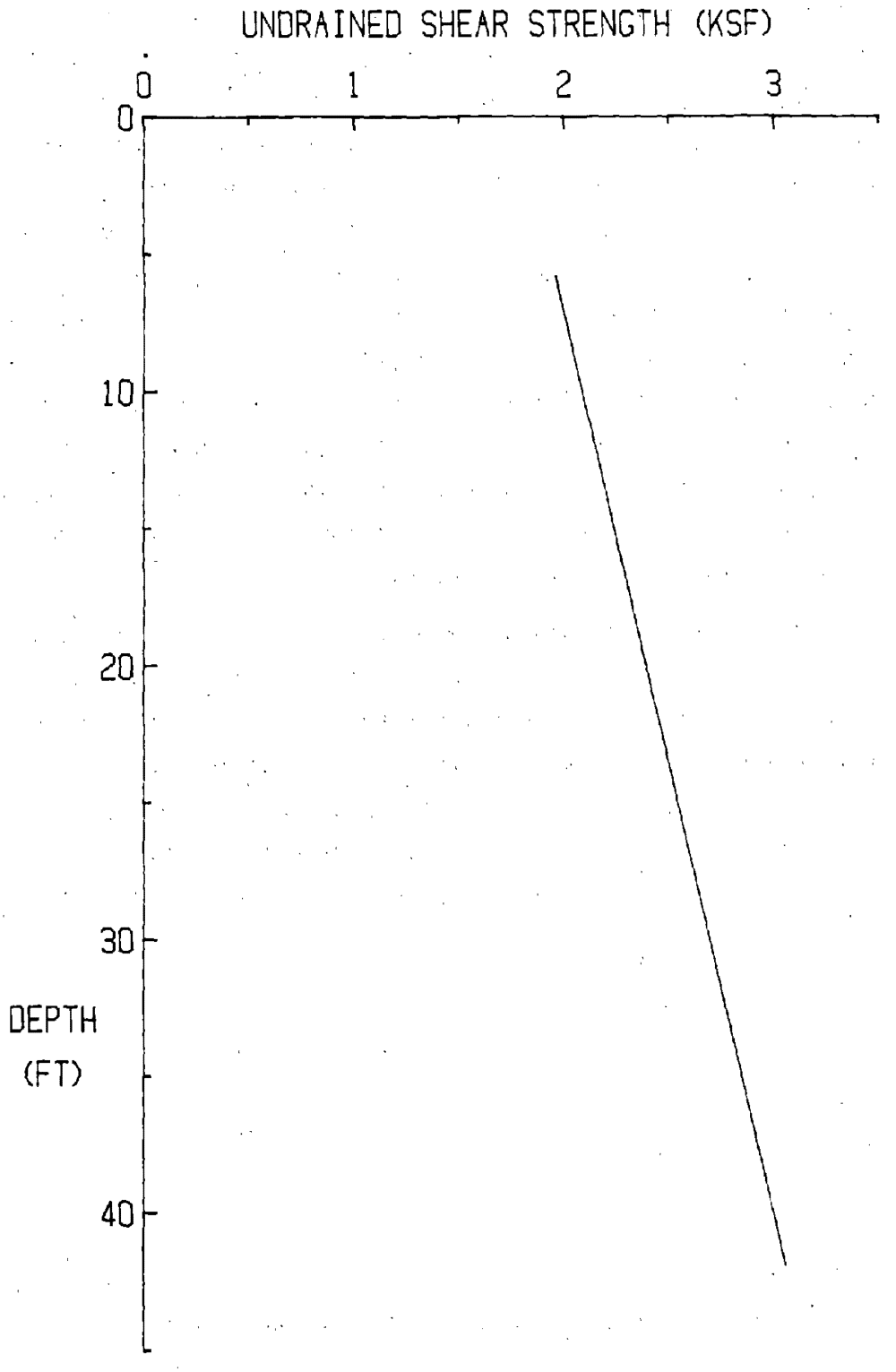

Figure 18. Desired undrained shear profile (1 ksf = 47.9 kPa; 1 ft = 0.305 m)

or repairing and replacing defective equipment. These tasks (which will be further discussed in this chapter) might require anywhere from 15 minutes to 24 hours to accomplish. When the task was complete, the problem of determining how long to centrifuge the specimen to reachieve steady state was encountered. The approach taken in solving this problem was that the specimen should be centrifuged for an amount of time equal to that at which it remained at one g. The exceptions to this were cases where the specimen was at rest for long periods of time. Since seven hours were found to be sufficient to achieve steady state during initial centrifuging, any instance in which the specimen remained at rest longer than seven hours required seven hours of additional centrifuging to restore the previously established steady state.

With this practice in mind, the following "generic test sequence" is presented. This is, as its name implies, a basic guideline which was followed throughout the testing program of 22 tests. Specifics of each test will be discussed in Chapter 6.

Test Sequence

1. Following static consolidation of specimen in the MTS, install in centrifuge with necessary equipment for vane test; insert vane to desired depth in desired position.
2. Centrifuge 7 hours to obtain equilibrium of pore pressure.
3. Perform vane test; record vane output manually.
4. Stop centrifuge and reinsert vane for new vane test.
5. Centrifuge as needed.
6. Perform vane test, record output.
7. Repeat steps 4, 5, and 6 until desired amount of vane shear data is obtained. Note on later tests; steps 4, 5, and 6 were eliminated as one vane test was deemed adequate.
8. Stop centrifuge; install/adjust pile loading equipment and instrumented pile(s).

9. Centrifuge as necessary.

10. Perform pile load test, recording data by analog or digital means as necessary.

11. Repeat steps 8, 9, and 10 as necessary, performing either 2nd axial load test (on different pile), lateral load test, or pile group (axial) test.

12. If desired, repeat steps 4, 5, and 6 if vane strength and pile capacity seem to be contradictory.

13. Stop centrifuge; make any one g measurements desired such as one g vane testing or water content measurement.

CHAPTER 6. TEST PROGRAM AND RESULTS

6.1 Discussion of Test Program

6.1.1 Goals of Program

As stated in the introduction, the aim of the testing described by this report was to demonstrate the effectiveness of centrifugal modeling as a means of duplicating in the laboratory results obtained in field pile load tests. Specific interest was placed on the following subjects.

1. Duplication of prototype shear strength profile.
2. Relationship between S_u and Single Pile Capacity.
3. Relationship between single pile and pile group capacities (group factor).
4. Relationship between single pile and pile group load transfer.
5. Comparison of model results from subjects 2, 3, and 4 above to prototype.
6. Comparison of model and prototype load-displacement curve.
7. Behavior of single piles (model) under lateral load.
8. Comparison of model results at different scaling factors (modeling of models).

6.1.2 Format of Program

The testing program as carried out is summarized in Table 5. Because exact reproduction of the desired S_u profile proved to be difficult, the first 15 tests were devoted to vane shear tests and single pile tests (with 2 trial lateral tests). This established a relationship between S_u at the pile mid-depth and single pile capacity that was used as a standard for judging subsequent tests. If the measured S_u of a particular model was above or below that of the prototype, the test was still valuable since these tests provided data on the relation between pile capacity and behavior and shear strength at the model scale being tested if the axial single pile capacity was correspondingly higher or lower. This concept of evaluating data will be further discussed in the next section, but here let it suffice to say that

Table 5. Summary of Testing Program.

Test No.	No. of vane tests	S_u at pile middepth	g level	Axial load test (single)	Axial load test (group)	Lateral load test	Load transfer (single)	Load transfer (group)	Moment vs. depth (lateral)
1	4	2.3	70	No displacement					
2	3	1.6	70	No displacement			X		
3	4	2.0	70	Good			3/5		
4	1	2.0	70	Good			4/5		
5	1	2.35	70	Good			3/5		
6	1	1.9	70	Good			4/5		
7	2	2.0	70	X					
8[1]	1	2.4	70	Good			3/5		
9[2]	2	2.1	70						
10[3]			70	X		Good			
11[4]	X		70						
12	2	3.0	70	No displacement		Good			
13	1	2.8	70	No displacement			4/5		
14[5]	2	very high	70						
15	1	2.35	70	Good		Good	5/5		4/5
16	1	2.75	50	Good		Good	3/5		3/5
17	1	2.45	70	No displacemt.	No displacemt.		3/5	14/20	
18	1	1.7	100	Good	Good				
19[5]	1	very high	70						
20	1	2.35	50	Good		Good	5/7		5/7
21	1	3.2	100	Good	Good				
22	1	1.8	70	Good	Good		4/5	14/24	

Legend:

A blank space indicates that the particular measurement in question was not attempted.

"No displacement" indicates that an ultimate load was measured.

"Good" indicates that the measurement was successfully made

"X" indicates that the measurement failed due to an equipment malfunction.

"3/5" indicates that 3 of 5 strain gauge signals were successfully recorded.

Notes:

1. Specimen No. 8 dried out to such a degree that its results are deemed useless.
2. Specimen No. 9 was devoted to vane testing only
3. The vane apparatus was not available for test No. 10 as it was being serviced.
4. An accident during vane testing prevented further testing on No. 11.
5. Specimen Nos. 14 and 19 were so stiff that no further testing was performed on them.

it was the reason for the large number of 70 g tests where only single pile tests were performed.

After the pile capacity S_u relationship was established, testing was conducted on 2 each of 50 g, 70 g, and 100 g specimens. The 50 g tests (nos. 16 and 20) involved single piles loaded both axially and laterally. The 70 g tests (nos. 17 and 22) involved single pile and pile group tests. The 100 g tests (nos. 18 and 21) also involved single pile and pile group tests. Specimen 19 was not tested as the vane strength proved too high to be of any value.

As can be seen in Table 5, a number of tests provided little or no useful data, for a variety of reasons. These were numbers 7, 8, 10, 11, 14, and 19. Also test number 9 was prepared for vane testing only, to resolve problems and doubts with that process, so no pile testing data was obtained from it.

6.2 Discussion of Results

All results are presented in graphic form in Appendices 1 through 3. All measured data are presented as prototype quantities by applying the scaling factors in Table 1. Pertinent parts of these appendices are presented along with this discussion as appropriate.

6.2.1 Determination of Undrained Shear Strength

Measurement of S_u proved quite successful with the equipment described in Chapter 4. Results from each test were internally consistent, and indicated a slope of the S_u profile consistent through all tests. These characteristics are illustrated in Figure 19. Because of these facts, only one vane shear test was performed on later specimens, and the previously established slope was applied to the one measured point. Occasionally an extra test was done if there was some question about the accuracy of the first measurement.

6.2.2 S_u vs. Single Pile Capacity

As previously stated, exact reproduction of the S_u profile of the prototype proved difficult. The desired S_u at pile mid-depth was 2.4 ksf (115 kPa) (O'Neill et al., 1980) but the measured value for the model tests

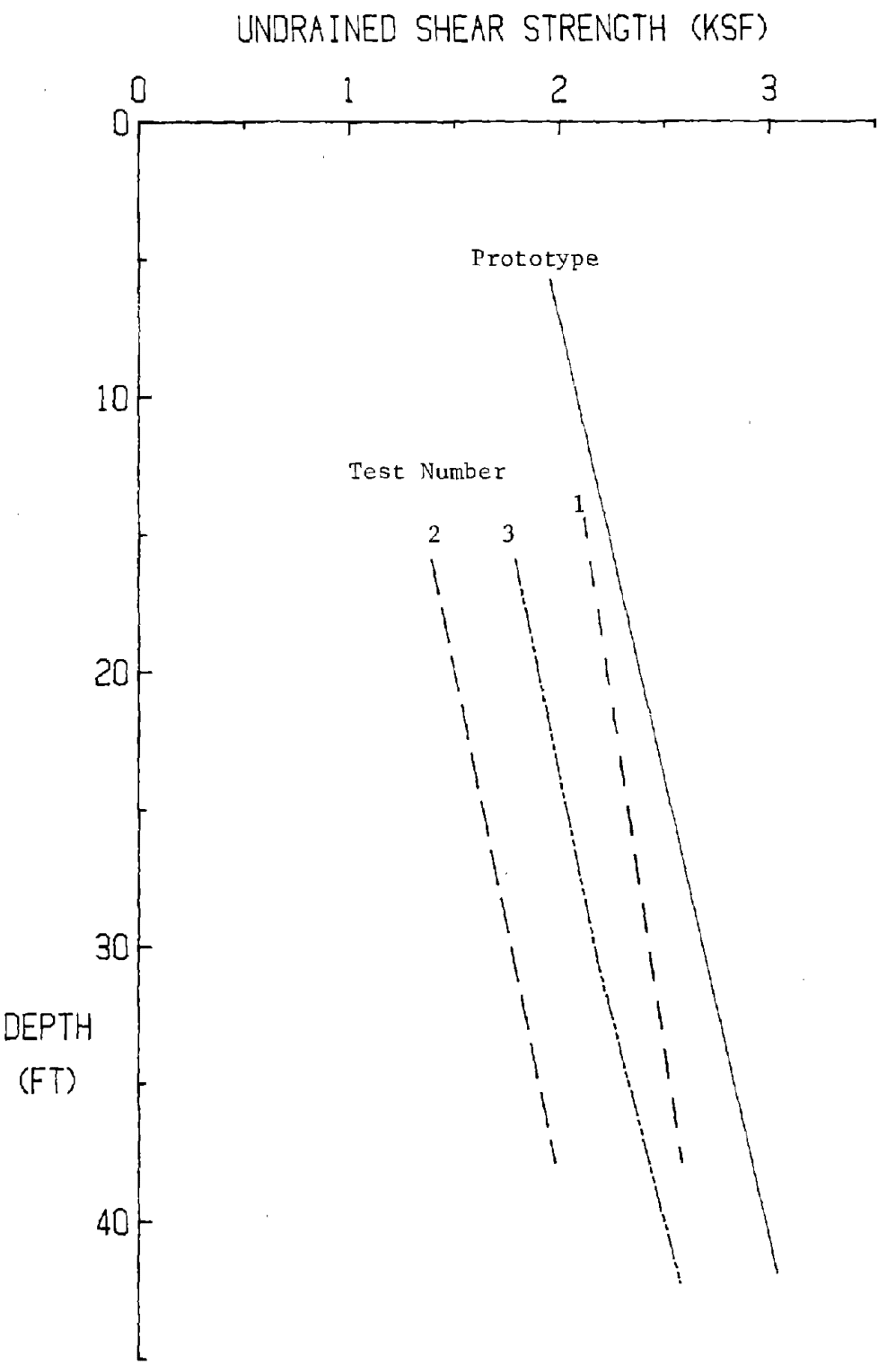

Figure 19. S_u profiles for initial tests (1 **ksf** = 47.9 **kPa**; 1 ft = 0.305 m)

generally varied from about 1.9 ksf (91 kPa) to 2.9 ksf (139 kPa). For this reason an experimental relationship was established between S_u at mid-depth and single pile capacity. This is illustrated in Figure 20. It should be noted that the prototype constitutes one point on the curve. When the S_u of the model was similar to that of the prototype, the single pile capacity also compared quite favorably to that of the prototype. When the S_u was higher or lower, the single pile capacity conformed closely with the relationship in Figure 20. This result is thought to establish amply the credibility of the centrifugal method for modeling the axial capacity of single piles for this prototype.

6.2.3 Group Capacities and Group Factors

Four group tests were performed, 2 each at 70 g and 100 g. Table 6 lists capacities from each test, both single and group, along with group factor. The group factor for the prototype was found to be approximately 0.98 (O'Neill et al., 1980). As shown in the table, that, for the four tests, compares well with this, with the most variation occurring with test 21 which had a group factor of about 1.04. This can probably be explained by the higher degree of irregularity incurred during installation of this group. Some degree of geometric irregularity was induced during the installation of all groups, but that induced in test no. 21 was the most severe. Post test excavation revealed that for this test the tips of the piles had wandered horizontally several diameters from their driven position and that several piles were touching each other at pile tip depth.

6.2.4 Load Transfer Data

Axial load transfer data obtained was very consistent through all tests. A typical load transfer curve is shown in Figure 21. All piles were essentially friction piles with only 10 to 20 percent of the total load being taken by the tip. The remaining 80 to 90 percent of the total load was transferred fairly uniformly throughout the length of the pile, resulting in the essentially linear transfer function shown in Figure 21.

Load transfer within pile groups was very similar to that measured for single piles, which would be expected as the group factors were very close to unity. Measurement of top loads in individual piles during group tests proved difficult due to bending stresses incurred during the capping of the group.

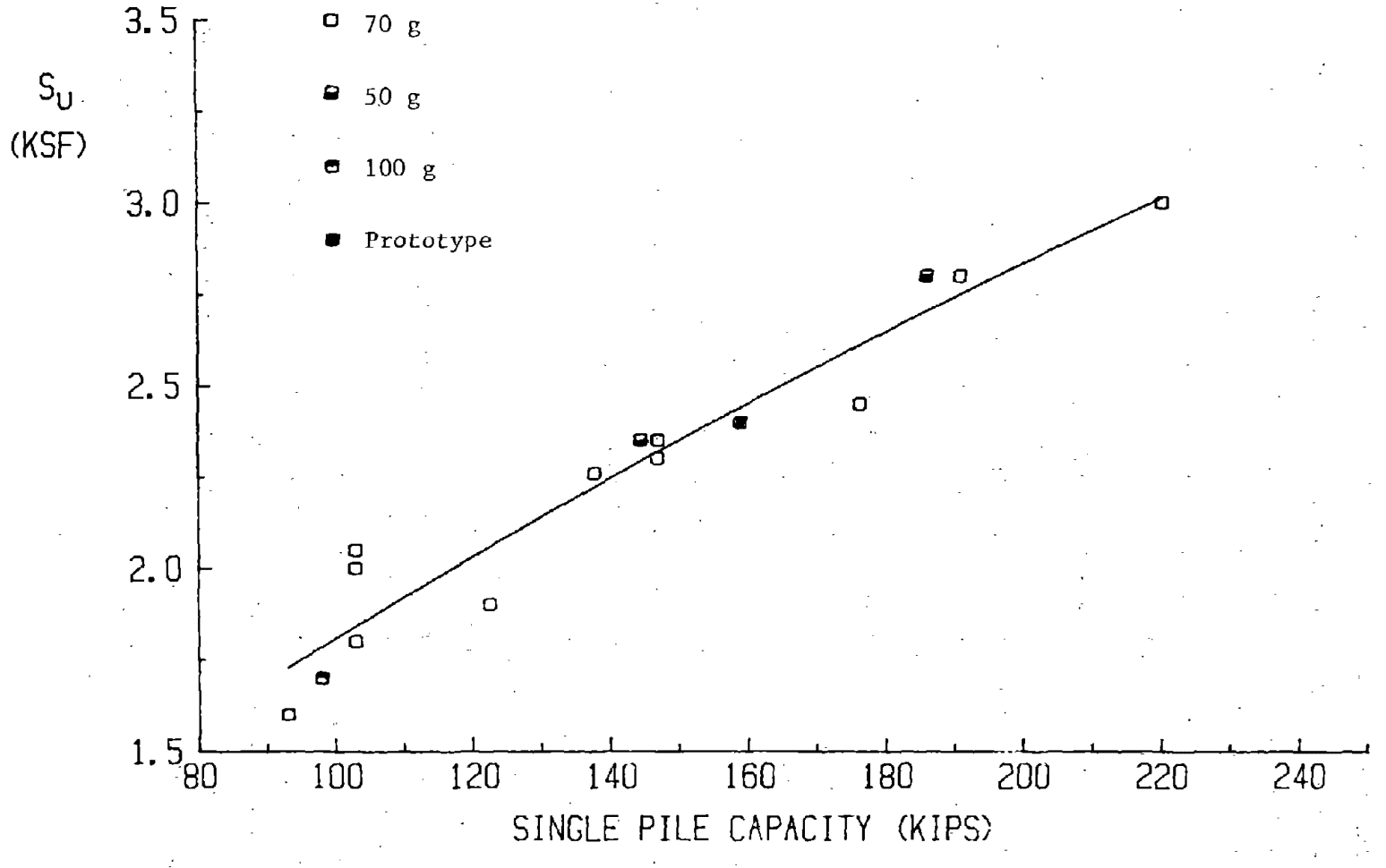

Figure 20. S_u vs. single pile capacity (1 ksf = 47.9 kPa; 1 KIP = 4.45 KN)

Table 6. Group Test Data.

Test No. g Level	17 70	18 100	21 100	22 70	Prototype 1
S_u at pile middepth, KSF	2.45	1.7	3.2	1.8	2.4
Single pile capacity, KIPS	176	98	330	104	160
Pile group capacity, KIPS	1520	850	3100	940	1140
Group factor	0.96	0.96	1.04	1.00	0.98

Conversion factors: 1 ksf = 47.9 kPa, 1 KIP = 4.45 KN

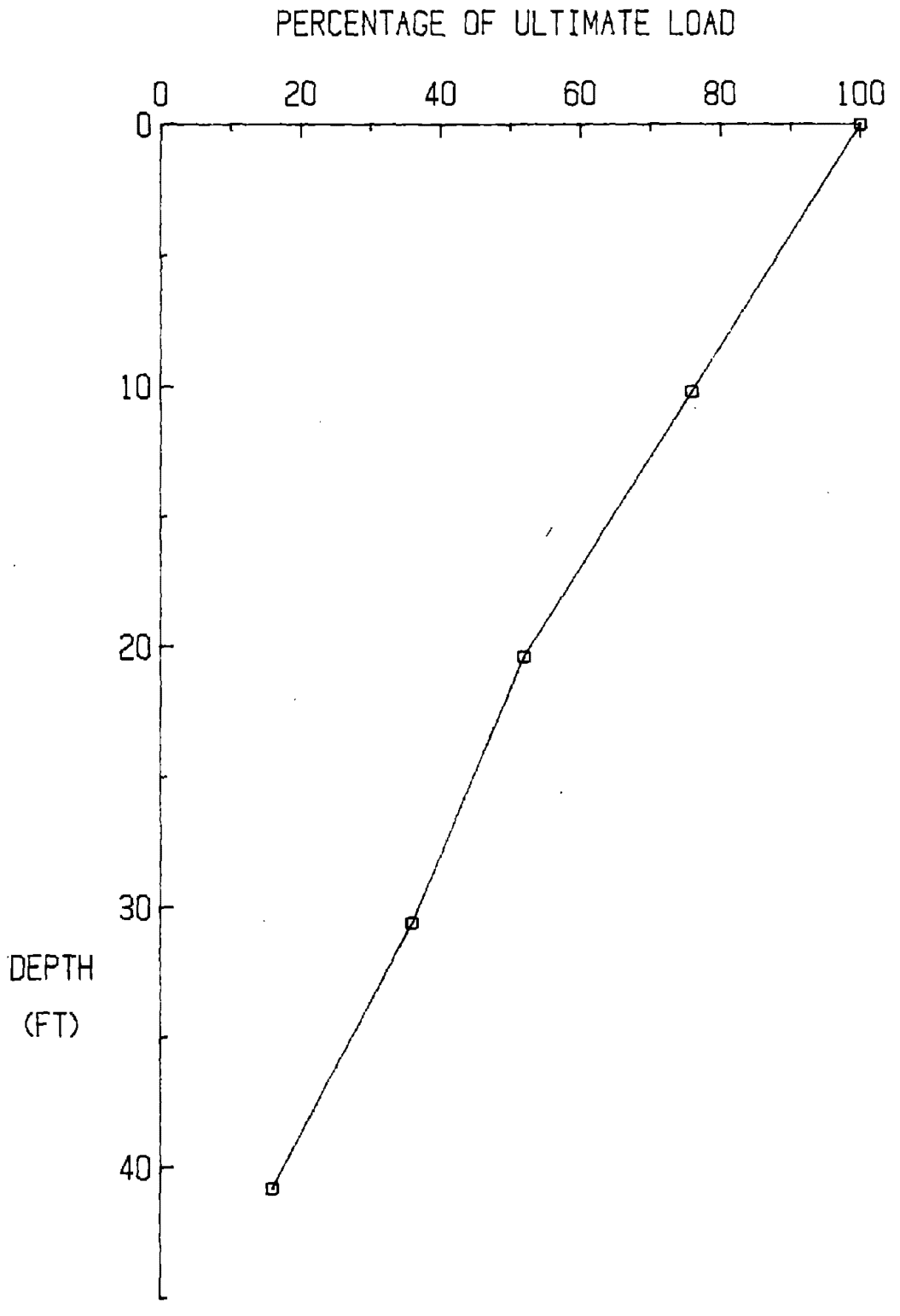

Figure 21. Typical load transfer curve (1 **kip** = 4.45 KN; 1 ft = 0.305 m)

The load-transfer measured in the prototype is very similar, and Figure 22 is provided for comparison. The only appreciable difference is in the top 10 ft (3 m) of the pile and is most likely due to the fact that the prototype piles were driven into 10 ft deep preaugered holes (O'Neill et al., 1980). This was attempted with the model, but the resulting holes were essentially produced by displacement, rather than augering, which doubtlessly affected the load transfer characteristics. All load-transfer curves are presented in Appendix 2.

6.2.5 Load-Displacement Characteristics

Load-displacement curves are not available for all tests as various problems were experienced with the LVDT used to measure displacements during load testing. Curves were obtained successfully, however, in well over half the tests, and several are presented in Figures 23 (single pile) and 24 (pile group) for comparison with prototype results. On the whole, the comparison seems good, with a slight tendency on the part of the model to show a stiffer response in the single pile tests. This may be attributed to two factors, the first being the preaugered holes used in the prototype as already discussed. The other is related to the axial stiffness of the model pile being greater than that of the prototype. As discussed in Chapter 4, the model piles were dimensioned according to the lateral stiffness (EI), rather than the axial stiffness. An exception to this observed behavior is the performance of the 50 g single pile tests. Here, the load displacement curves showed a noticably softer response than the prototype, although the ultimate capacities compare well. Load-displacement curves for all tests are presented in Appendix 3.

6.2.6 Lateral Load Behavior

Although no lateral loading data was available from the prototype, lateral load tests were performed on 5 model specimens. Load-displacement curves are shown in Figure 25 and are fairly consistent with the measured shear strength of their respective specimens. Some scatter is caused by the fact that the distance above the ground surface at which the load was applied was not very consistent between tests. This occurred because axial tests were performed prior to lateral tests, and it was not often easy to control the depth of penetration during failure of the pile under axial loading.

A representative moment vs. depth curve was obtained from specimen no. 20 and this is presented in Figure 26. One can see that the maximum moment

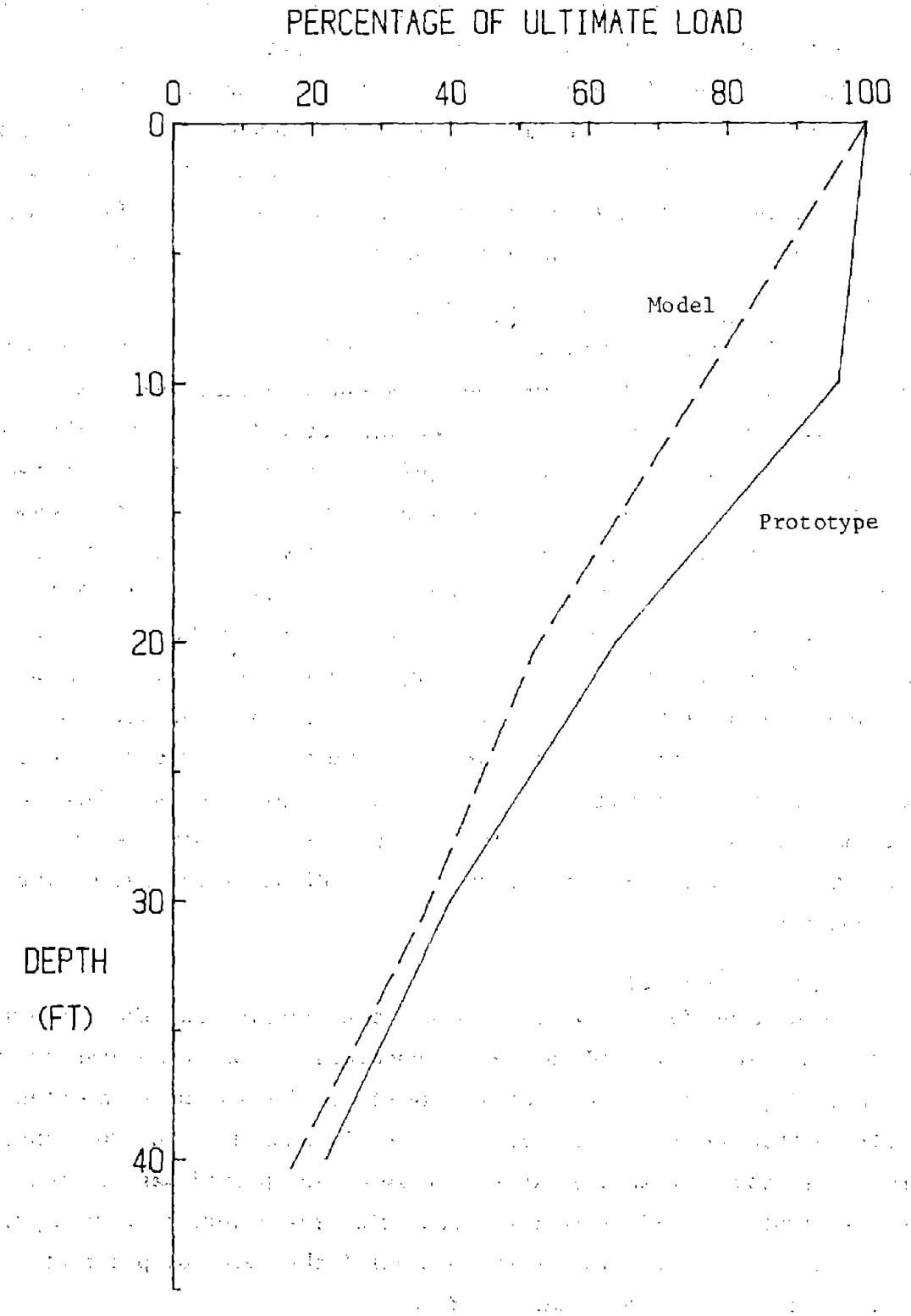

Figure 22. Load transfer curves from model and prototype (1 kip = 4.45 KN; 1 ft = 0.305 m)

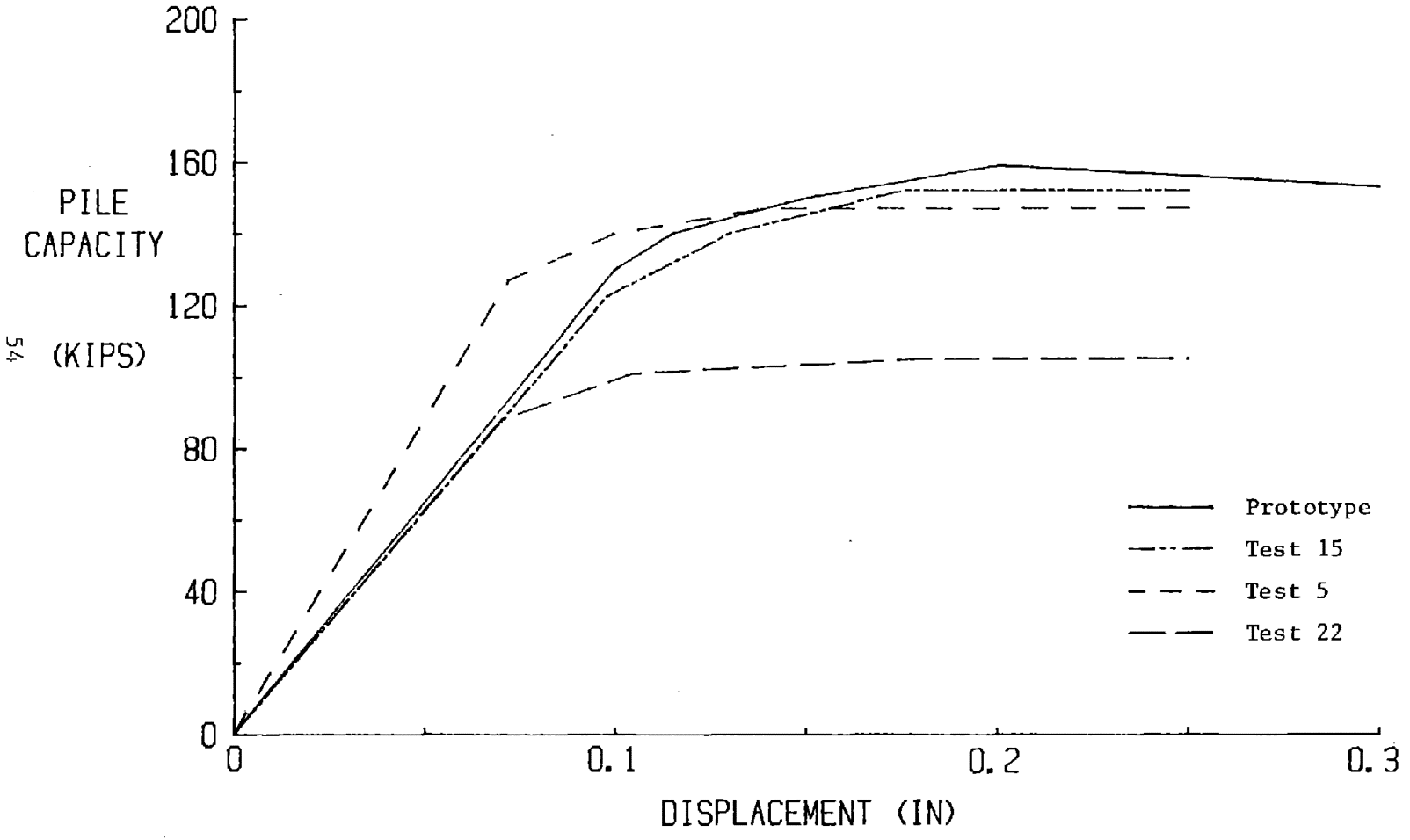

Figure 23. Load deflection curves, single piles (1 **kip** = 4.45 KN; 1 in = 2.54 cm)

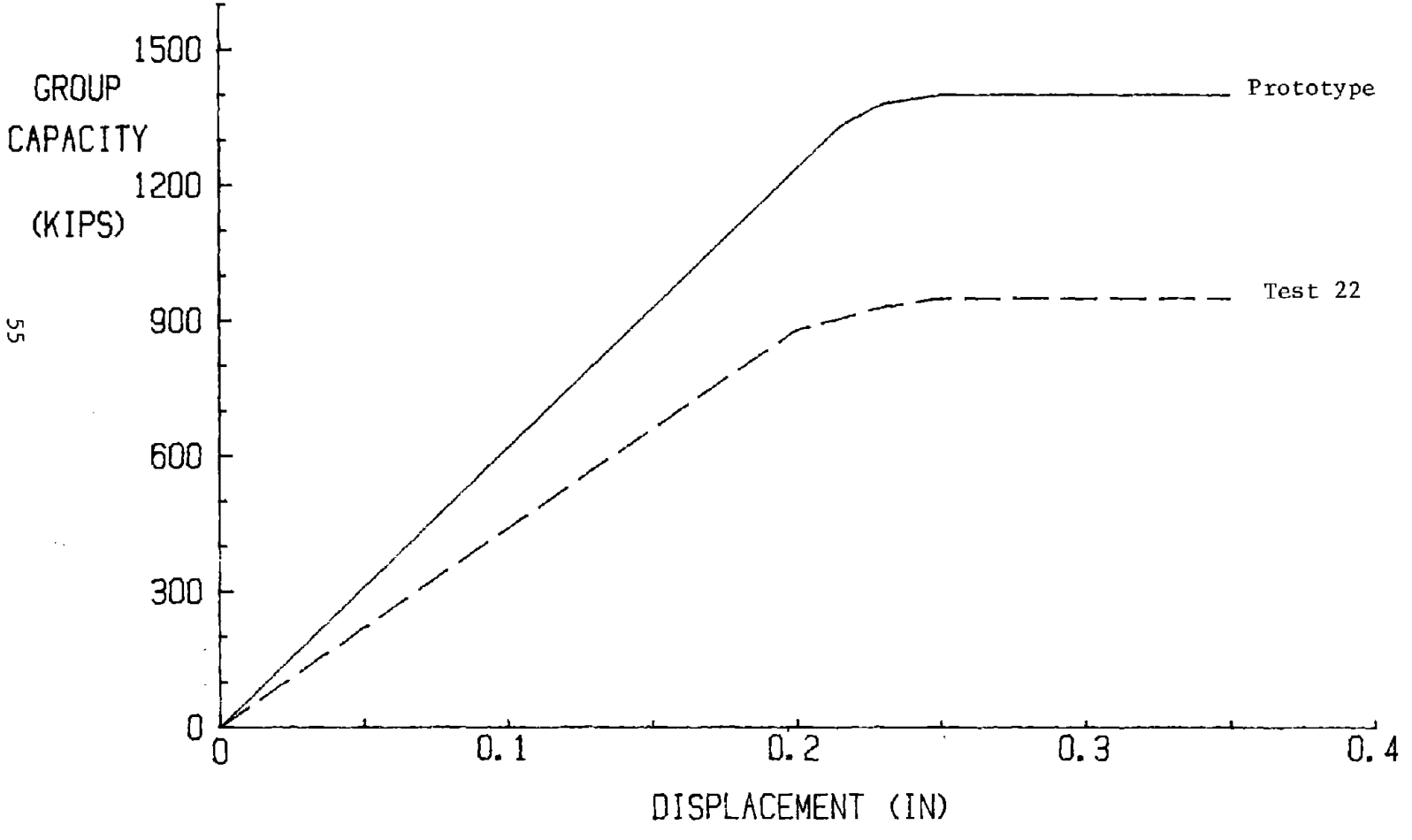

Figure 24. Load-deflection curves, group (1 **kip** = 4.45 KN; 1 in = 2.54 cm)

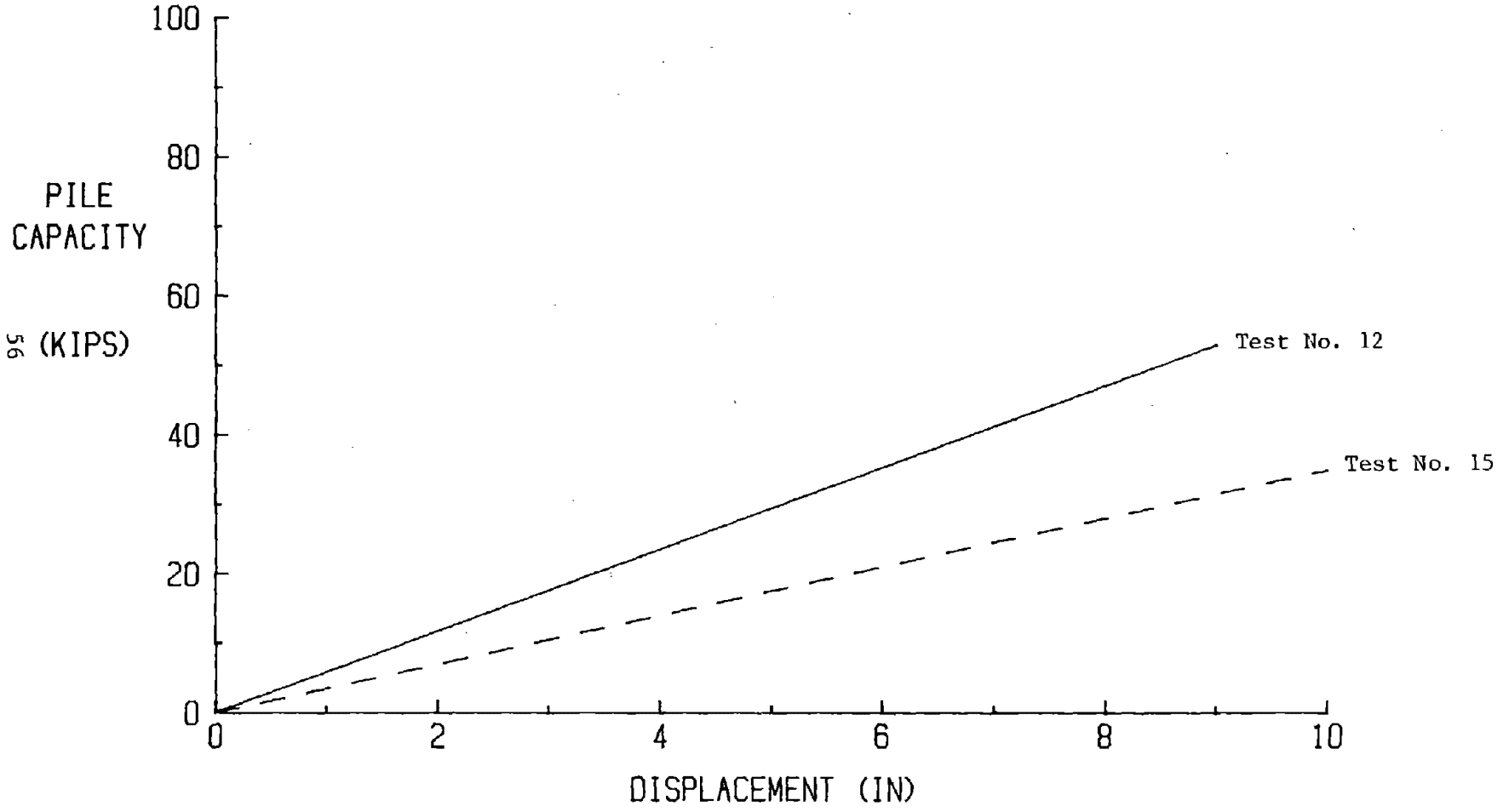

Figure 25. Lateral load-displacement curves (1 kip = 4.45 KN; 1 in = 2.54 cm)

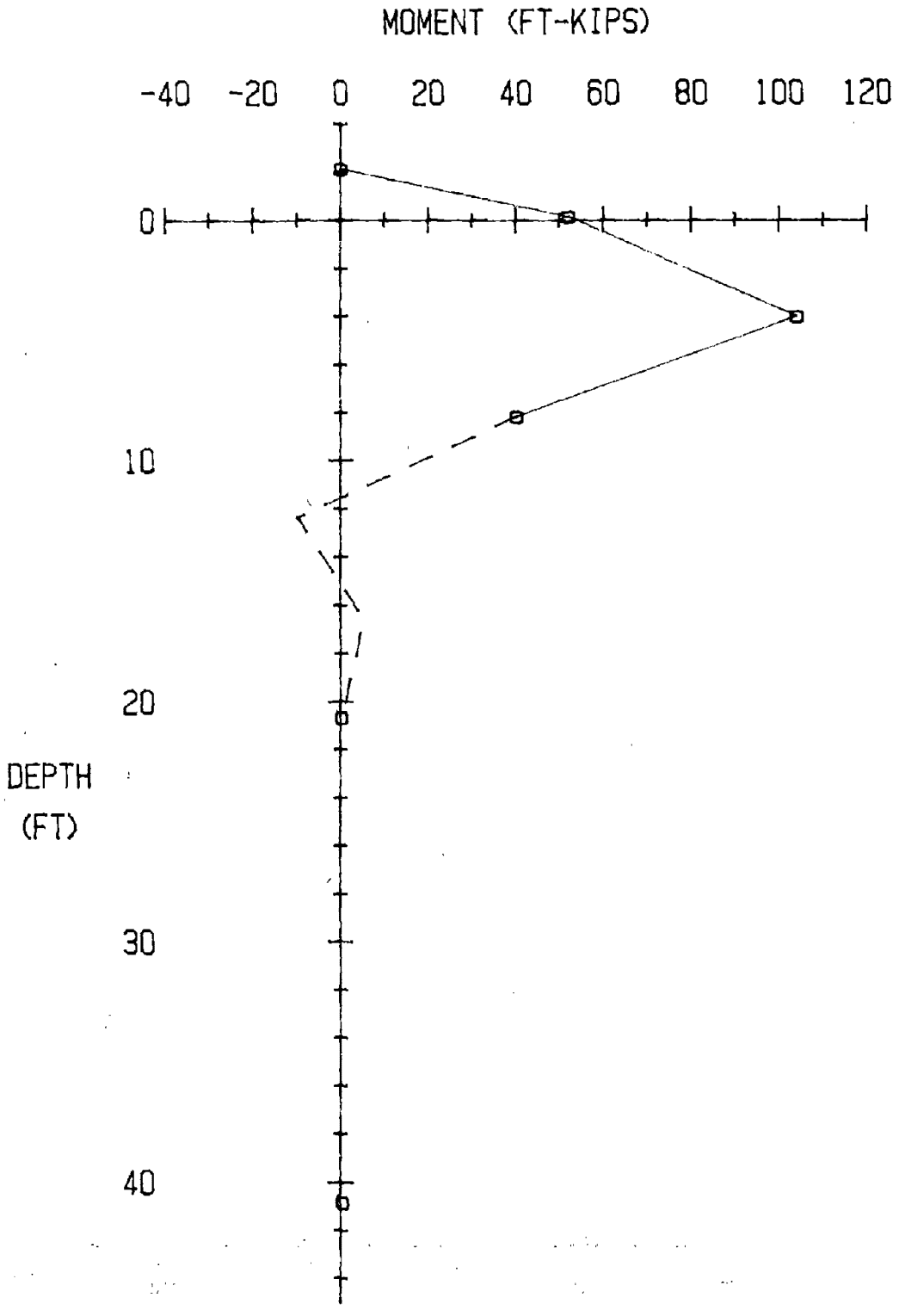

Figure 26. Moment vs. depth curve, from model test (1 ft-kip = 1.36 m-KN; 1 ft = 0.305 m)

occurs at a depth of approximately 9 feet in the prototype. These lateral load tests are thought to show that the centrifugal approach is applicable as well to modeling lateral loading conditions.

6.2.7 Modeling of Models

As has been stated, 2 each 50 g and 100 g tests were performed to verify the similitude relations internally, that is, independent of the prototype. It was found that both the 50 g and 100 g tests agreed quite well with the 70 g tests. This is best illustrated in Figure 20, where S_u at mid-depth and single pile capacities are plotted in prototype scale for 50 g, 70 g, and 100 g tests. All points fall on or reasonably near the curve. Modeling of models for groups is verified in Table 6, as the group factors at 70 g and 100 g are compatible.

The only exception is the load-displacement curves for the 50 g tests. Although the capacities conform well, the curves are much less steep than the 70 g and 100 g single pile tests.

CHAPTER 7. ANALYSIS

7.1 The Use of Model Tests in Developing Analytical Techniques

As discussed in the introduction, confidence among modern engineers in the ability of analytical techniques to predict pile behavior is not overwhelming. Certainly the lack of data available on behavior of piles and pile groups contributes to this uncertainty. Development of an accurate computer model is difficult to nearly impossible without accurate, comprehensive data for all conditions to which the model is applicable. It then seems feasible that centrifugal model tests could be used as a data base for development of analytical models. If so, data for a wide range of soil types, pile geometries, and loading conditions could be generated and used at a fraction of the cost of generating the data from full scale field tests.

Another related possibility is the use of model test data to calibrate a computer model. Often an analytical technique may be theoretically correct, but it may require that certain variables be input that are difficult to quantify without expensive field tests. Results from centrifugal model tests can be used to back-calculate these input variables for a variety of conditions, and thus avoid or at least reduce the effect of a major fault with many analytical techniques.

These concepts were demonstrated through the use of a program called PILGPI (Ha and O'Neill,1981) developed at the University of Houston. PILGPI models single pile behavior by a finite difference approach, and extends this to pile groups by a solution of Mindlin's equation (Ha and O'Neill,1981).

7.2 Axial Behavior

In analyzing axial load behavior using PILGPI, pile geometry and properties, loading conditions, soil properties, Q-z curves, and f-z curves must be input. F-z curves relate unit shear stress from skin friction mobilized at a point along the shaft of the pile to deformation at that point. The Q-z curve is the load-deformation curve for the pile tip. Soil properties here are only the elastic properties of the soil and are used to calculate group effect. All other soil properties are inherent in the f-z curves and Q-z curves.

7.2.1 Determination of f-z and Q-z Curves

Centrifuge model tests can be used to produce f-z curves if load-transfer data and pile head displacements are recorded. The f value over a particular section of a pile can be determined for a given applied load by Equation 7.1, where P_1 is the shaft load at the top of that section, P_2 is the shaft load at the bottom of the section, and A is the exposed area of the pile at the section.

$$f = \frac{P_1 - P_2}{A} \tag{7.1}$$

For the tests described here, the load transfer was essentially linear, so f-values are constant through the depth of the pile for a given load.

The z value that corresponds to the f value given by Equation 7.1 can be easily obtained by Equation 7.2, where z_H is the displacement of the pile load in relation to the ground (as measured in the load deformation test) and Δ is the elastic deformation of the pile between the head and the point where the z value is needed.

$$z = z_H - \Delta \tag{7.2}$$

To determine Δ, the load in the pile (P) is described as a function of depth, x, such that $P = f(x)$. Then imagine a small differential length of the pile, dx. The deformation (Δ_i) of the differential length dx is given by Equation 7.3, which is derived from Hooke's Law.

$$\Delta_i = \frac{Pdx}{AE} \tag{7.3}$$

P is the load in the pile at the center of segment dx, and A and E are the cross sectional area and Young's modulus of the pile, respectively. The deformation, Δ, then of the entire pile above a depth D can be obtained by Equation 7.4.

$$\Delta = \int_0^D \frac{Pdx}{AE} \tag{7.4}$$

Recall that P = f(x), so Equation 7.4 is integrated with respect to x. f-z curves at the pile head and at the tip from the model tests are given in Figures 27 and 28. PILGP1 interpolates linearly to obtain f-z curves for all points in between.

The Q-z curve for a pile is also easily obtained. The Q value is merely the load taken by the tip of the pile. The z value is calculated in the same manner as that for the f-z curves. The Q-z curve from the model pile test is given in Figure 29.

7.2.2 Results

The predicted load-displacement curves for single pile and pile groups using PILGP1 are shown in Figures 30 and 31. The results from a representative model test (test number 22) are plotted with them for comparison. The single pile prediction is quite reasonable up to the yield load, which would have to be expected if the f-z curves were properly calculated. The discrepancy after yield may be explained by the fact that the program was executed at the model scale (1/70th). The program, when executed with the same data at prototype scale, yielded good results (O'Neill et al., 1981), even after yield.

The pile group prediction (Figure 31) is somewhat in error, even though the single pile behavior is accurate. Some group effect is obviously predicted, whereas the model tests (as well as the prototype) all show little or no group effect. One might conclude that the linear elastic solution to Mindlin's equation is not an entirely satisfactory method for predicting pile-soil interaction in the case of pile groups.

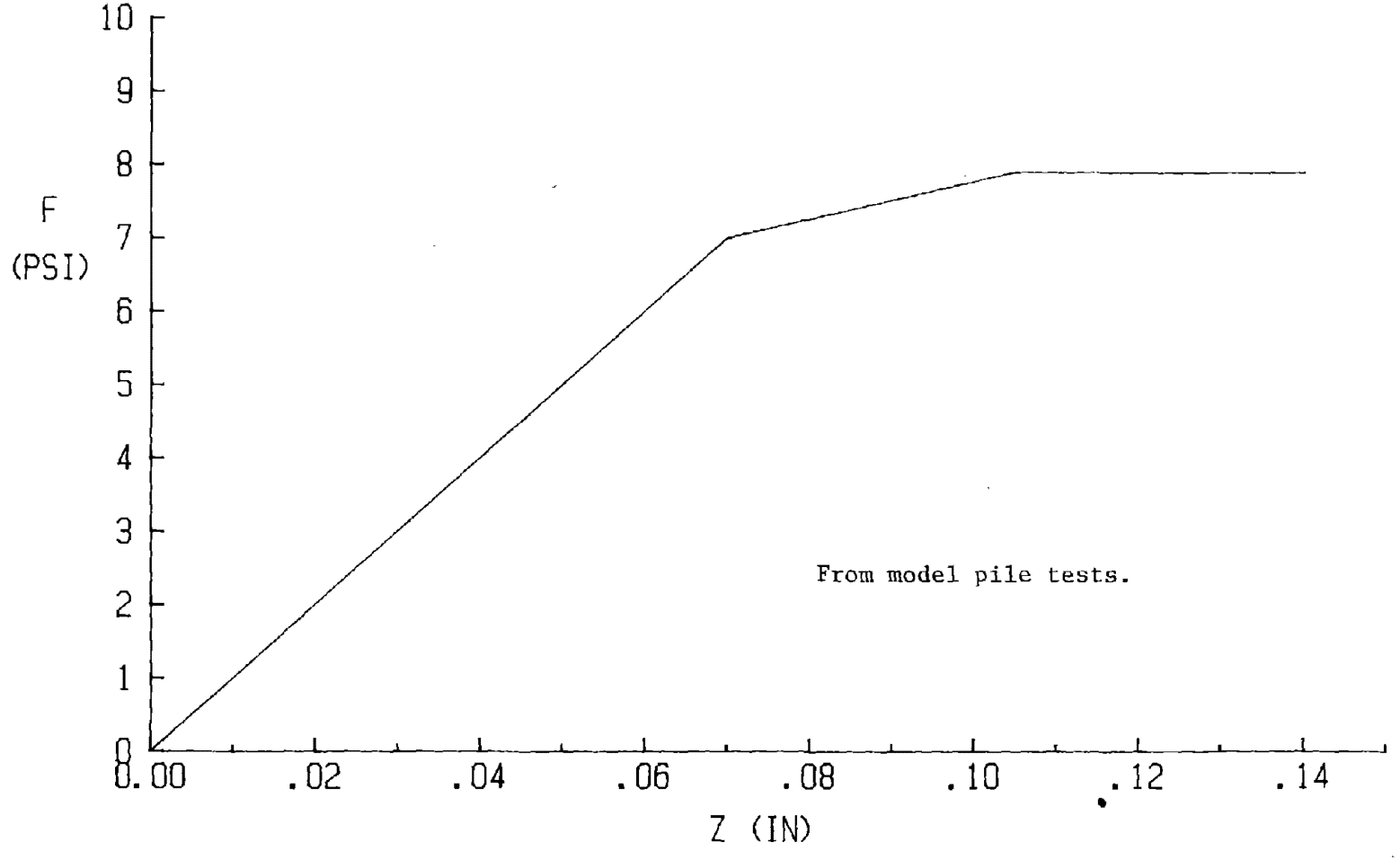

Figure 27. Unit skin friction vs. deflection, pile head (1 psi = 6.9 kPa; 1 in = 2.54 cm)

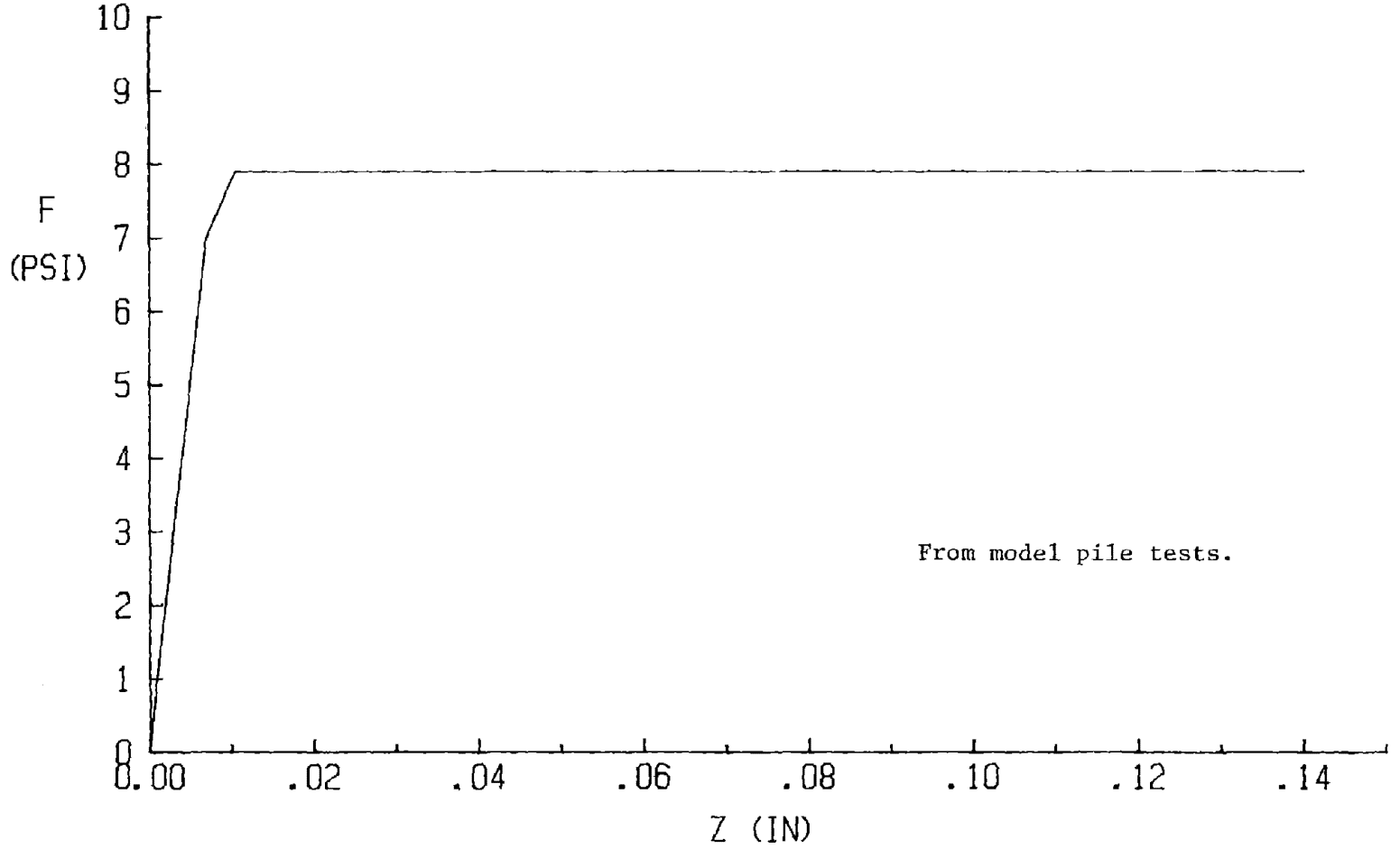

Figure 28. Unit skin friction vs. deflection, pile tip (1 psi = 6.9 kPa; 1 in = 2.54 cm)

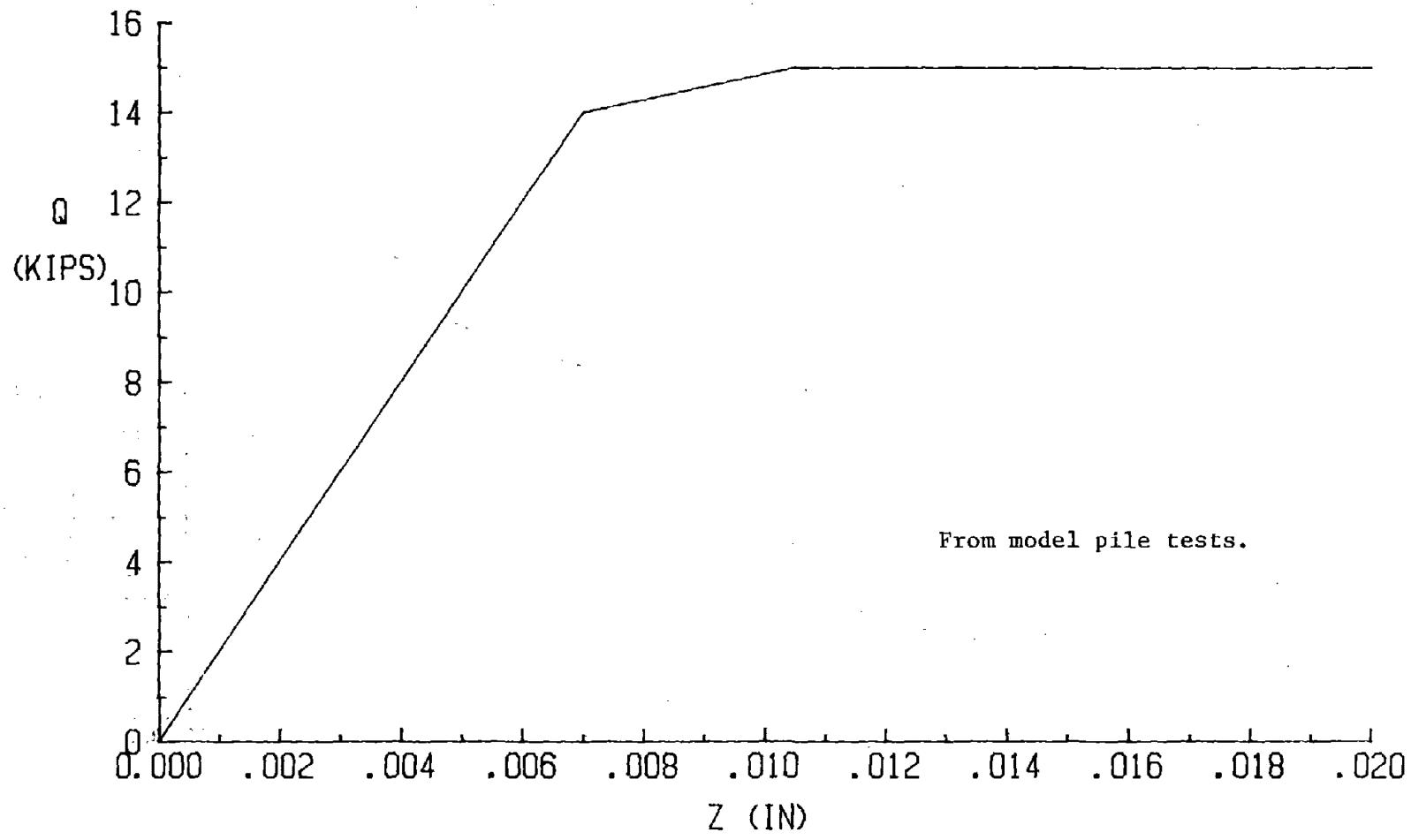

Figure 29. Tip load vs. deflection (1 **kip** = 4.45 KN; 1 in = 2.54 cm)

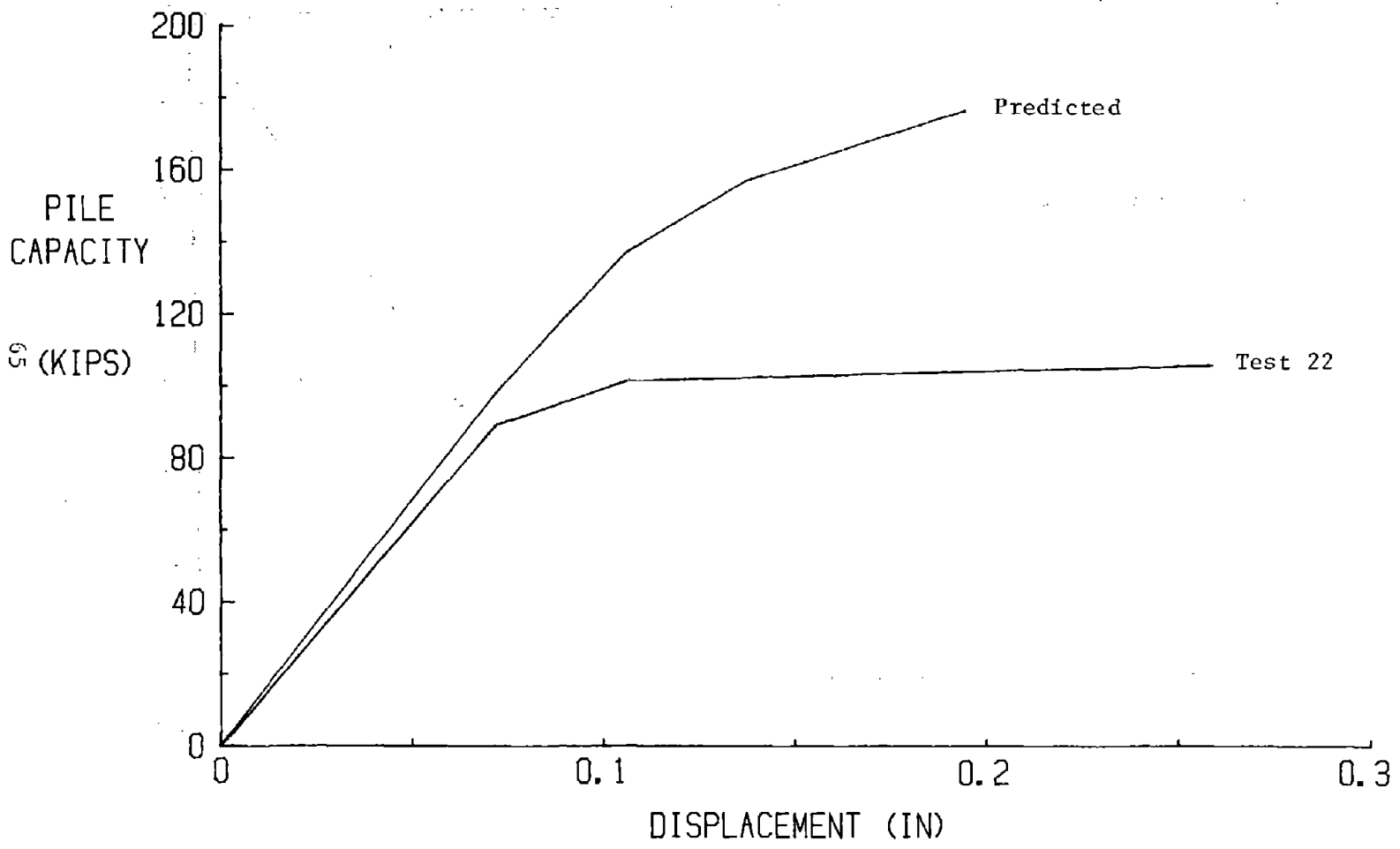

Figure 30. Single pile load-displacement as predicted by PILGP1 (1 kip = 4.45 KN; 1 in = 2.54 cm).

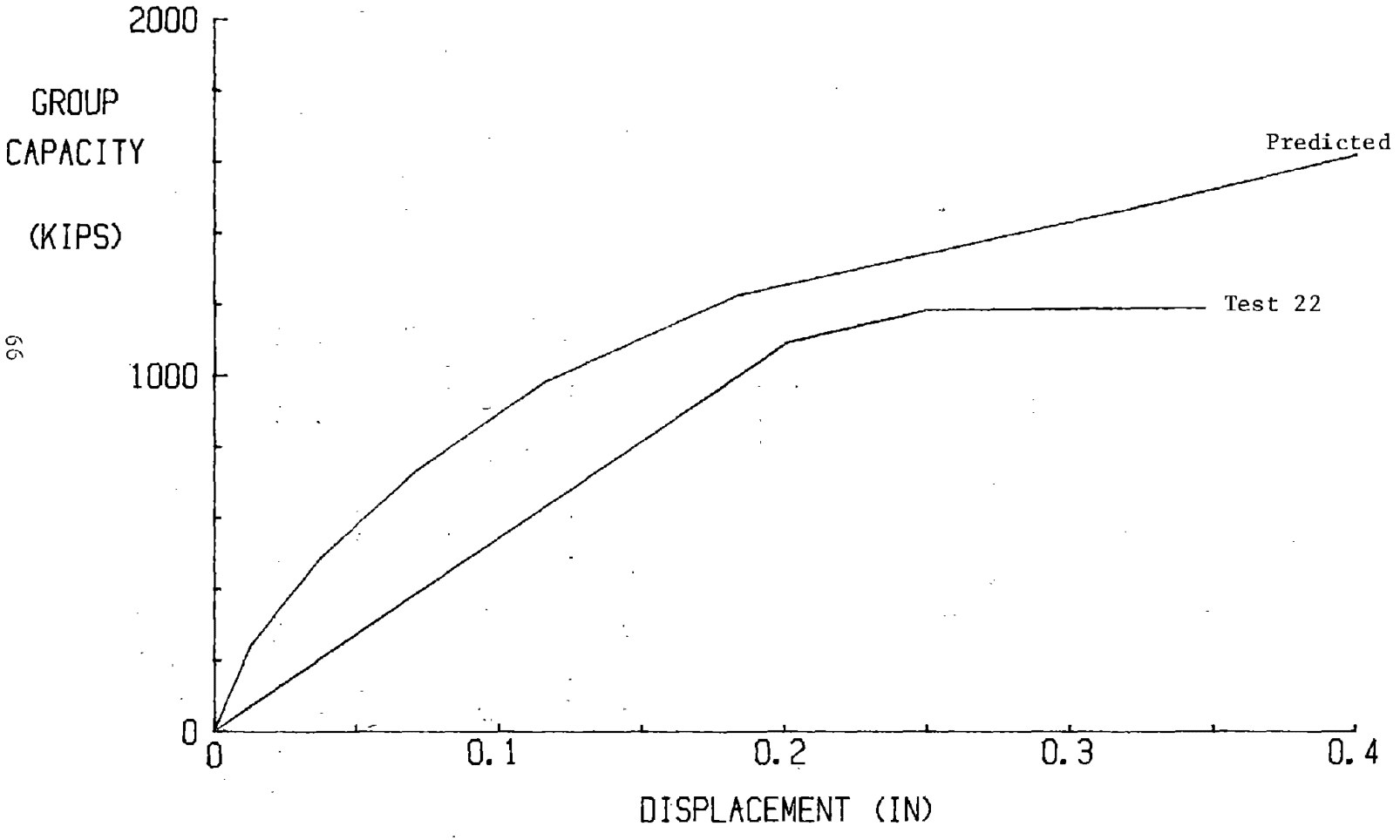

Figure 31. Pile group load-displacement as predicted by PILGP1 (1 kip = 4.45 KN; 1 in = 2.54 cm).

CHAPTER 8. CONCLUSION

8.1 Summary of Work Performed

The results of the work described by this report as discussed in Chapter 6 are thought to demonstrate the applicability of the centrifugal method to modeling of pile foundations in clay for the prototype in question. The capacity of single piles and pile groups as related to the undrained shear strength profile compares well with the prototype (Figure 20). The load transfer curves as shown in Figure 22 also provide a good comparison, with the slight discrepancies discussed in Chapter 6. The load-displacement curves as recorded and shown in Figures 23 and 24 are reasonably close to the prototype behavior, with a tendency of the single pile tests to show a somewhat stiffer response than the prototype. Possible causes for this discrepancy are suggested in Chapter 6.

8.2 Problems Encountered

Several problems encountered during the testing program have already been mentioned. Possibly the one which prolonged the testing program the most was the uncertainty encountered in reproducing the desired undrained shear strength profile. This caused some of the tests performed to be of little value. A more certain procedure of reproducing the S_u profile would certainly have made the testing program more productive.

The method used for capping the driven piles in the case of group test led to problems. Rather than casting a cap to the piles as is the practice in the field, the cap was bolted to the piles, as time restraints and the desire to reuse the test piles ruled out any cast or epoxied cap. Despite efforts to insure that the piles were driven in the proper configuration, some bending moment was undoubtedly induced in installing the pile cap. This bending moment made load transfer measurement near the pile top difficult. It also undoubtedly affected to some degree the behavior of the pile group.

Another problem encountered is related to the actual size of the instrumented model piles. The relative size of the strain gauges in relation to the pile itself limits the number of gauges that can be installed along the

length of the pile, and thus indicates restraints on the minimum spacing between gauges. Large spaces between gauge stations are not an exceptional problem with axial loading, especially if the load transfer curves are fairly linear as in this case. It does present a problem in the case of lateral loading, however, as the moment typically increases quickly with depth to a peak and then falls off. Large spaces between gauge stations can cause inaccuracy in estimating both the location and magnitude of the maximum moment.

Finally, problems endemic to all centrifuge testing certainly exist. The variation of gravity with depth has already been discussed in Chapter 2. Another point which bears mentioning is that instrumentation often does not function well in the high gravity environment induced in the centrifuge. This problem is most apparent in the load transfer data, where it was very difficult to maintain balance in the one-half Wheatstone bridges.

8.3 Recommendations for Future Research

In any research activities undertaken in the future with regard to centrifugal modeling of pile groups in clay, attention should be given to the problem addressed in the previous sections. Particular attention should be given to developing better methods of duplicating the prototype S_u profile and capping the pile group. The problem associated with the actual size of the model pile can be reduced by using as large a model (as low a gravity) as is possible. The variable gravity field is unavoidable but it will be much less severe in a large radius centrifuge.

In future studies undertaken to verify the concept of centrifugal modeling as applied to pile groups in clay, efforts should be made to obtain prototype results in which there is a definite group effect. The adequacy of the centrifugal method remains unverified for this situation.

REFERENCES

Atkinson, J.H. and Bransby, P.L. (1978), The Mechanics of Soils, McGraw-Hill Book Company (UK), Ltd., London.

Bucky, P.B. (1931), "The Use of Models for the Study of Mining Problems," Transactions of the American Institute of Mining Engineers, 96.

Bucky, P.B., Solakian, A.G., and Baldwin, L.S. (1935), "Centrifugal Method of Testing Models," Civil Engineering, ASCE, 5(5), pp. 287-290.

Bucky, P.B. and Taborelli, R.J. (1938), "Effect of Immediate Roof Thickness in Long Wall Mining as Determined by Barodynamic Experiments," Transactions of the American Institute of Mining Engineers, 130, pp. 314-332.

Cargill, K.W. (1980), "Centrifugal Modeling of Transient Water Flow in Earth Embankments," M.S. Thesis, Department of Civil Engineering, University of Colorado, Boulder, Colorado.

Croce, P. (1982), "Evaluation of Consolidation Theories by Centrifugal Model Tests," M.S. Thesis, Department of Civil Engineering, University of Colorado, Boulder, Colorado.

Ferguson, K.A. (1980), "Centrifugal Modeling of the Quasi-Static Zone Penetrometer," M.S. Thesis, Department of Civil Engineering, University of Colorado, Boulder, Colorado.

Fumagalli, E. (1973), Statical and Geomechanical Models, Springer-Verlag, Wien.

Ha, H.B. and O'Neill, M.W.(1981), "Field Study of Pile Group Action (Appendices)," FHWA Report RD-81/003 and RD-81/004.

Hougnon, J.H. (1980), "Centrifugal Modeling of Axially Loaded Piles," M.S. Thesis, Department of Civil Engineering, University of Colorado, Boulder, Colorado.

Kim, M.M. (1980), "Centrifugal Model Testing of Soil Slopes," Ph.D. Thesis, Department of Civil Engineering, University of Colorado, Boulder, Colorado.

Ladd, C.C. and Foote, R. (1974), "New Design Procedure for Stability of Soft Clays," Journal of the Geotechnical Engineering Division, ASCE, 100(GT7), pp. 763-786.

Lambe, T.W. (1954), Soil Testing for Engineers, John Wiley & Sons, Inc., New York.

Mayne, P.W. (1980), "Cam-Clay Predictions of Undrained Strength," Journal of the Geotechnical Engineering Division, ASCE, 106(GT11), pp. 1219-1242.

Mikasa, M. and Takada, N. (1973), "Significance of Centrifugal Model Test in Soil Mechanics," 8th International Conference on Soil Mechanics and Foundation Engineering, Vol. 1, pp. 273-278.

O'Neill, M.W.(1979), "Field Study of Pile Group Action (Interim Report)," FHWA Report No. RD-81/001.

O'Neill, M.W.,Hawkins, R.A. and Mahar, L.J. (1980), "Field Study of Pile Group Action (Final Report)," FHWA Report No. RD-81/002.

Pokrovsky, G. and Fedorov, I.S. (1936), "Studies of Soil Pressures and Soil Deformations by Means of a Centrifuge," 1st International Conference on Soil Mechanics and Foundation Engineering, Vol. 1, p. 70.

Popov, E.P. (1976), Mechanics of Materials, Prentice-Hall, Inc., Englewood Cliffs, N.J.

Poulos, H.G. and Davis, E.H. (1980), Pile Foundation Analysis and Design, John Wiley and Sons, Inc., New York.

Rocha, M. (1957), "The Possibility of Solving Soil Mechanics Problems by the Use of Models," 4th International Conference on Soil Mechanics and Foundation Engineering, 1, pp. 183-188.

Roscoe, K.H. (1968), "Soils and Model Tests," Journal of Strain Analysis, 3, pp. 57-64.

Saffery, M.R. and Tate, A.P.K. (1961), "Model Tests on Pile Groups in a Clay Soil with Particular Reference to the Behavior of the Group When it is Loaded Eccentrically," 5th International Conference on Soil Mechanics and Foundation Engineering, 2, pp. 129-134.

Schofield, A.N. (1980), "Cambridge Geotechnical Centrifuge Operations," 20th Rankine Lecture, Geotechnique, 30, pp. 227-268.

Scott, R.F. (1979), "Centrifuge Studies of Cyclic Lateral Load-Displacement Behavior of Single Piles," Report to American Petroleum Institute, OSAPR Project 8.

Skempton, A.W. (1957), "Discussion: The Planning and Design of the New Hong Kong Airport," Proceedings of the Institute of Civil Engineers London, 7, pp. 305-307.

Sowers, G.F. (1979), Introductory Soil Mechanics and Foundations: Geotechnical Engineering, Macmillan Publishing Co., Inc., New York.

Sowers, G.F., Martin, C.B., Wilson, L.L., and Fausold, M., "The Bearing Capacity of Friction Pile Groups in Homogeneous Clay from Model Studies," 5th International Conference on Soil Mechanics and Foundation Engineering, 2, pp. 155-159.

Vesic, A.S. (1977), "Design of Pile Foundations," National Cooperative Highway Research Program Pamphlet No. 42.

Whitaker, T. (1957), "Experiments with Model Piles in Groups," Geotechnique, 7, pp. 147-167.

APPENDIX 1

In this appendix, undrained shear strength profiles are presented as measured in-flight by the vane shear apparatus. Results from test nos. 9, 10, 11, 14, and 19 are not included as either the equipment malfunctioned or the specimens were too stiff to allow proper measurement of S_u.

Actual measurements (at a given depth) are denoted by circles. After the initial specimens established a fairly constant slope to the S_u profile, usually only one vane shear test was performed per specimen. The previously established slope was then applied to this point.

These profiles are presented in Figures 32 through 48.

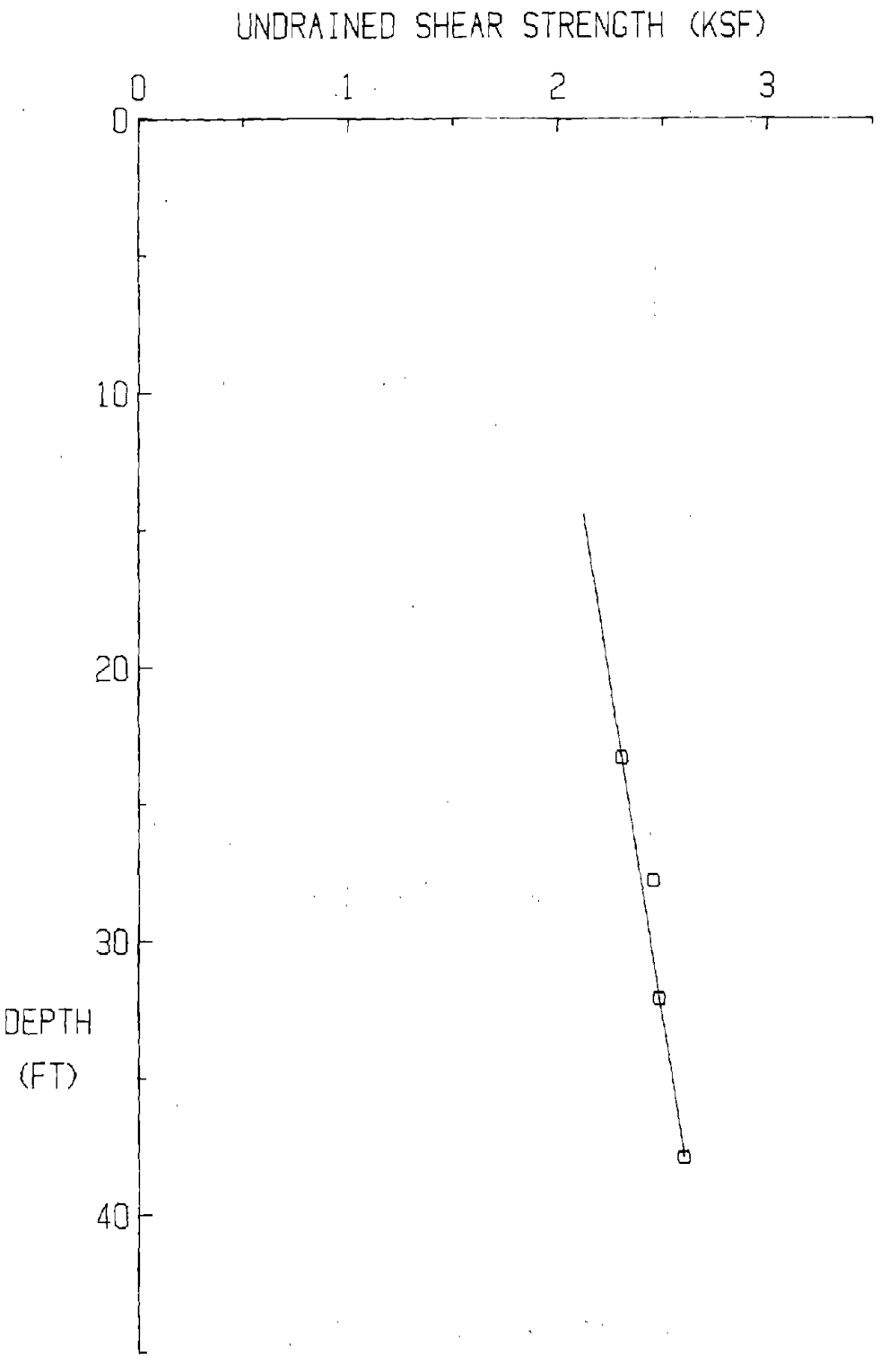

Figure 32. Test 1, S_u profile (1 ksf = 47.9 kPa; 1 ft = 0.305 m).

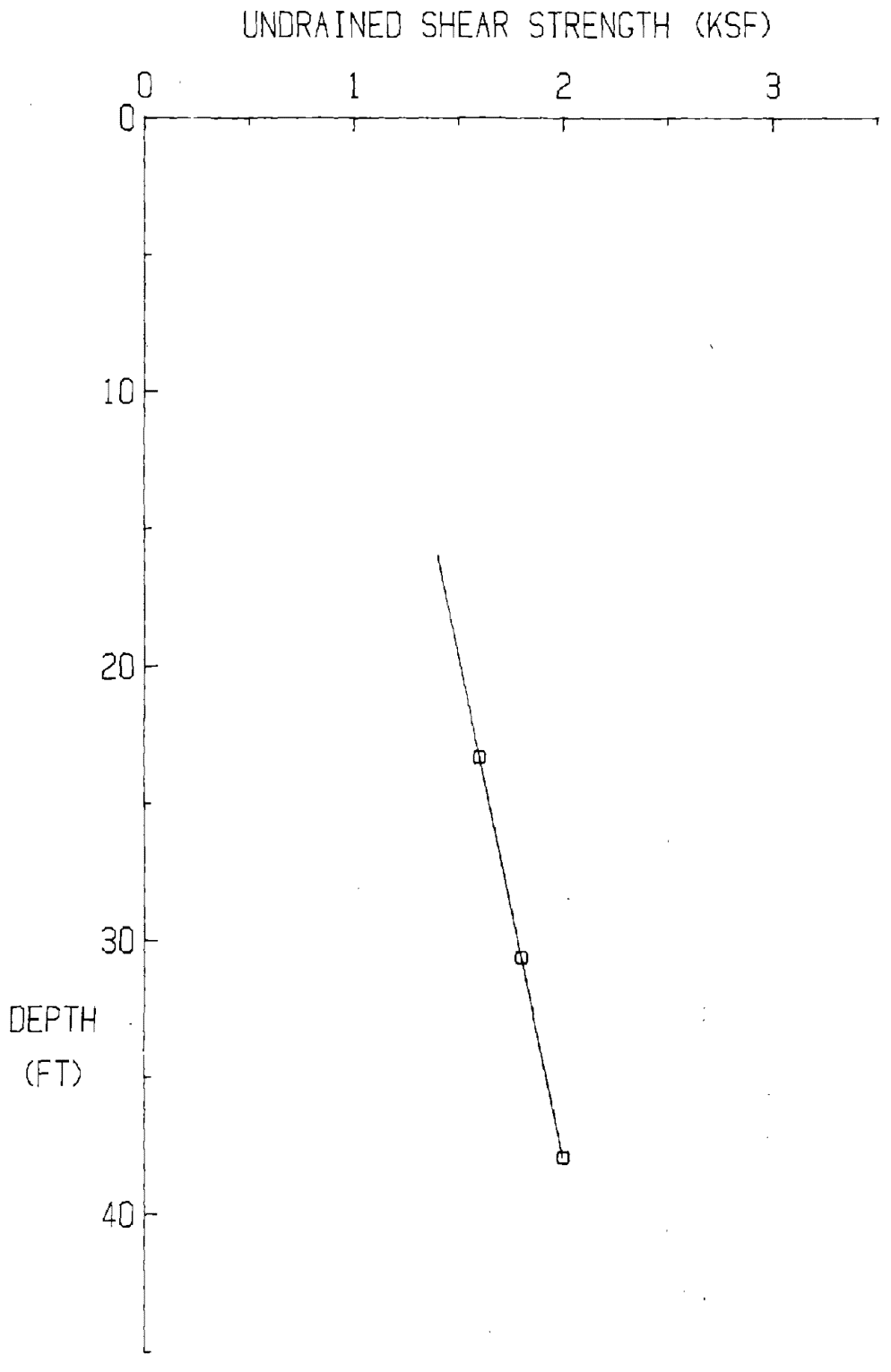

Figure 33. Test 2, S_u profile (1 ksf = 47.9 kPa; 1 ft = 0.305 m)

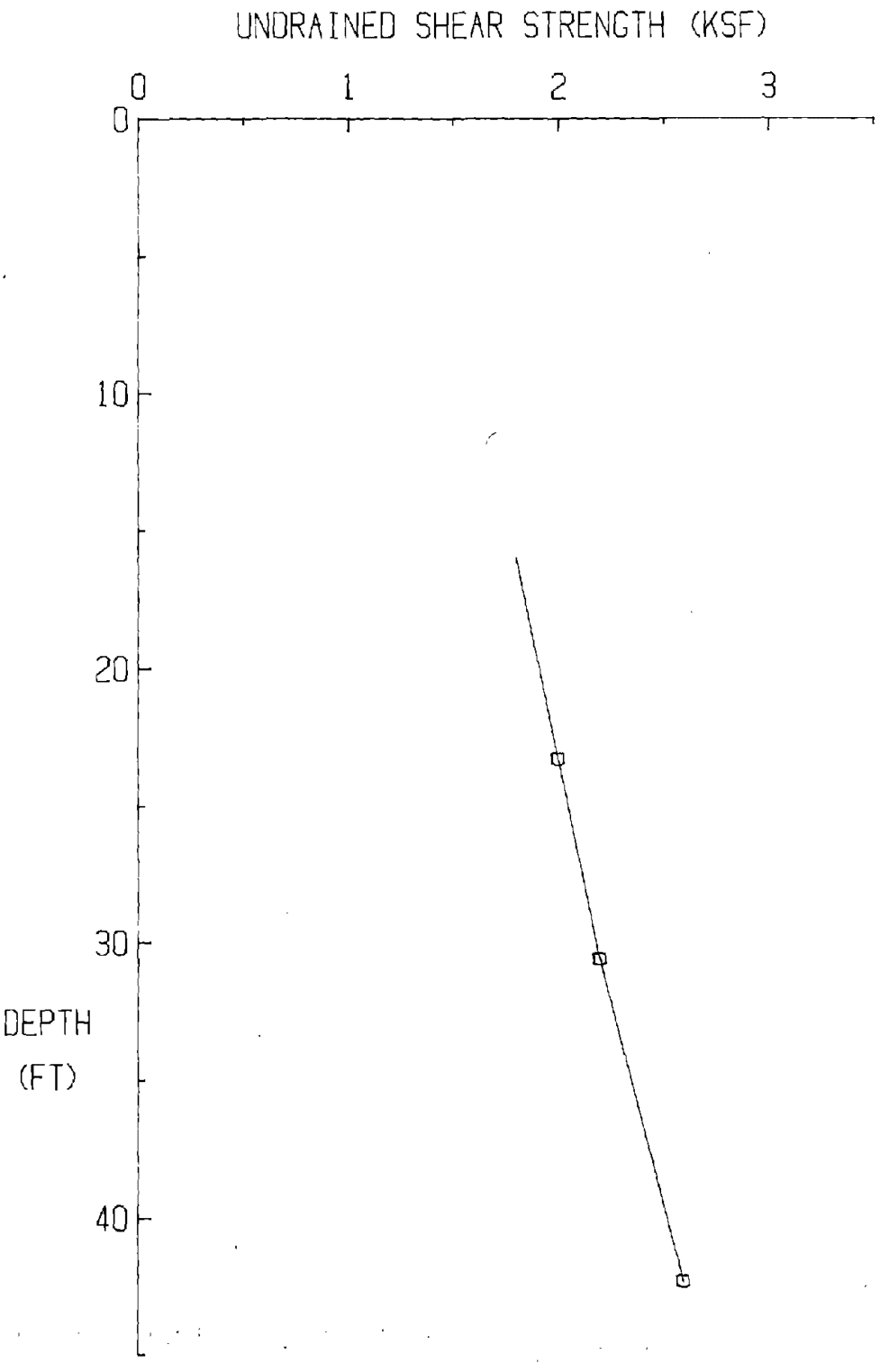

Figure 34. Test 3, S_u profile (1 ksf = 47.9 kPa; 1 ft = 0.305 m)

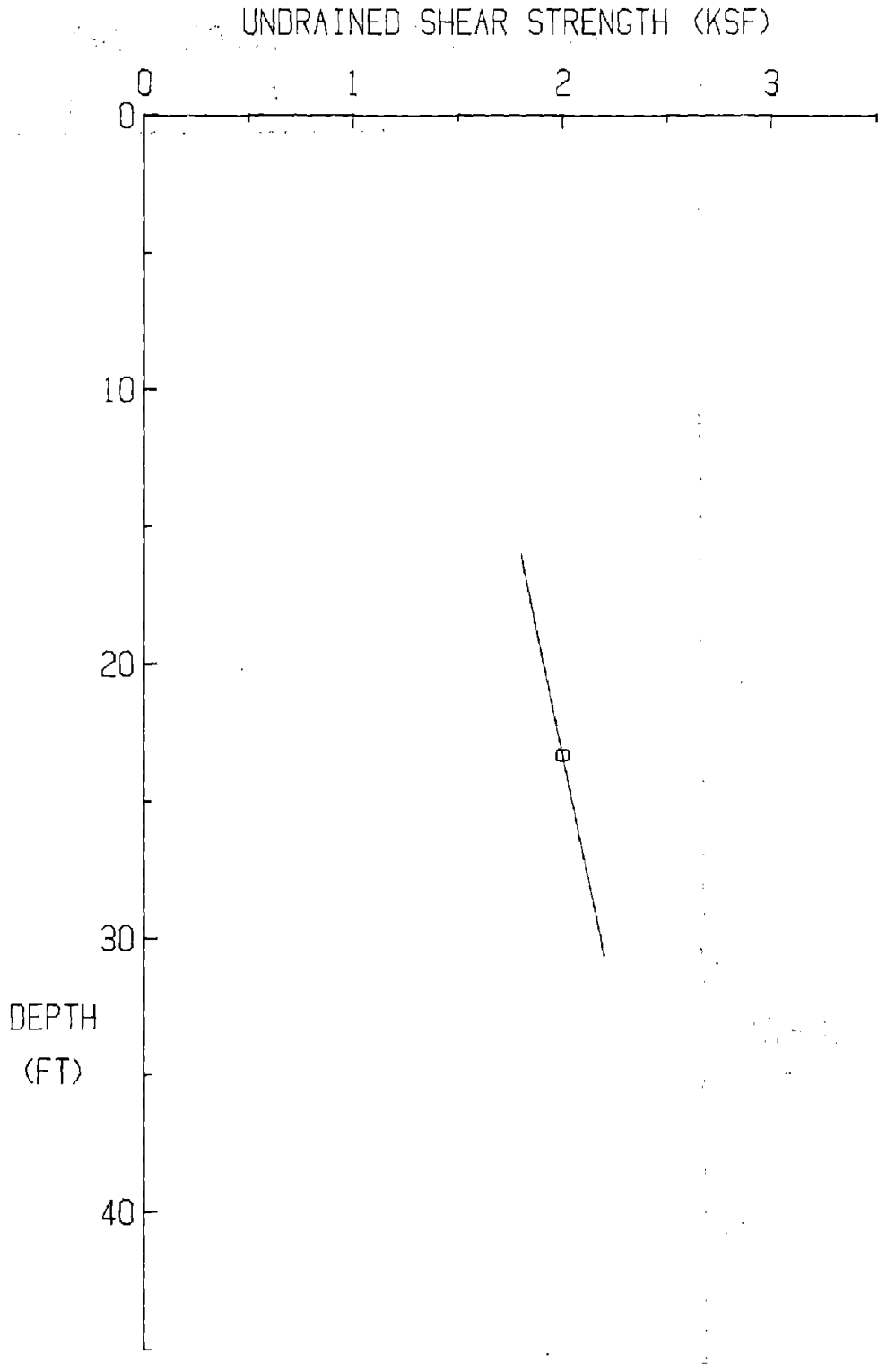

Figure 35. Test 4, S_u profile (1 ksf = 47.9 kPa; 1 ft = 0.305 m)

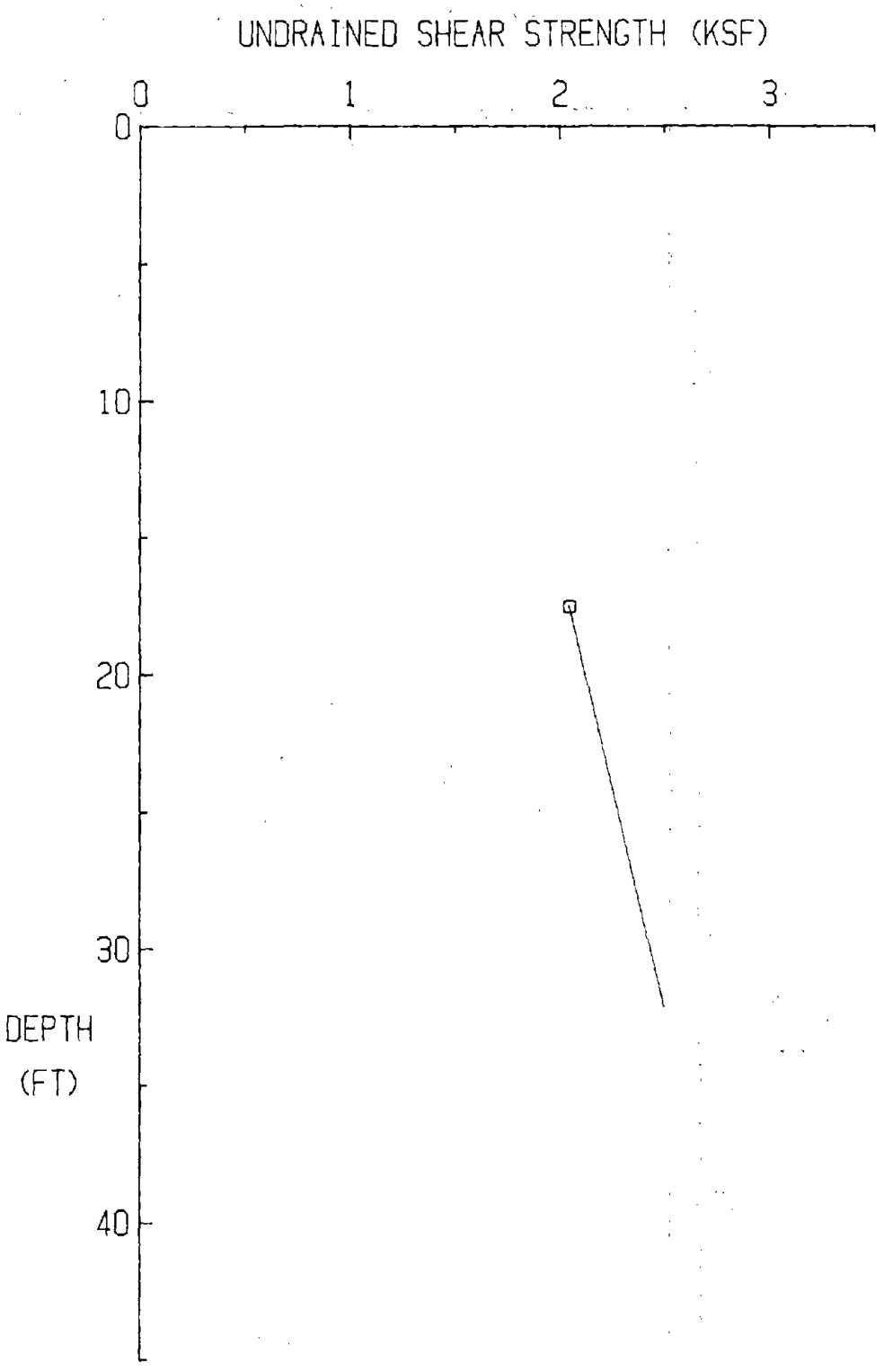

Figure 36. Test 5, S_u profile (1 ksf = 47.9 kPa; 1 ft = 0.305 m)

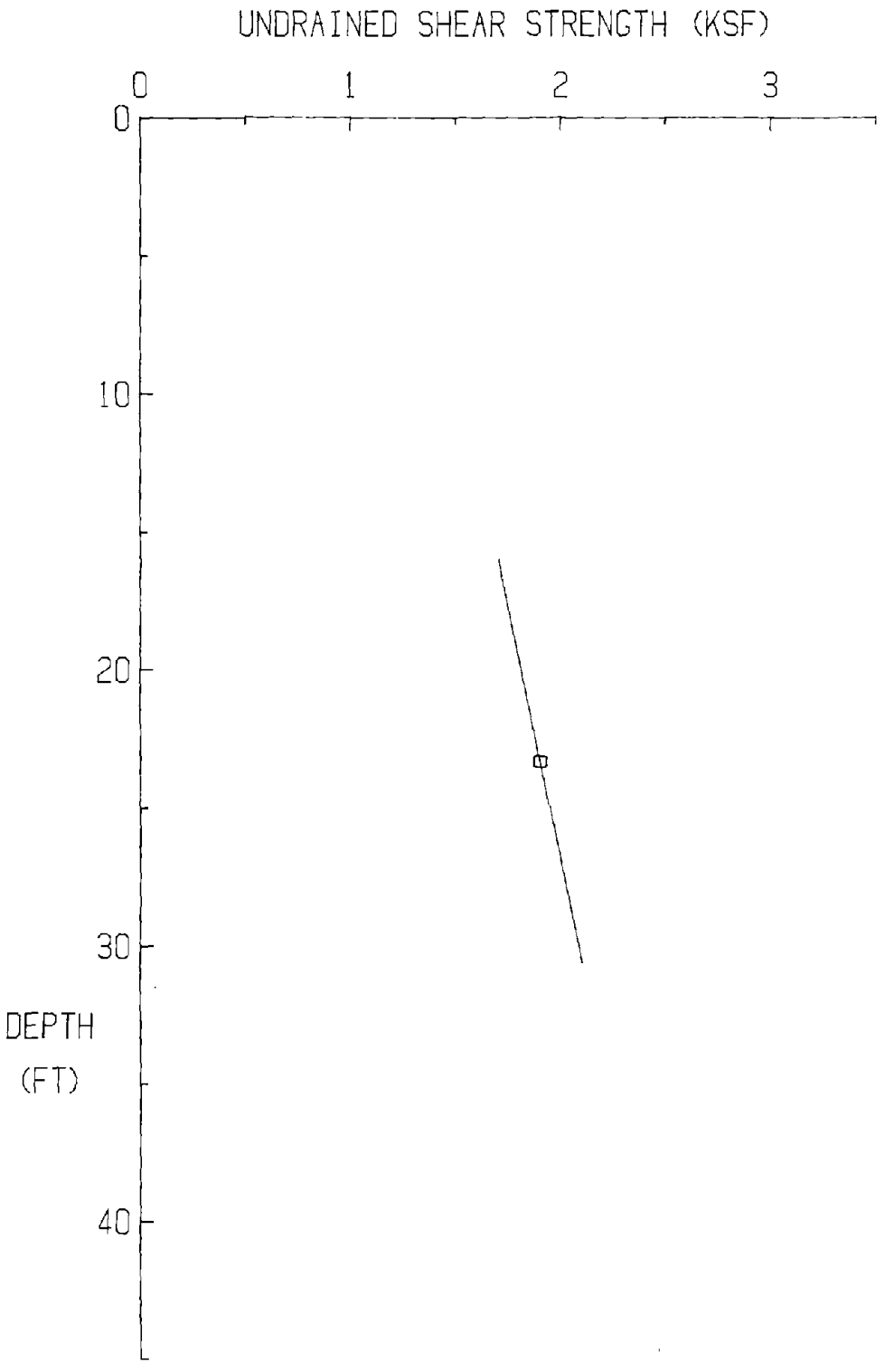

Figure 37. Test 6, S_u profile (1 ksf = 47.9 kPa; 1 ft = 0.305 m)

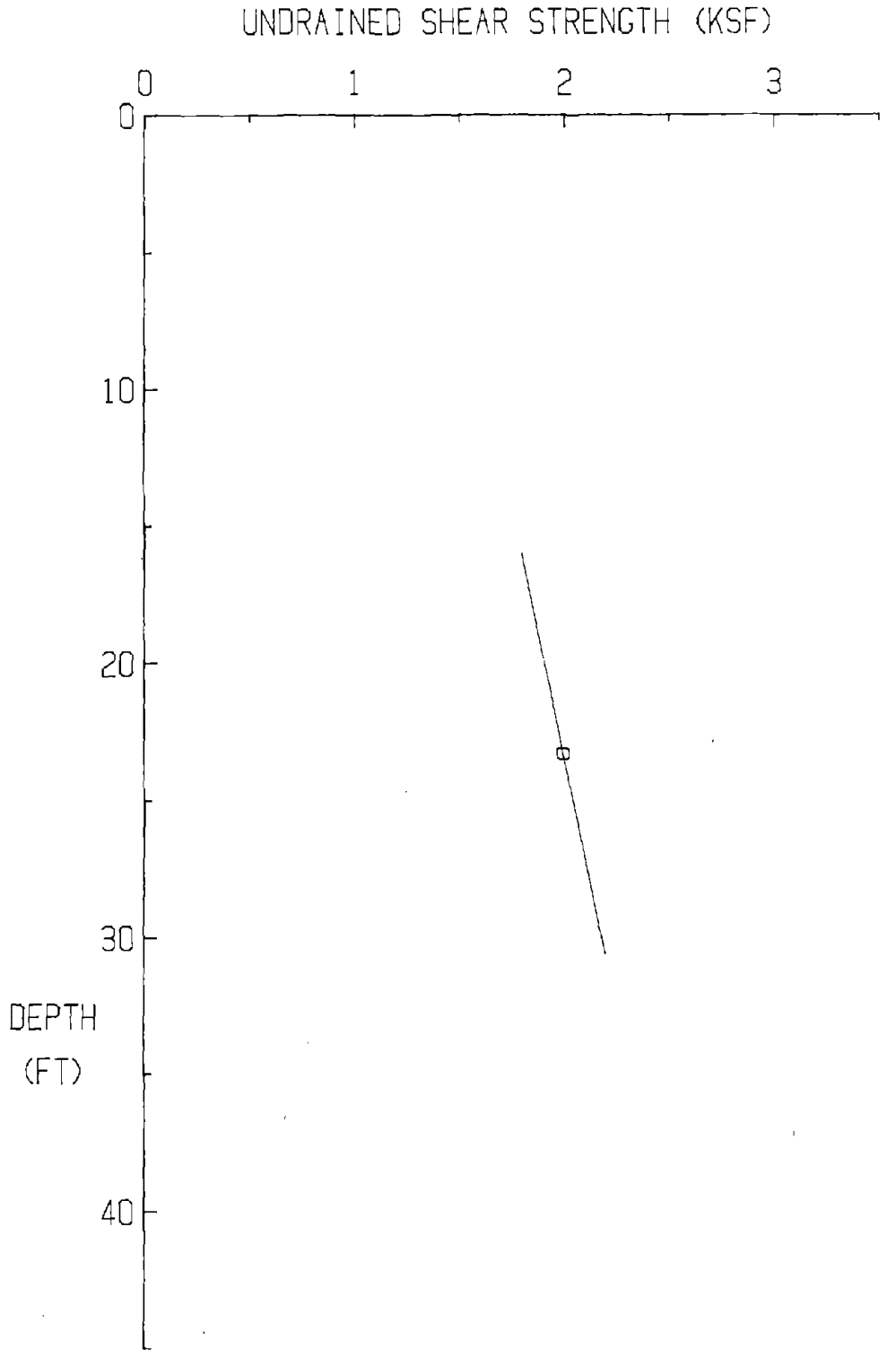

Figure 38. Test 7, S_u profile (1 ksf = 47.9 kPa; 1 ft = 0.305 m)

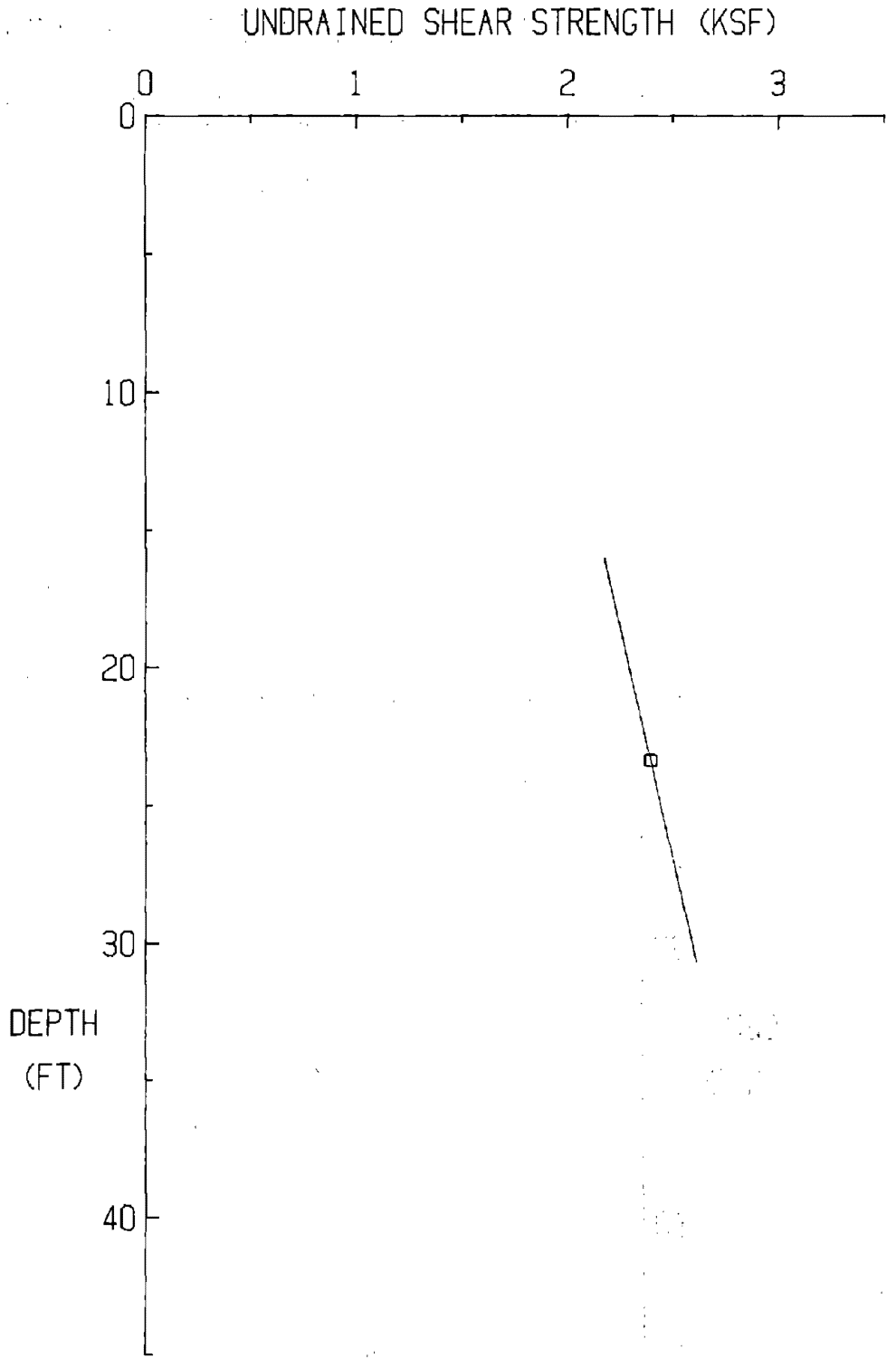

Figure 39. Test 8, S_u profile (1 ksf = 47.9 kPa; 1 ft = 0.305 m)

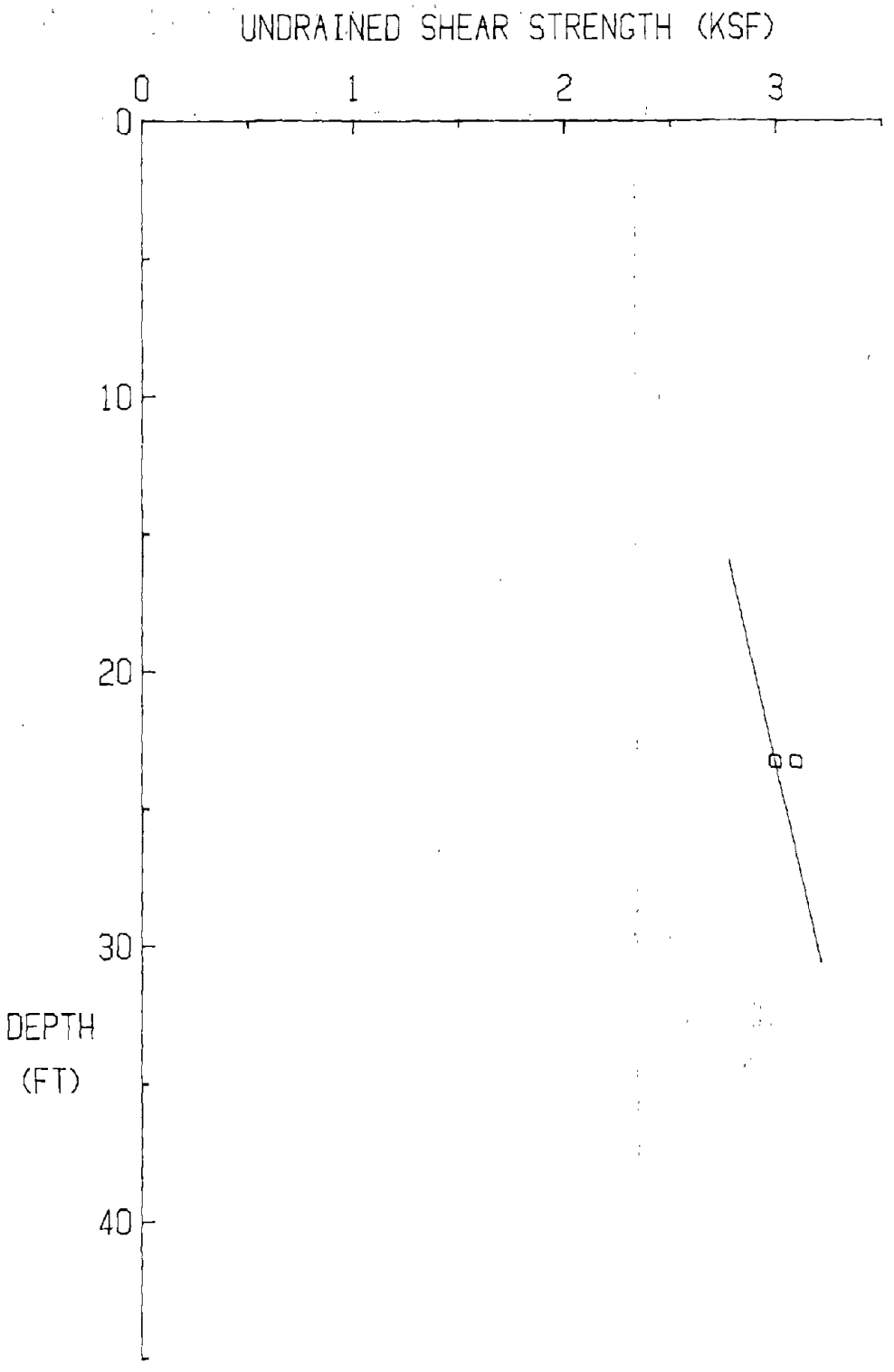

Figure 40. Test 12, S_u profile (1 ksf = 47.9 kPa, 1 ft = 0.305 m)

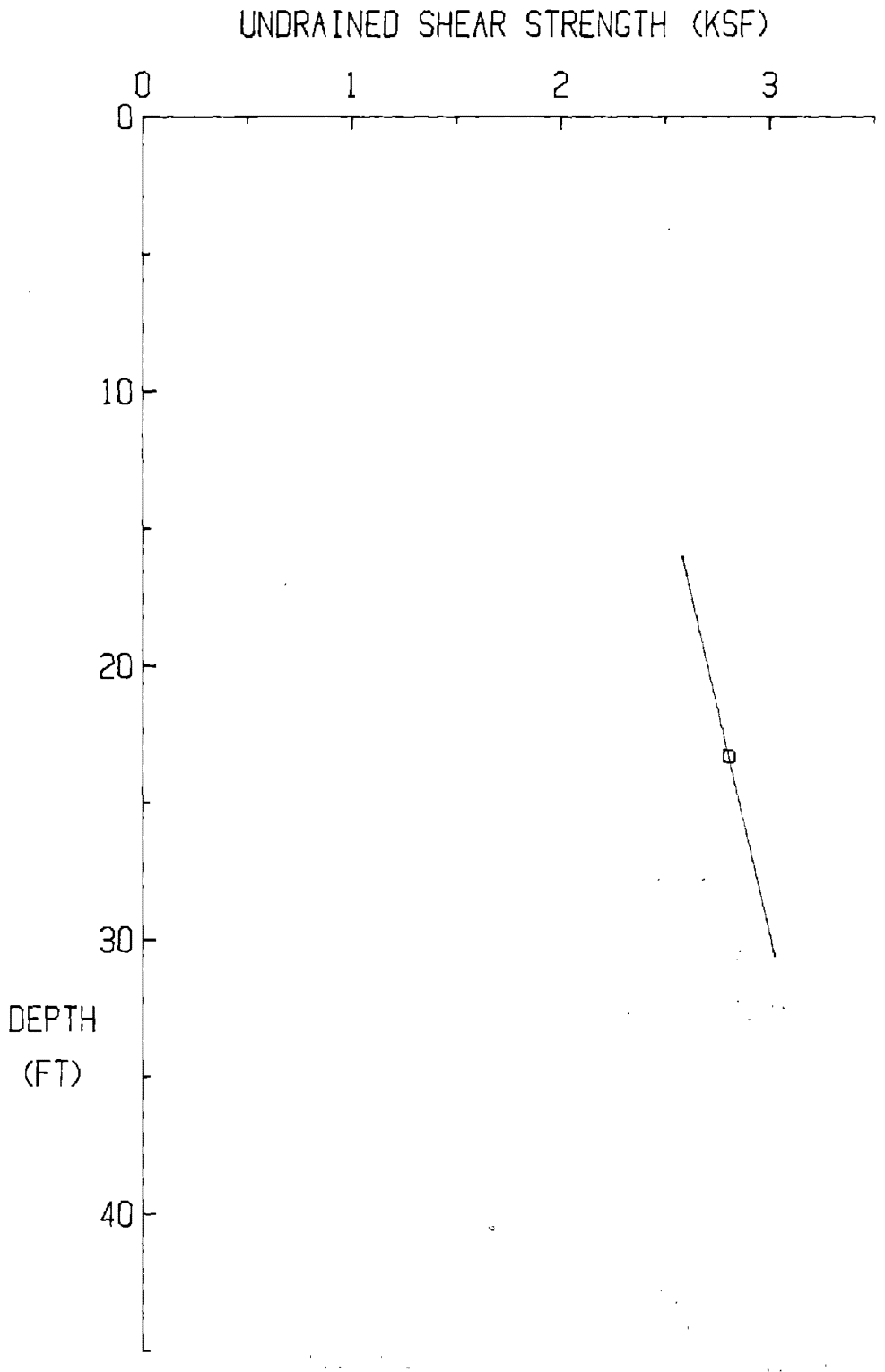

Figure 41. Test 13, S_u profile (1 ksf = 47.9 kPa; 1 ft = 0.305 m)

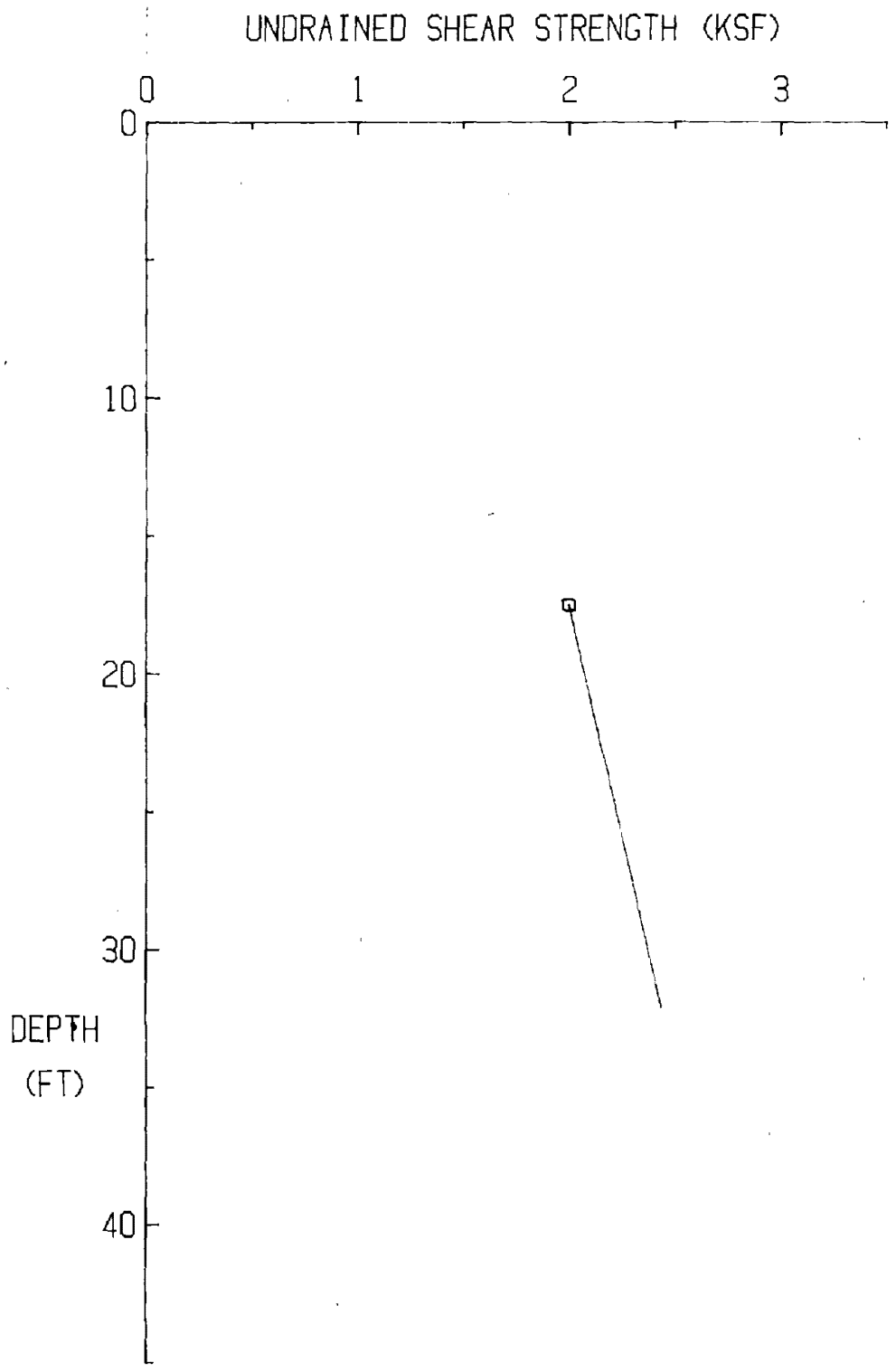

Figure 42. Test 15, S_u profile (1 ksf = 47.9 kPa; 1 ft = 0.305 m)

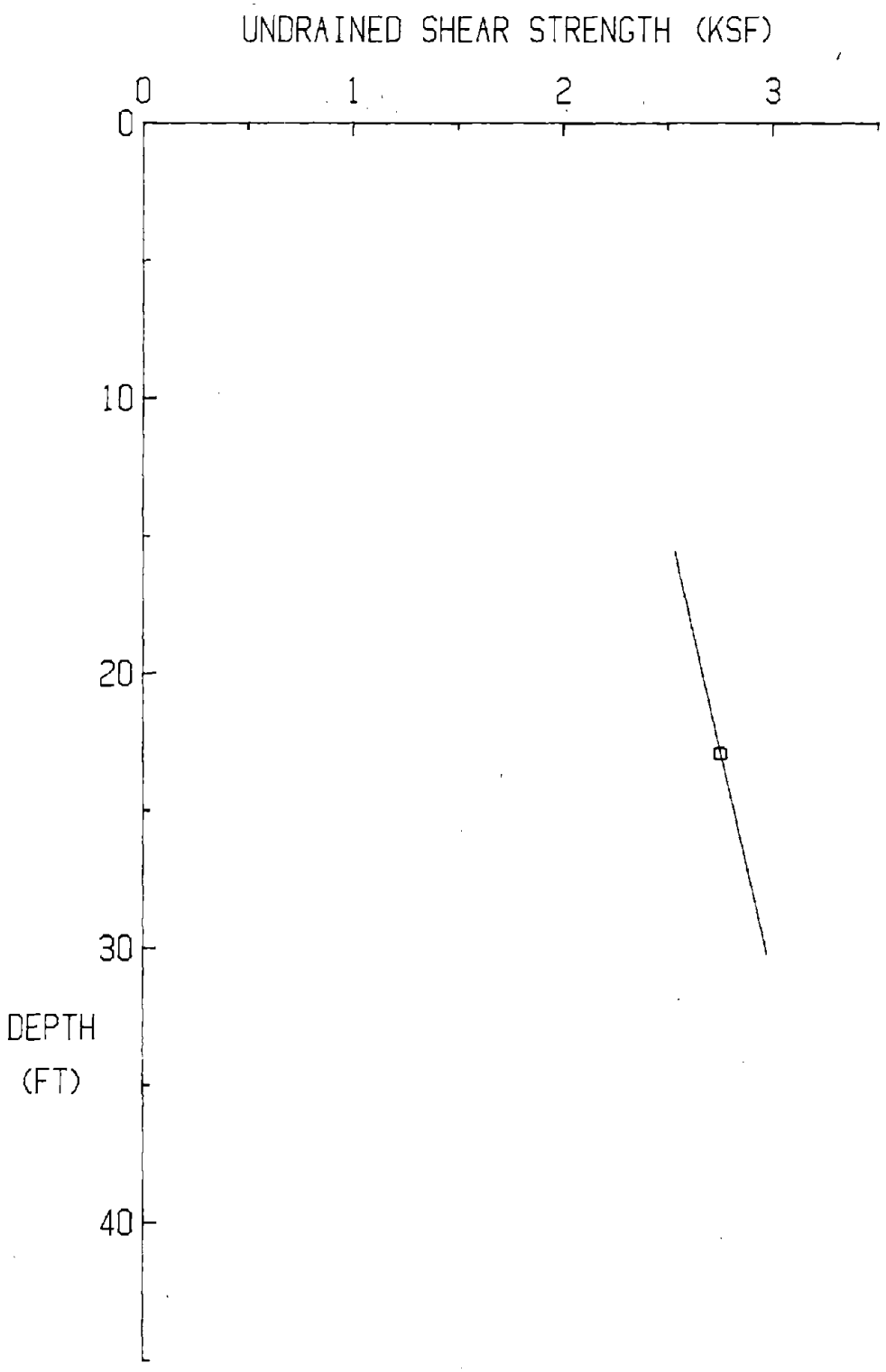

Figure 43. Test 16, S_u profile (1 ksf = 47.9 kPa; 1 ft = 0.305 m)

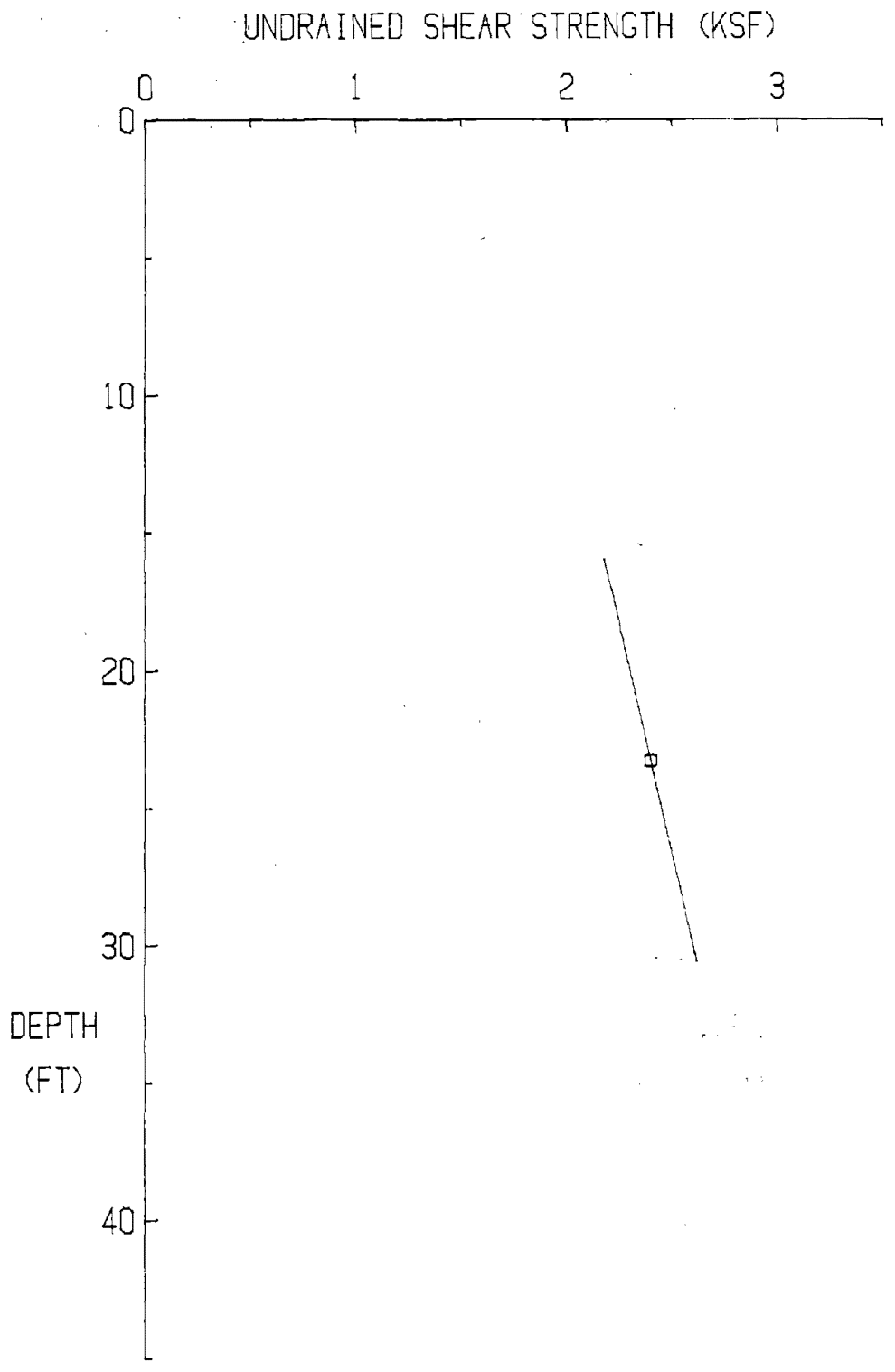

Figure 44. Test 17, S_u profile (1 ksf = 47.9 kPa; 1 ft = 0.305 m)

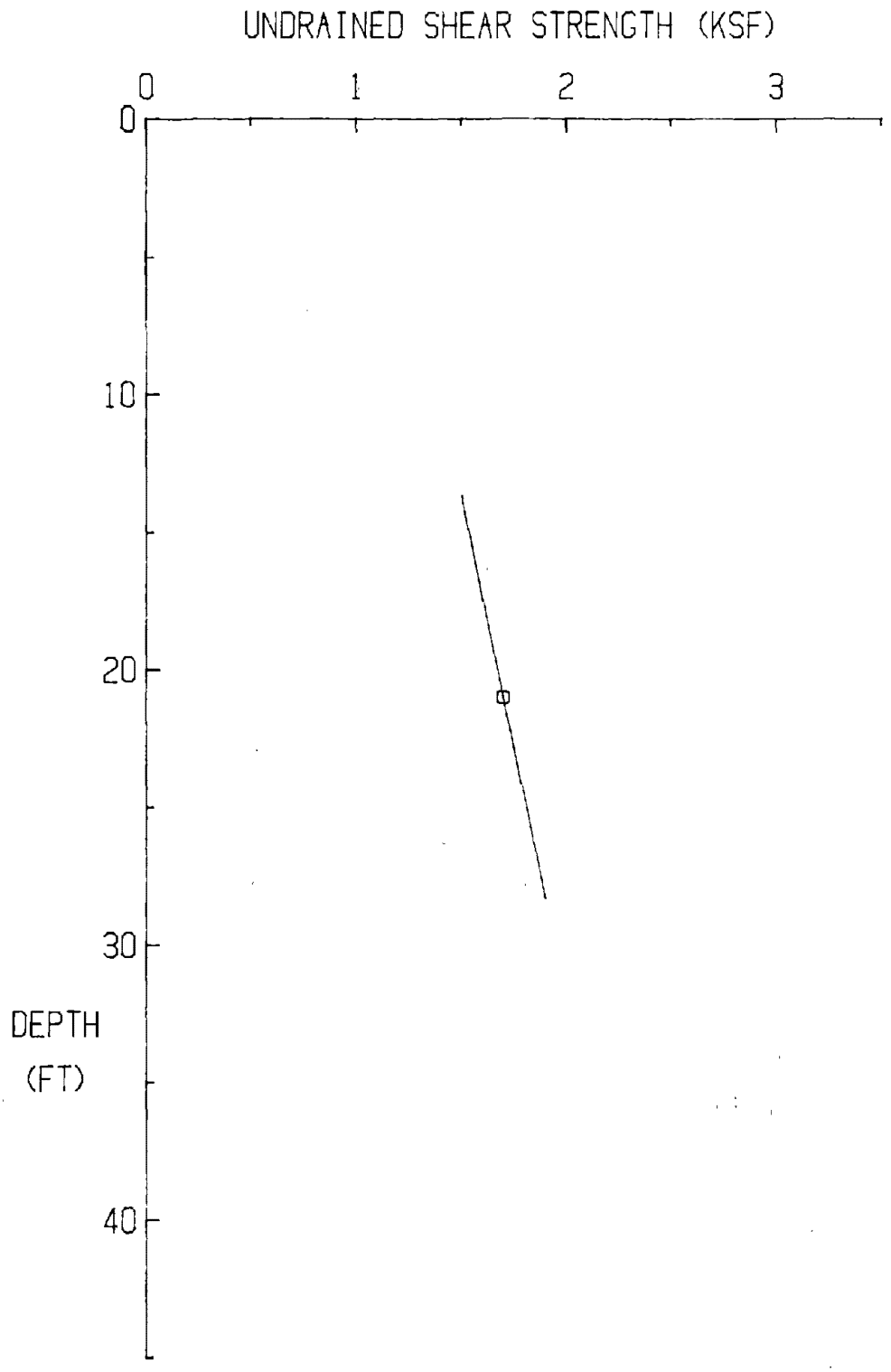

Figure 45. Test 18, S_u profile (1 ksf = 47.9 kPa; 1 ft = 0.305 m)

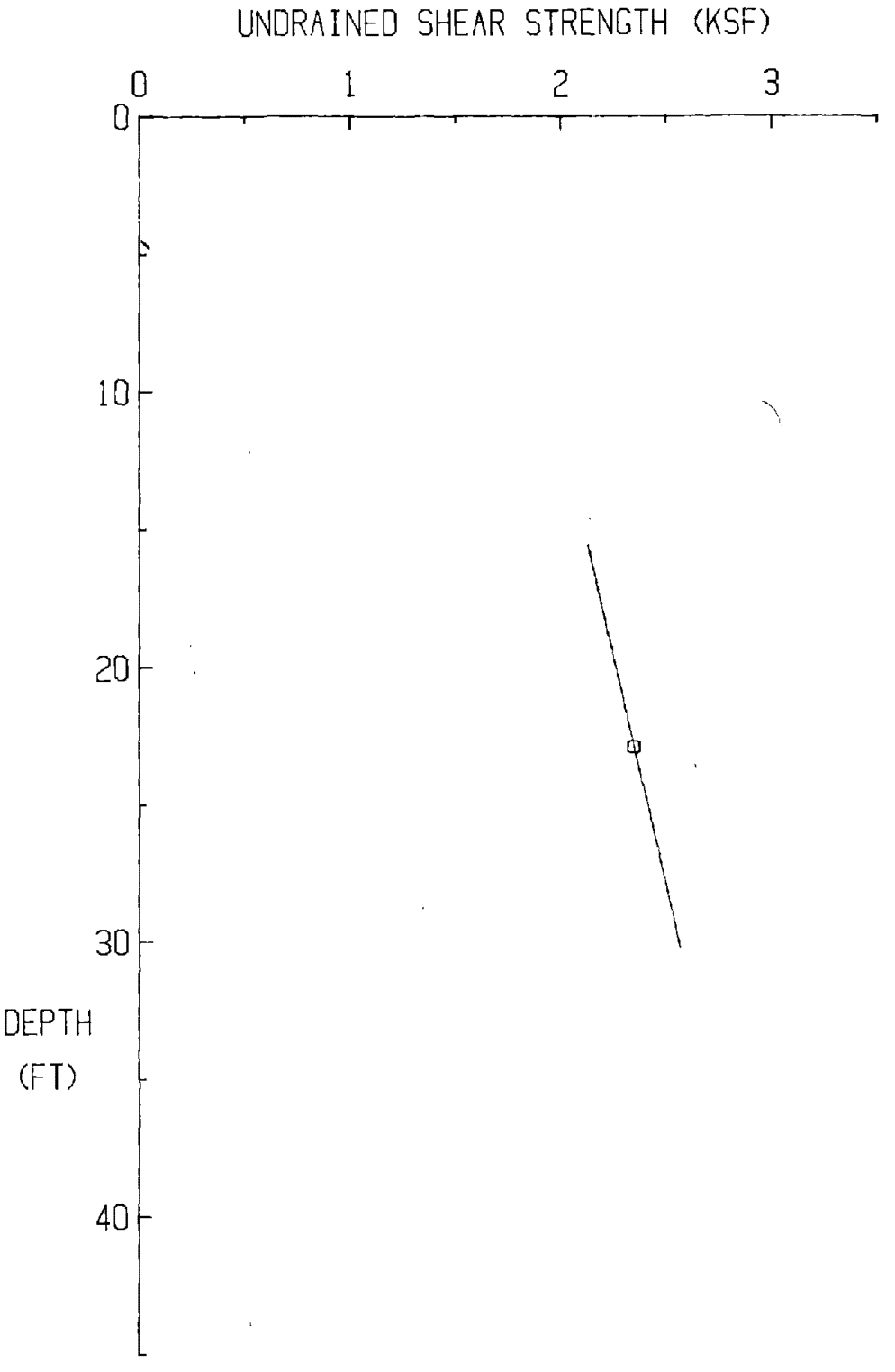

Figure 46. Test 20, S_u profile (1 ksf = 47.9 kPa; 1 ft = 0.305 m)

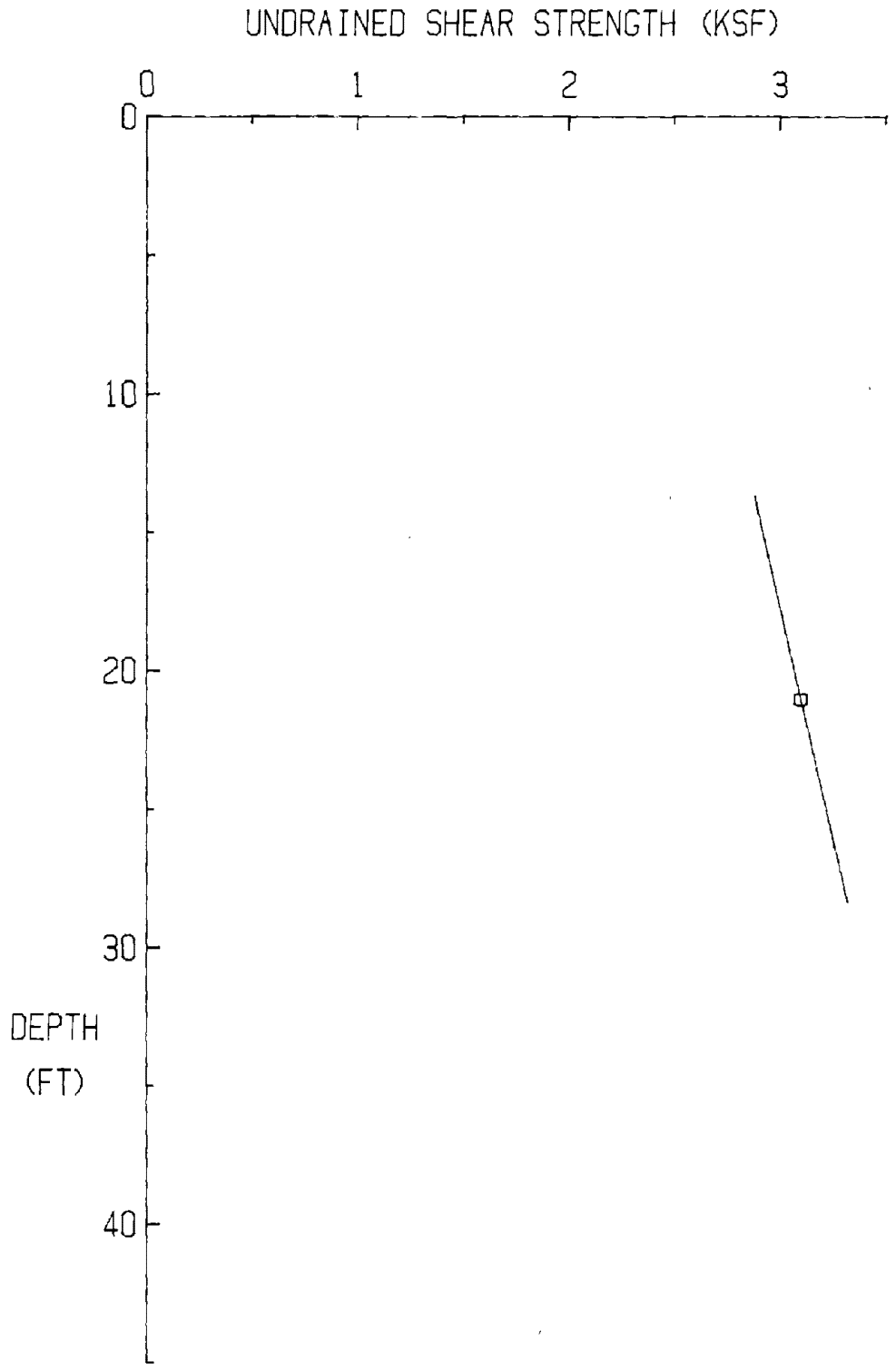

Figure 47. Test 21, S_u profile (1 ksf = 47.9 kPa; 1 ft = 0.305 m)

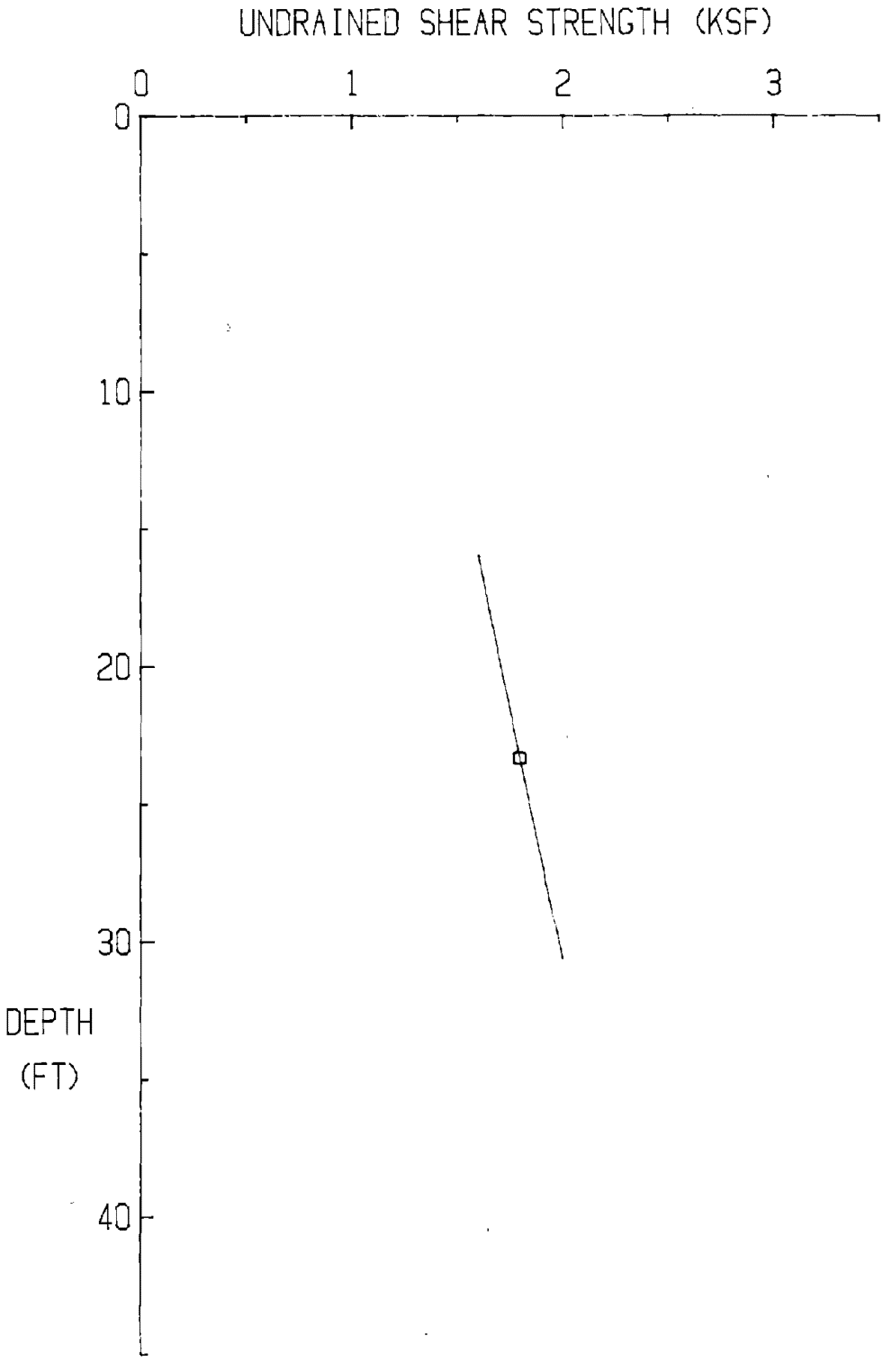

Figure 48. Test 22, S_u profile (1 ksf = 47.9 kPa; 1 ft = 0.305 m)

APPENDIX 2

In this appendix, load transfer curves for axial load tests (single and group) are presented. All quantities are given in prototype scale. Included are results from tests 3, 4, 5, 6, 13, 15, 16, 17, 20, and 22. Two curves are presented for test 4 as two different load tests (on different piles) were performed. Group data is presented for tests 13 and 22. The prototype data is also included (Figures 49 through 63).

Not included are results from tests 1, 2, 7, 8, 9, 10, 11, 12, 14, 18, 19, and 21. This can be attributed to a number of reasons as seen in Table 5. These measurements were not attempted on tests 1, 2, and 12. Load transfer was not recorded on tests 7, 8, 10, 11, 14, and 19 as various malfunctions prevented load tests from being properly performed. Tests 18 and 21 were at 100 g and therefore no load transfer was recorded as the smaller scale piles were not instrumented.

Actual measured values are denoted by circles. Interpolation between points is linear as presented here.

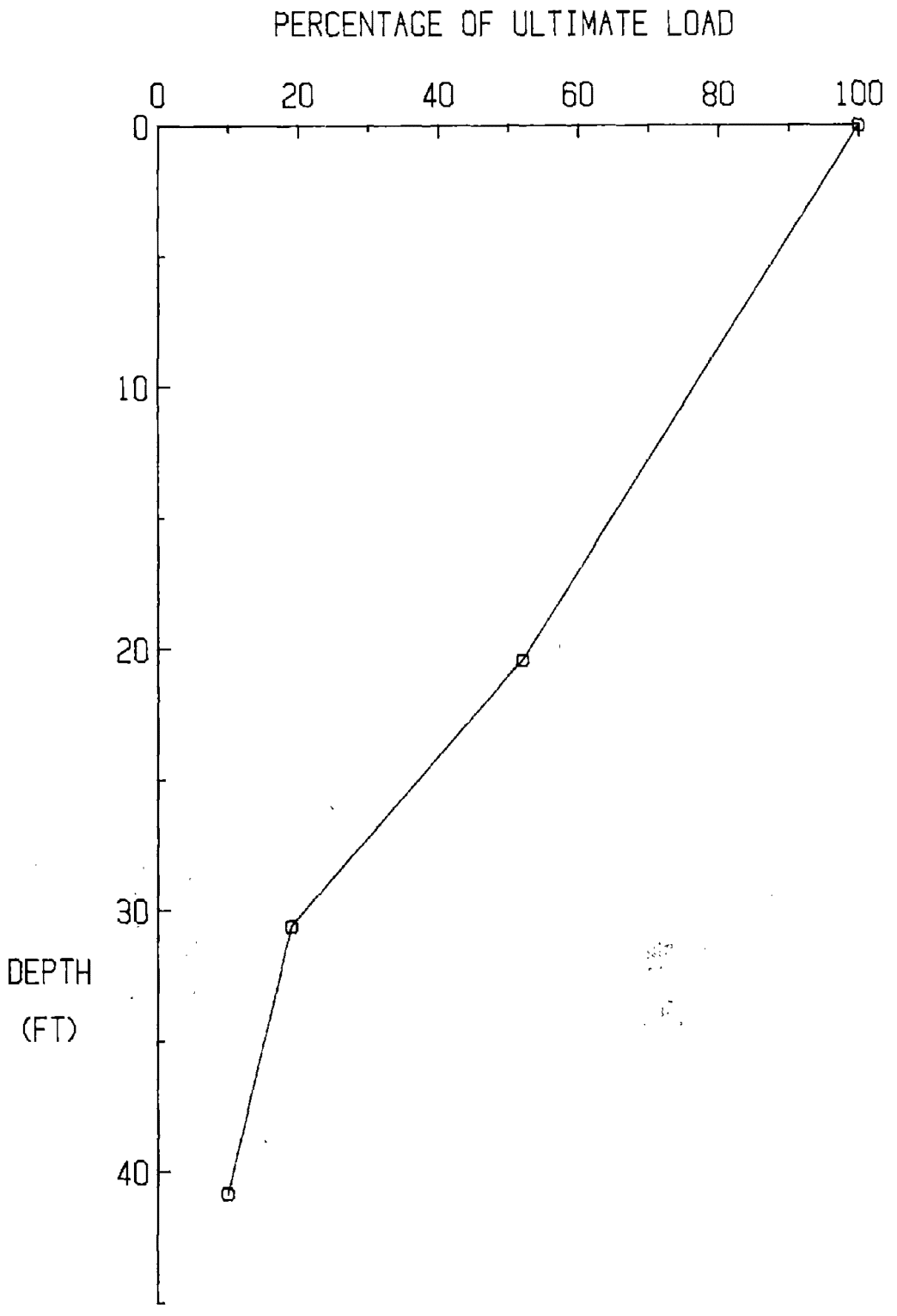

Figure 49. Test 3, load transfer curve (1 kip = 4.45 KN; 1 ft = 0.305 m)

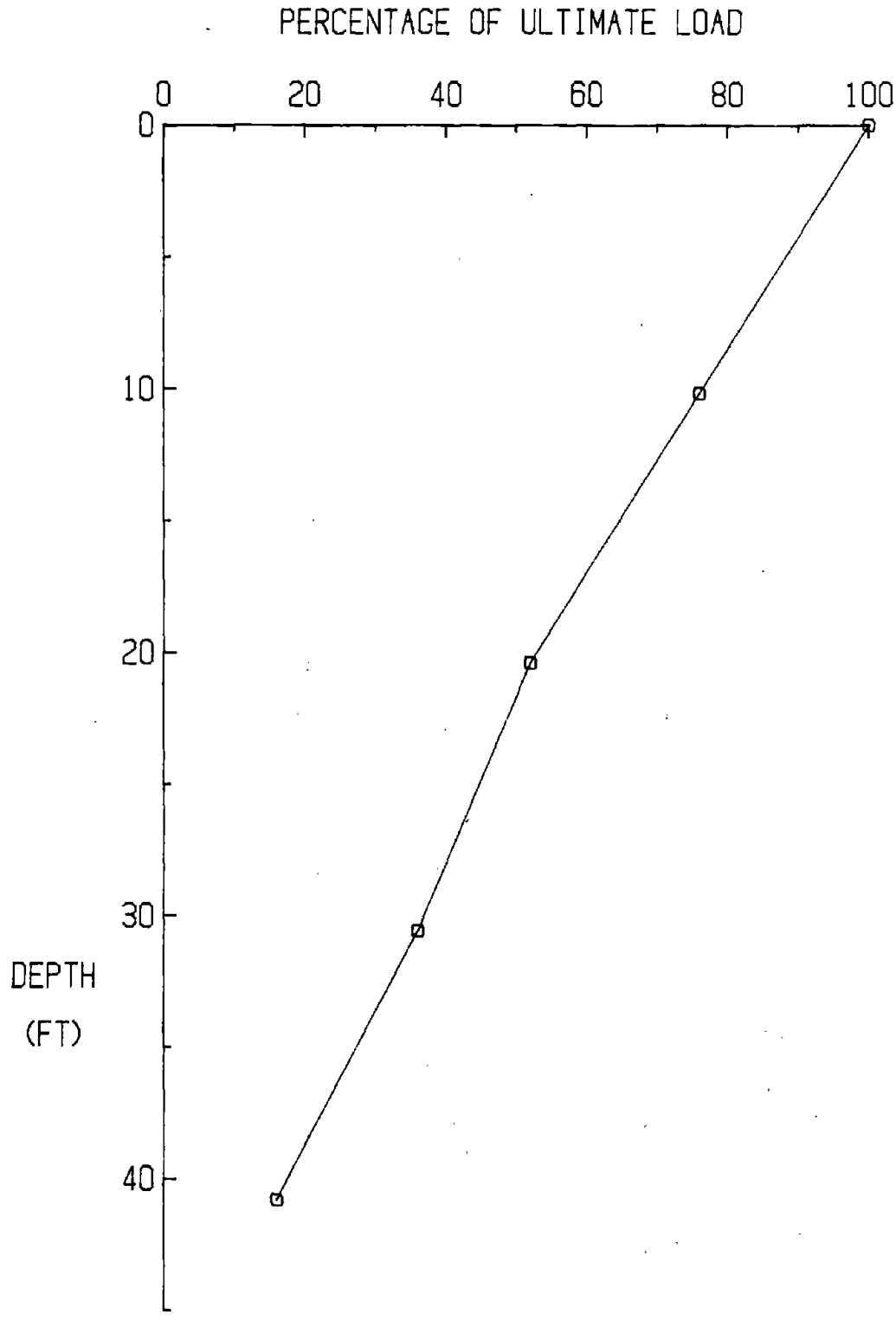

Figure 50. Test 4a, load transfer curve (1 kip = 4.45 KN; 1 ft = 0.305 m)

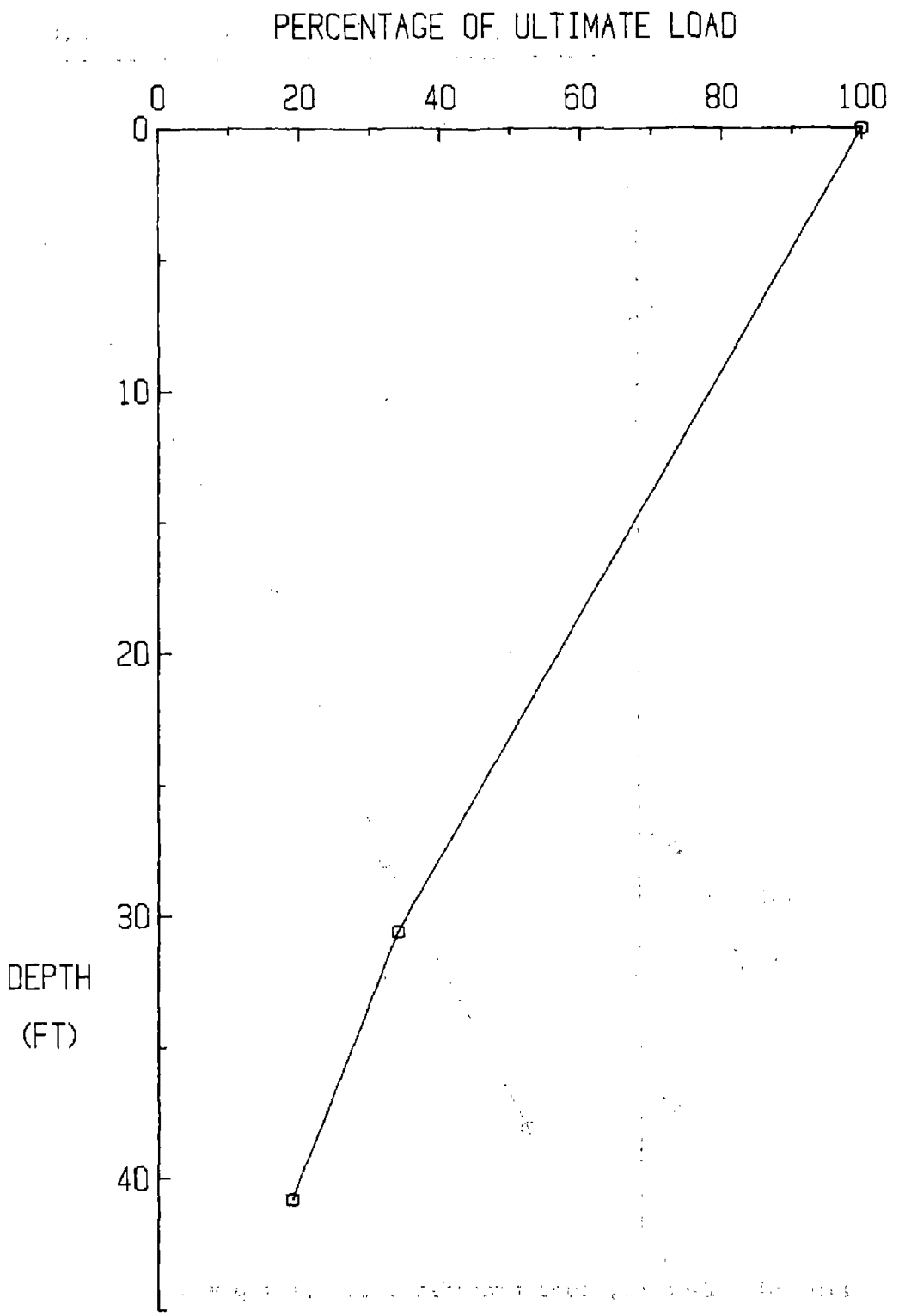

Figure 51. Test 4b, load transfer curve (1 kip = 4.45 KN; 1 ft = 0.305 m)

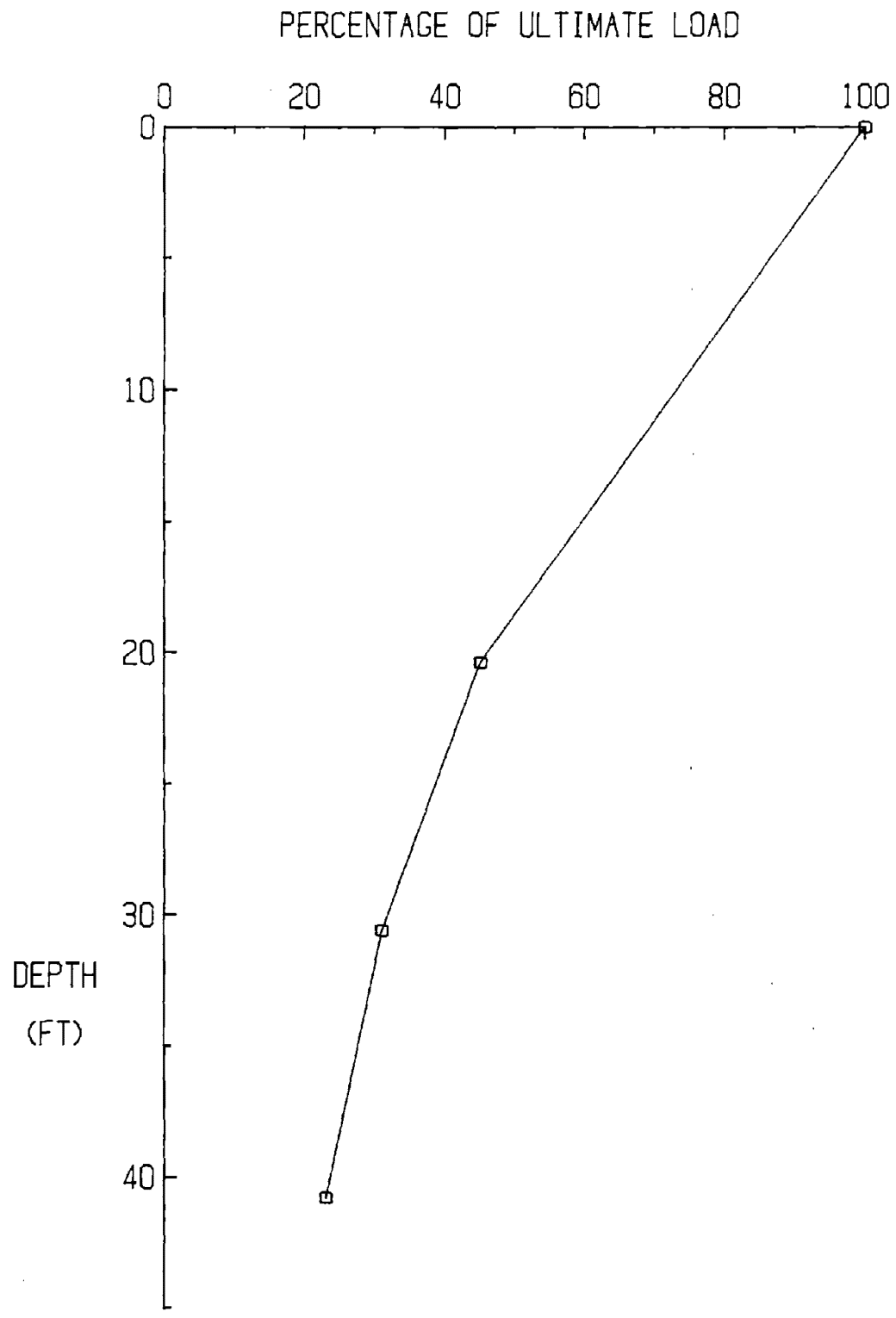

Figure 52. Test 5, load transfer curve (1 kip = 4.45 KN; 1 ft = 0.305 m)

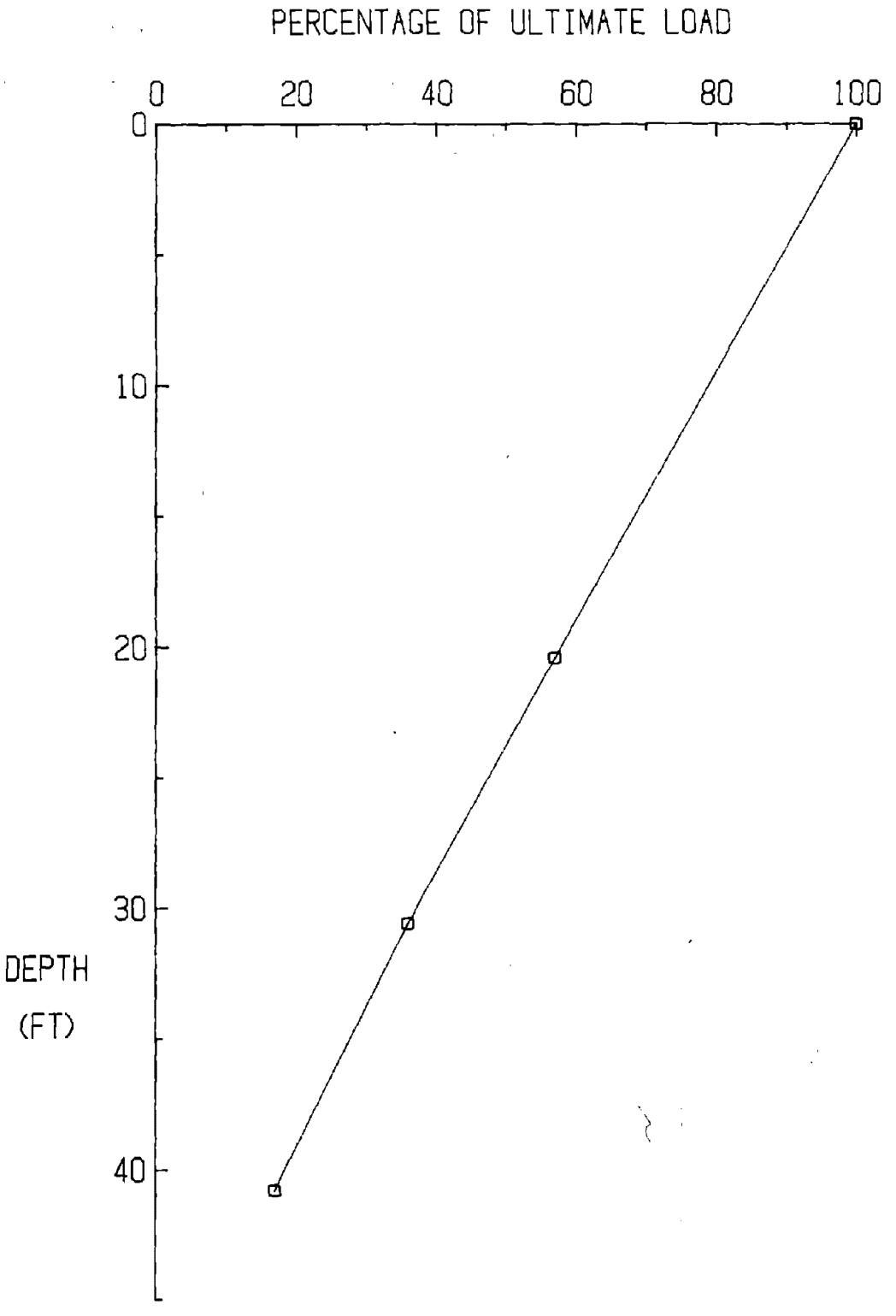

Figure 53. Test 6, load transfer curve (1 kip = 4.45 KN; 1 ft = 0.305 m)

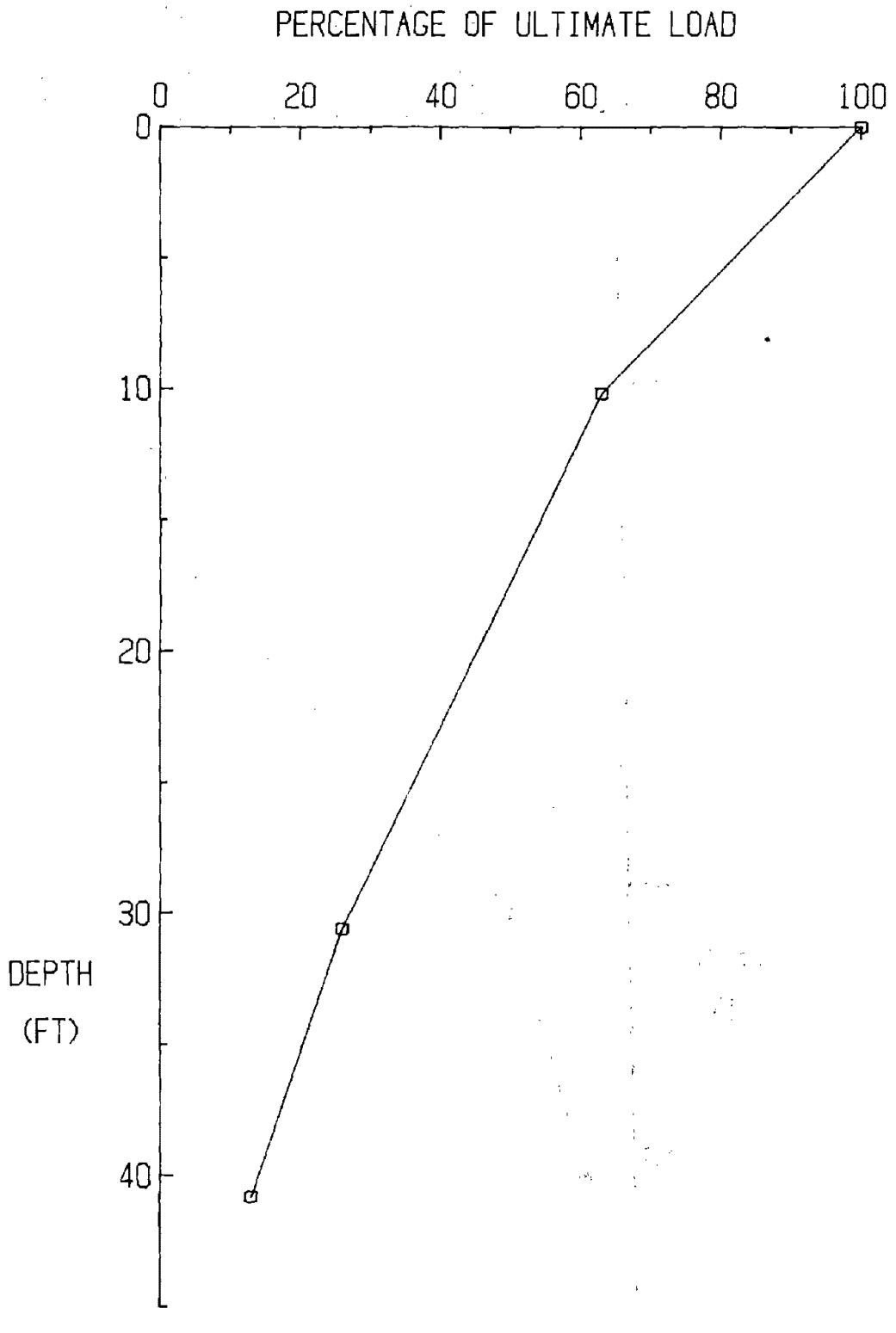

Figure 54. Test 13, load transfer curve (1 kip = 4.45 KN; 1 ft = 0.305 m)

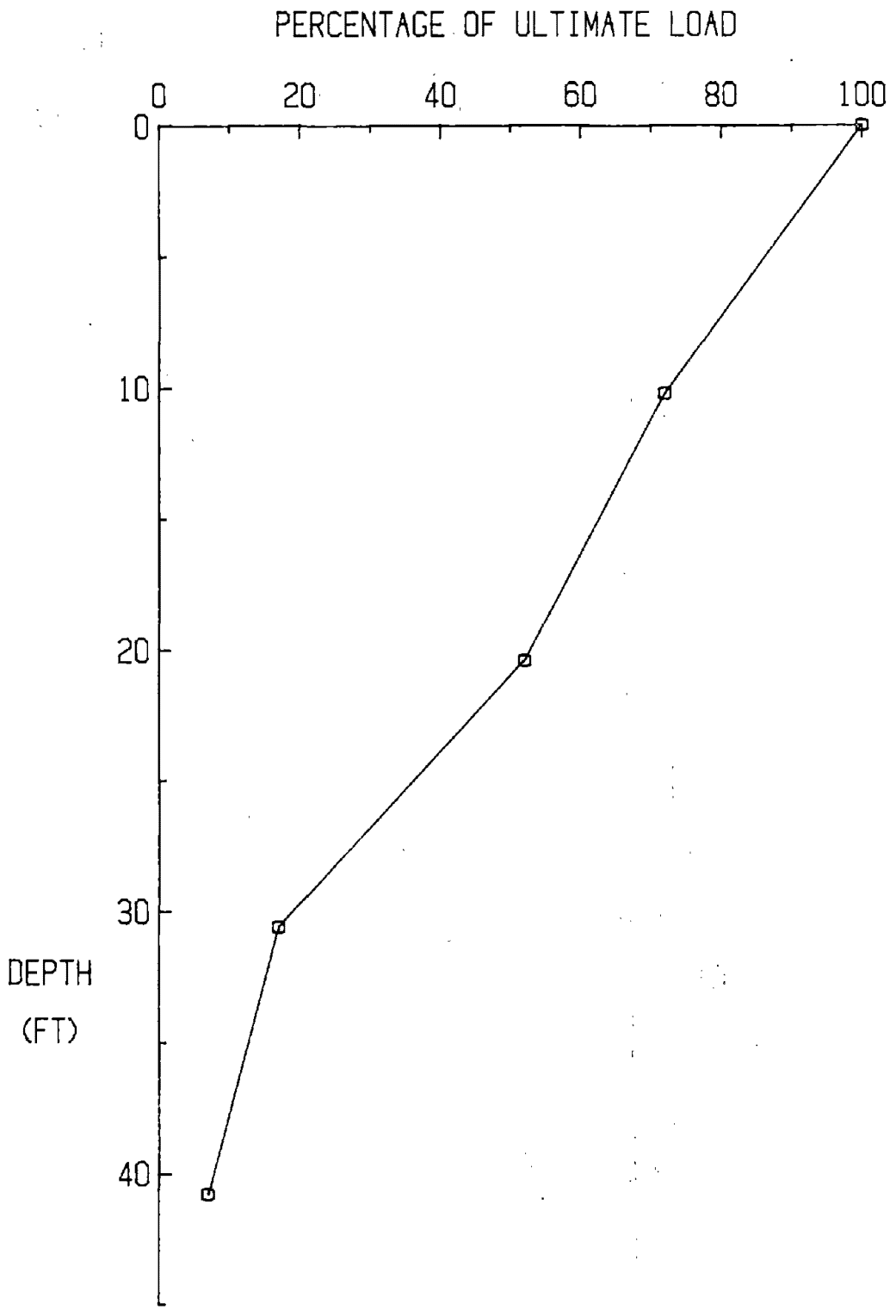

Figure 55. Test 15, load transfer curve (1 kip = 4.45 KN; 1 ft = 0.305 m)

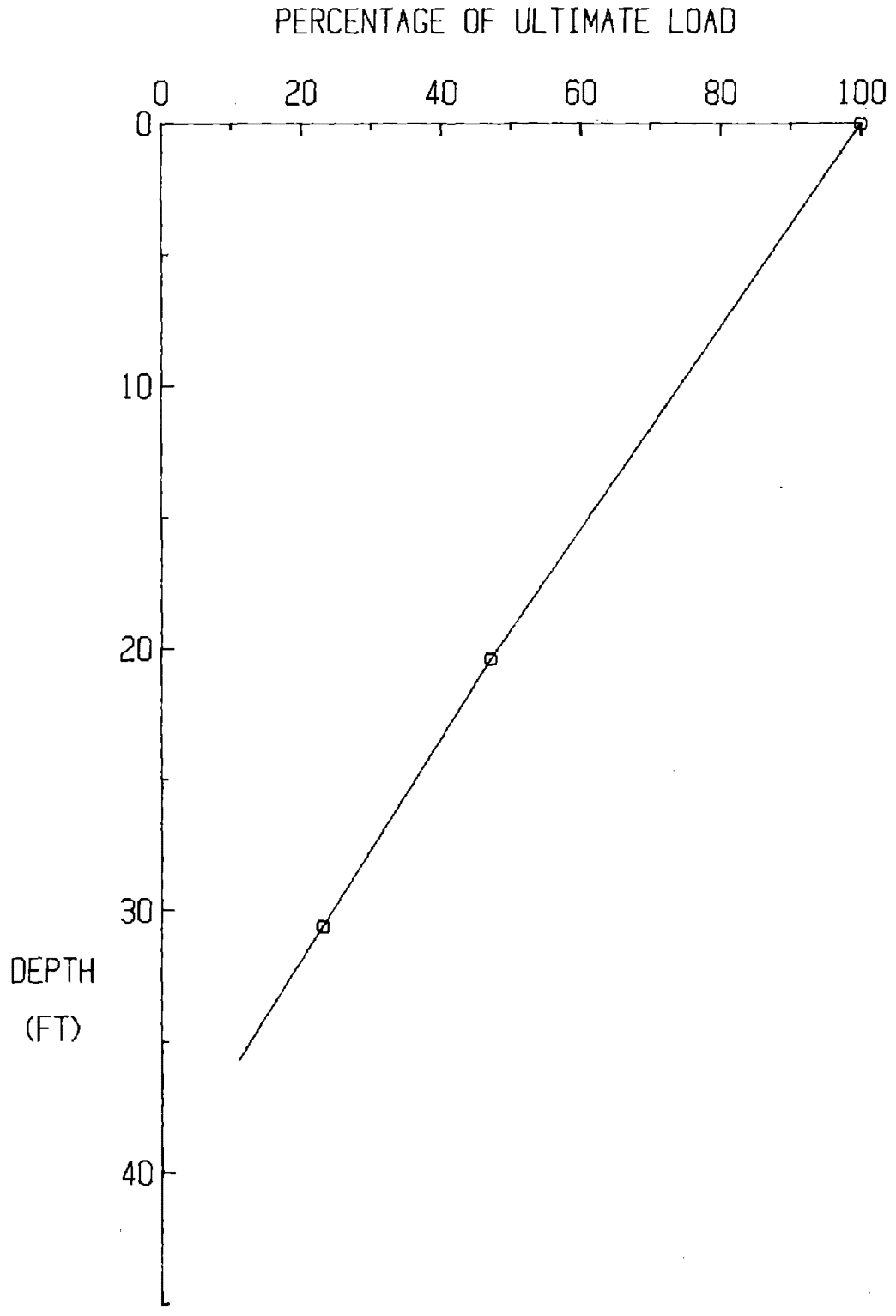

Figure 56. Test 16, load transfer curve (1 kip = 4.45 KN; 1 ft = 0.305 m)

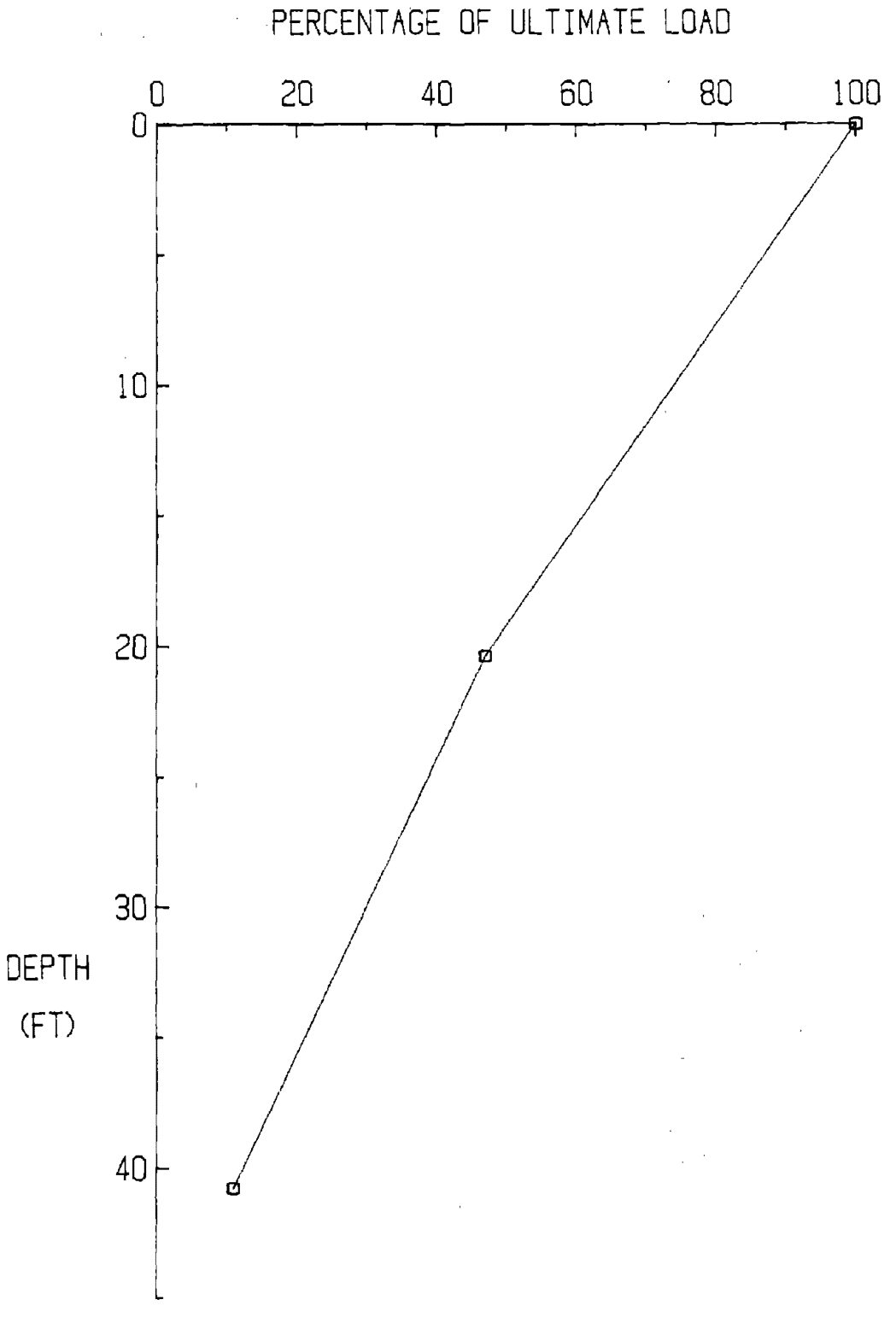

Figure 57. Test 17, load transfer curve (1 kip = 4.45 KN; 1 ft = 0.305 m)

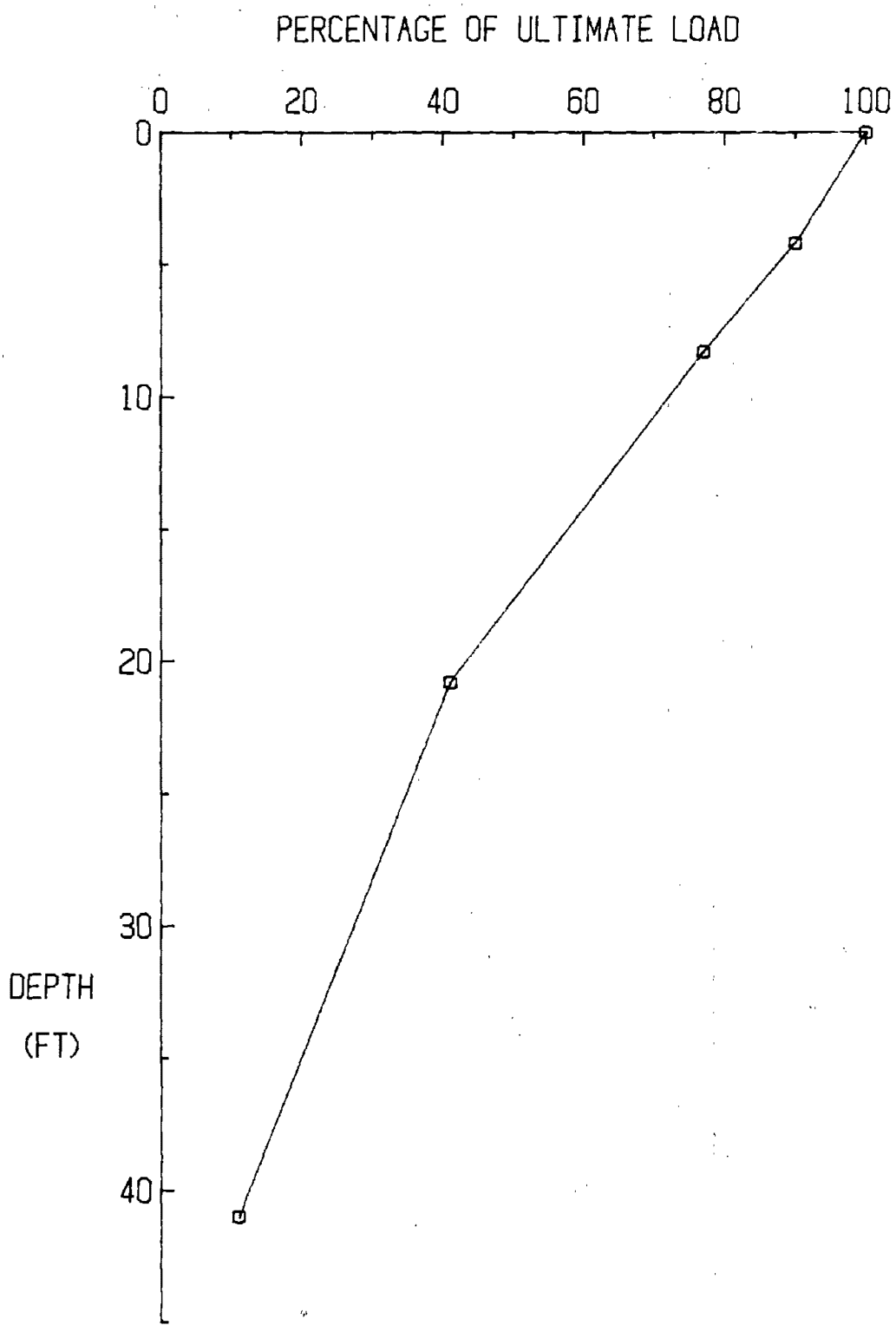

Figure 58. Test 20, load transfer curve (1 kip = 4.45 KN; 1 ft = 0.305 m)

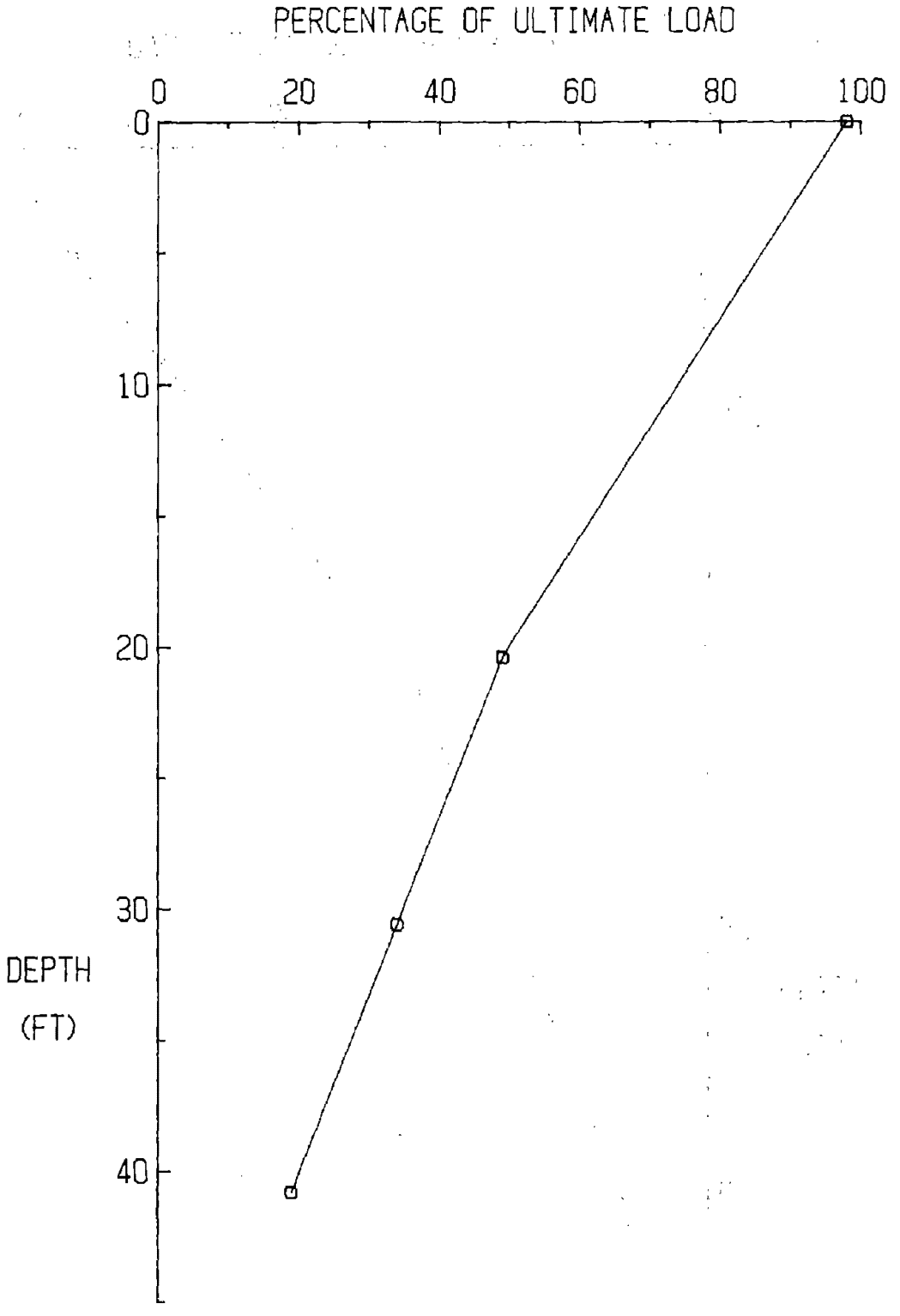

Figure 59. Test 22, load transfer curve (1 kip = 4.45 KN; 1 ft = 0.305 m)

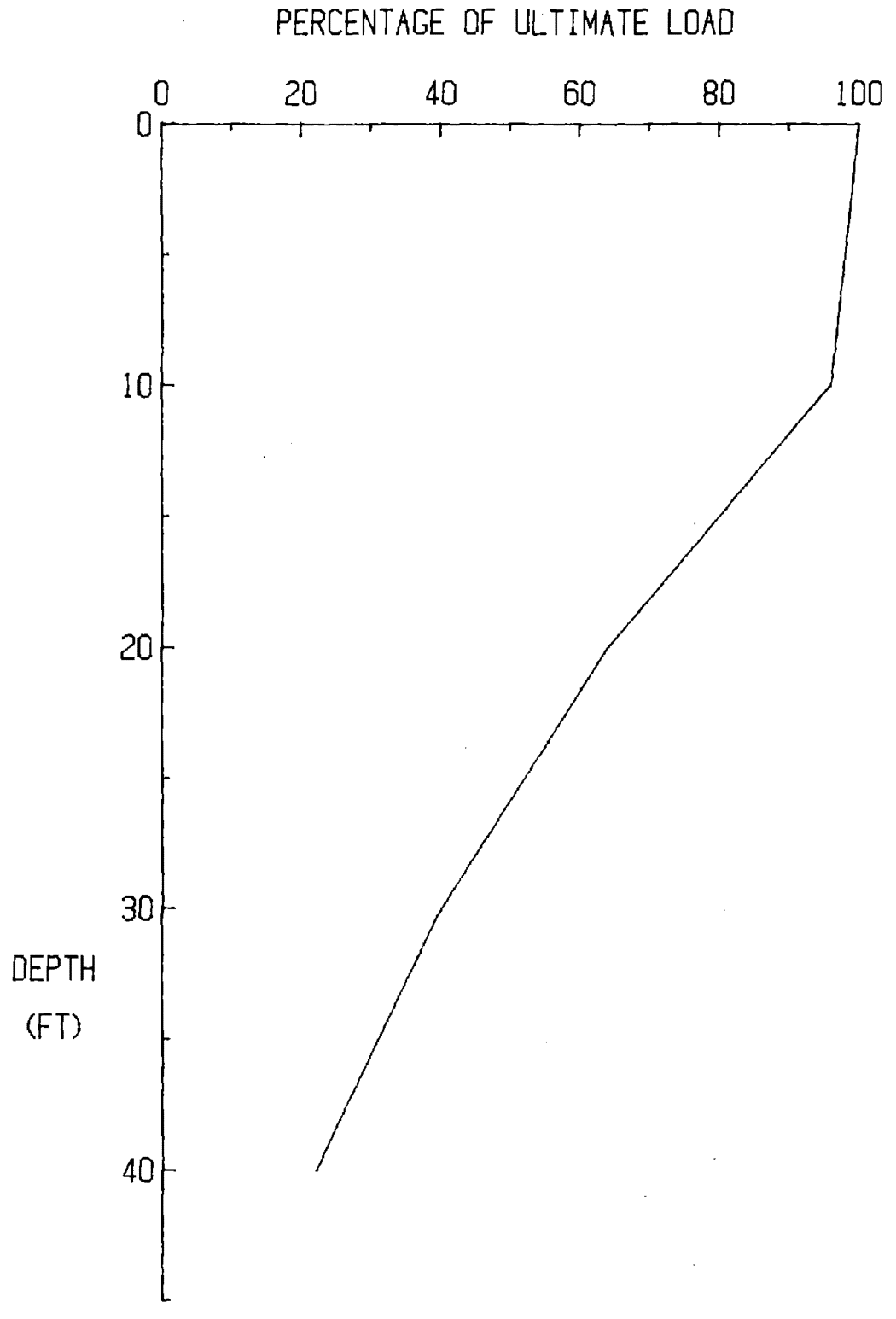

Figure 60. Prototype, load transfer curve (1 kip = 4.45 KN; 1 ft = 0.305 m)

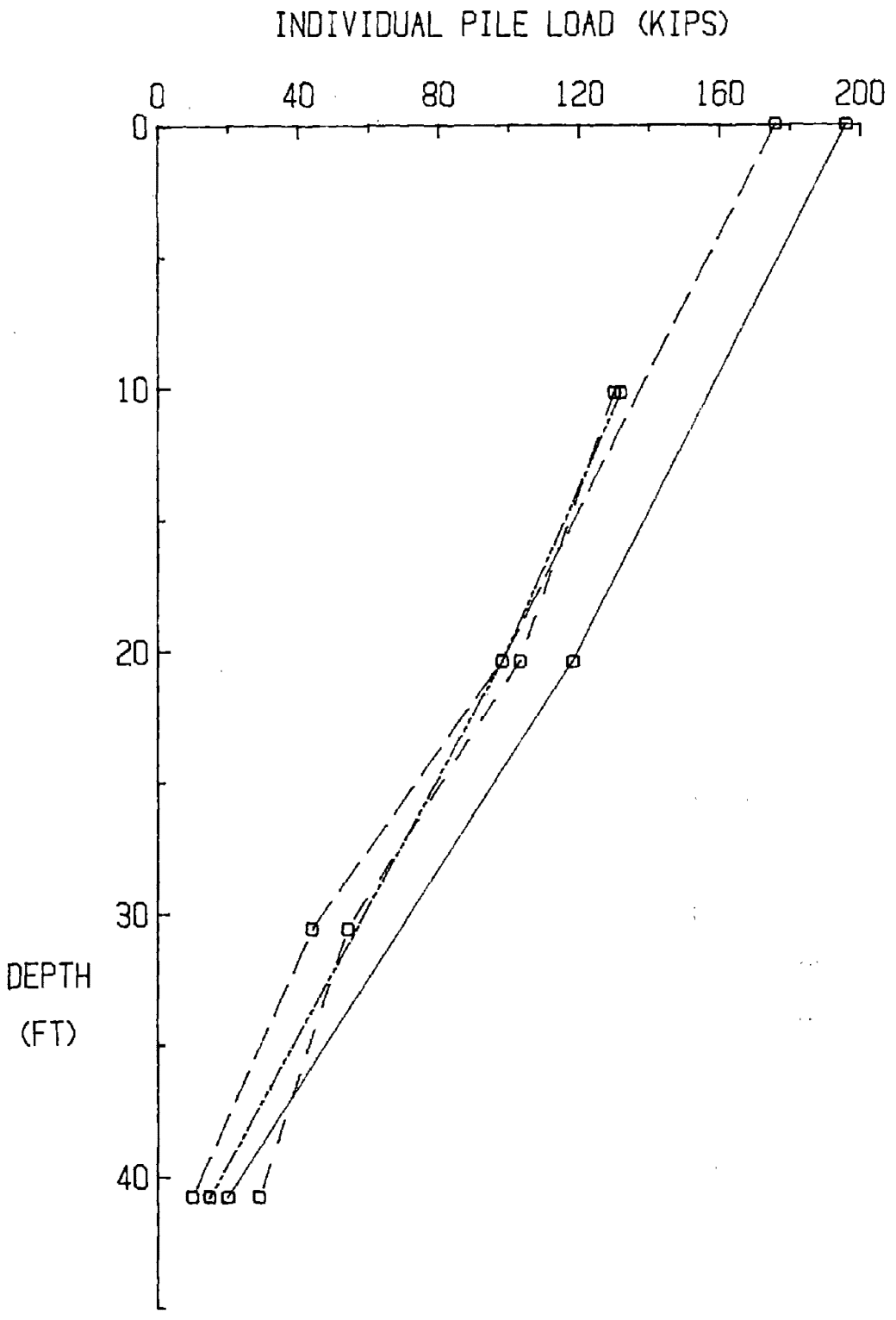

Figure 61. Test 17, group load transfer curves (1 kip = 4.45 KN; 1 ft = 0.305 m)

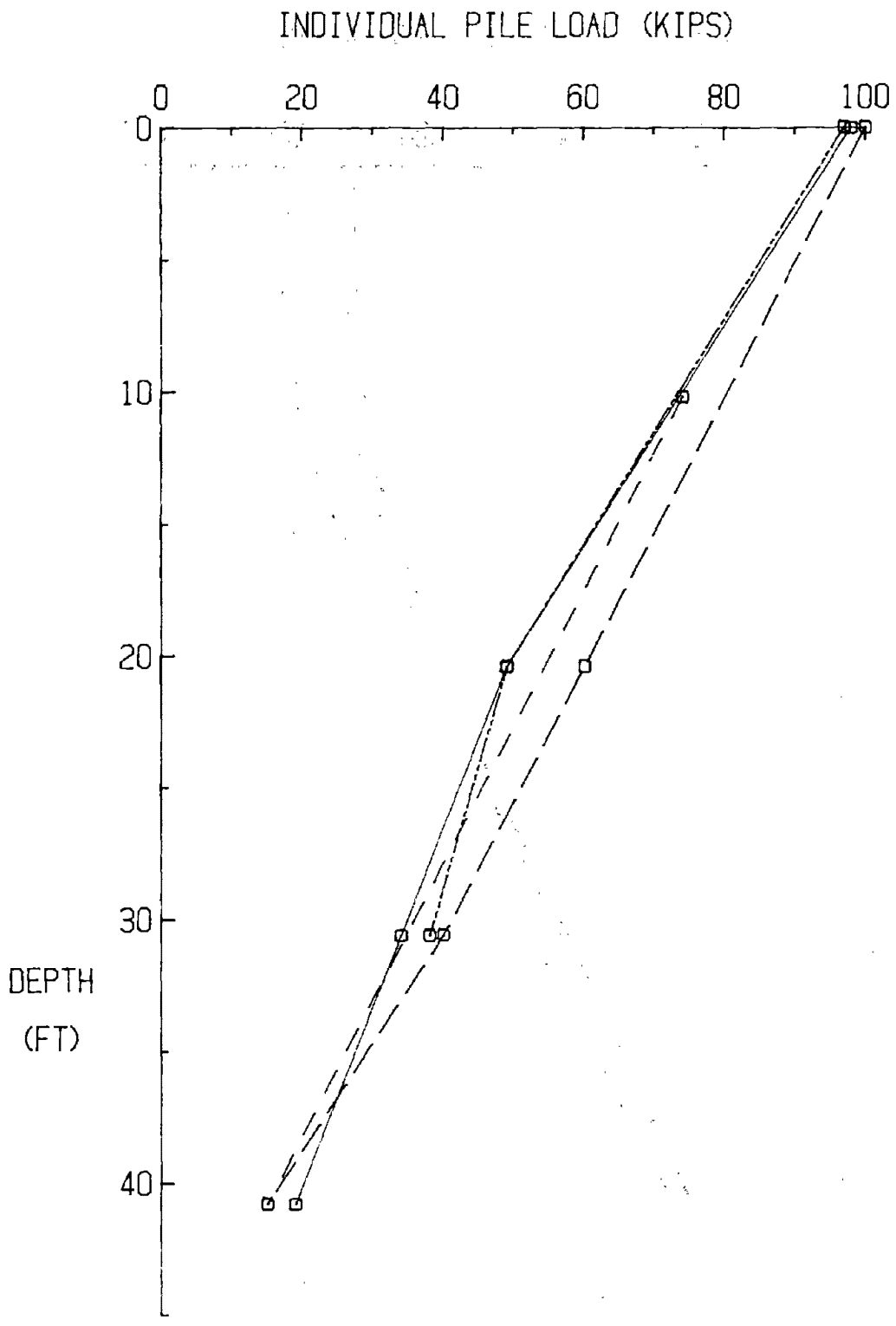

Figure 62. Test 22, group load transfer curves (1 kip = 4.45 KN; 1 ft = 0.305 m)

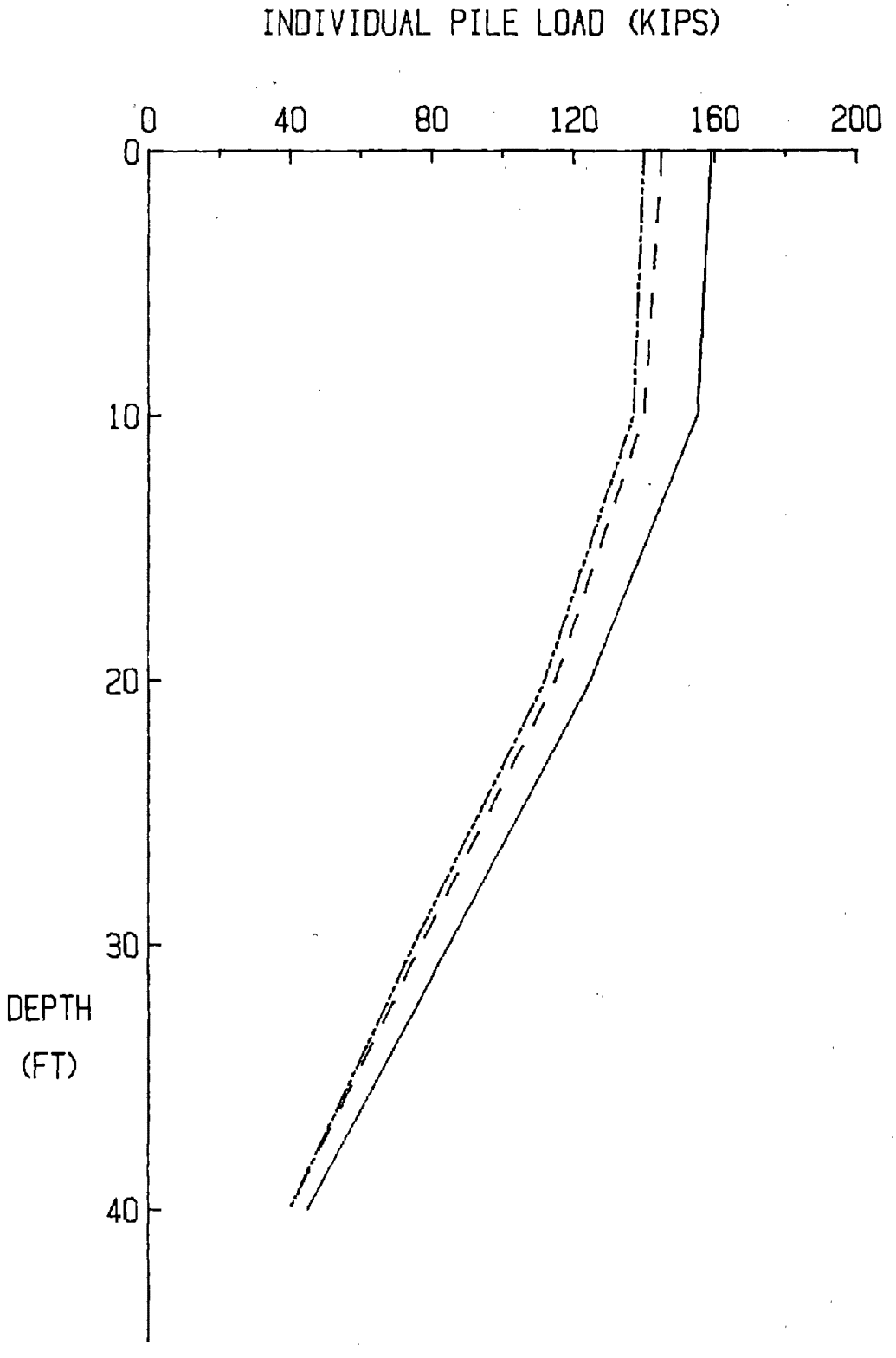

Figure 63. Prototype, group load transfer curves (1 kip = 4.45 KN; 1 ft = 0.305 m)

APPENDIX 3

In this appendix, axial load-displacement curves are presented for both single piles and pile groups. Single pile load-displacement curves are presented for tests 3, 4, 5, 6, 15, 16, 18, 20, 21, 22, and the prototype. Pile Group load displacement curves are presented for tests 18, 21, 22, and the prototype. Malfunctions typically prevented recording of displacements for the remaining tests. Those tests where ultimate loads were recorded without any displacement data are presented in Table 7.

The curves are presented here as piece-wise linear approximations. The curves were originally recorded directly on an x-y recorder. (Figures 64 through 122)

Table 7. Ultimate Loads for Single Pile Tests.

Test Number	Capacity (KIPS)
1	137.3
2	93.1
3	102.9
4	122.5
5	147.0
6	102.9
12	220.5
13	191.1
15	151.0
16	186.2
17	176.4
18	98.1
20	144.5
21	330.0
22	103.0
Prototype	159.0

1 kip = 4.45 KN

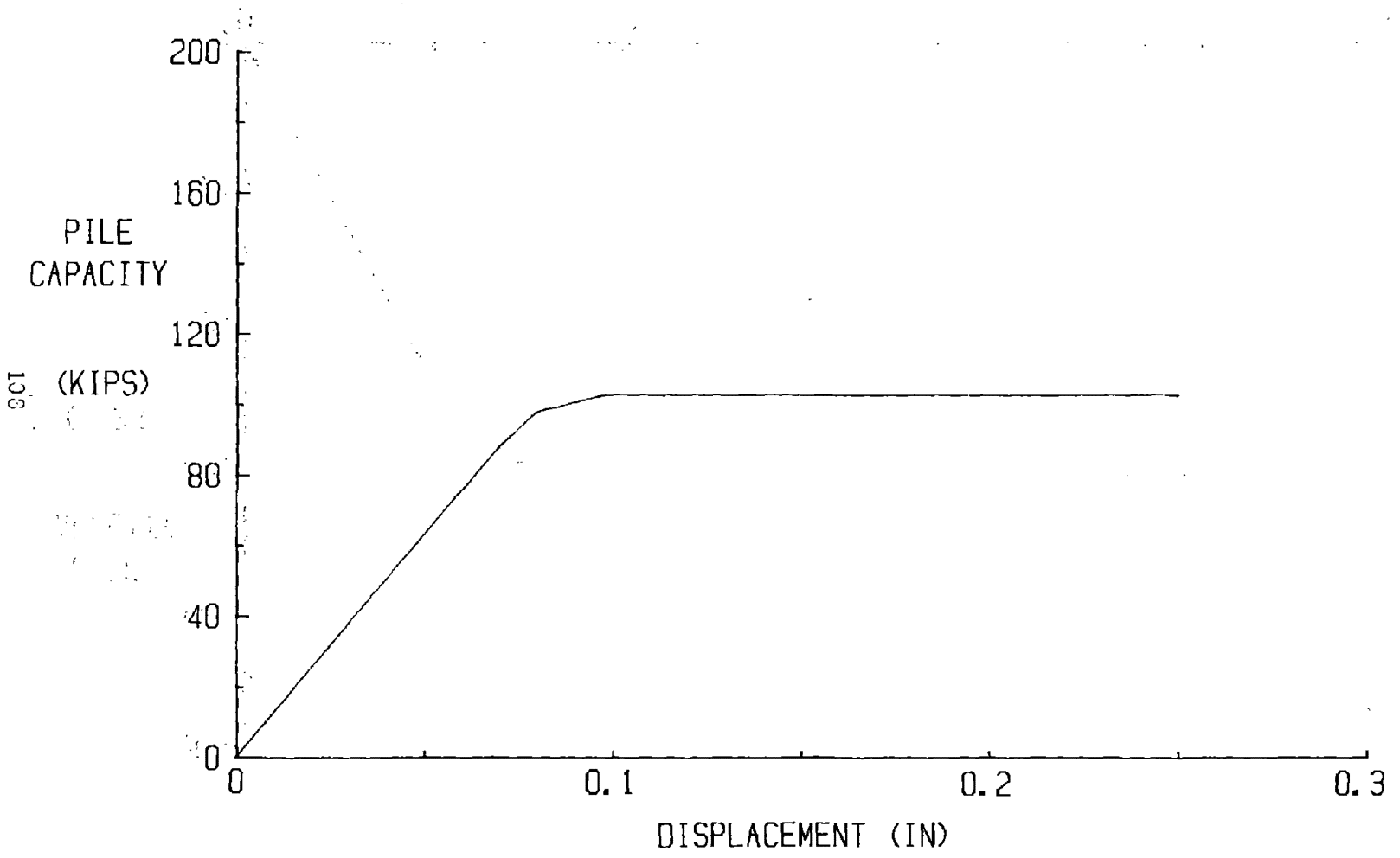

Figure 64. Test 3, load-displacement curve (1 kip = 4.45 KN; 1 in = 2.54 cm)

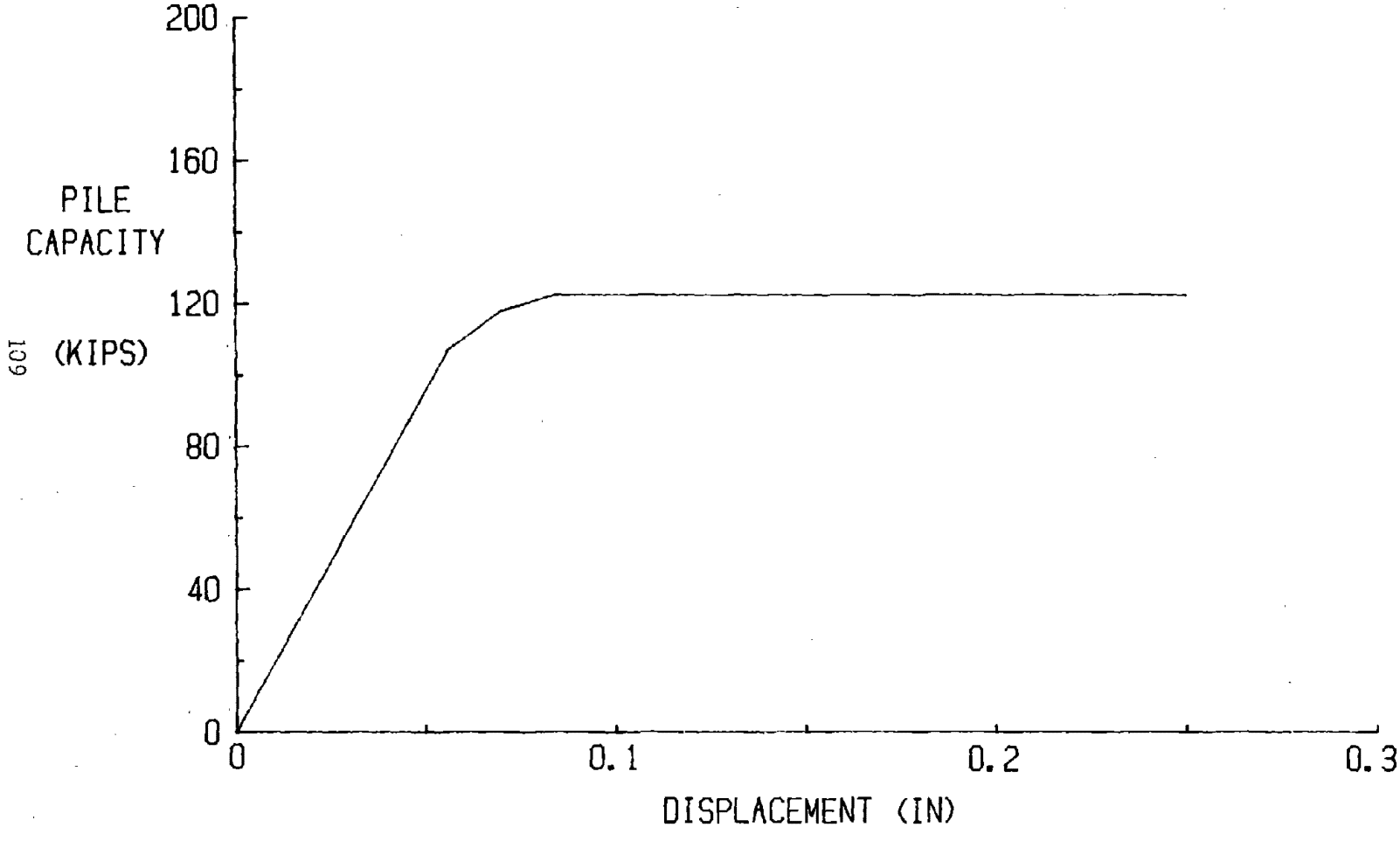

Figure 65. Test 4, load-displacement curve (1 kip = 4.45 KN; 1 in = 2.54 cm)

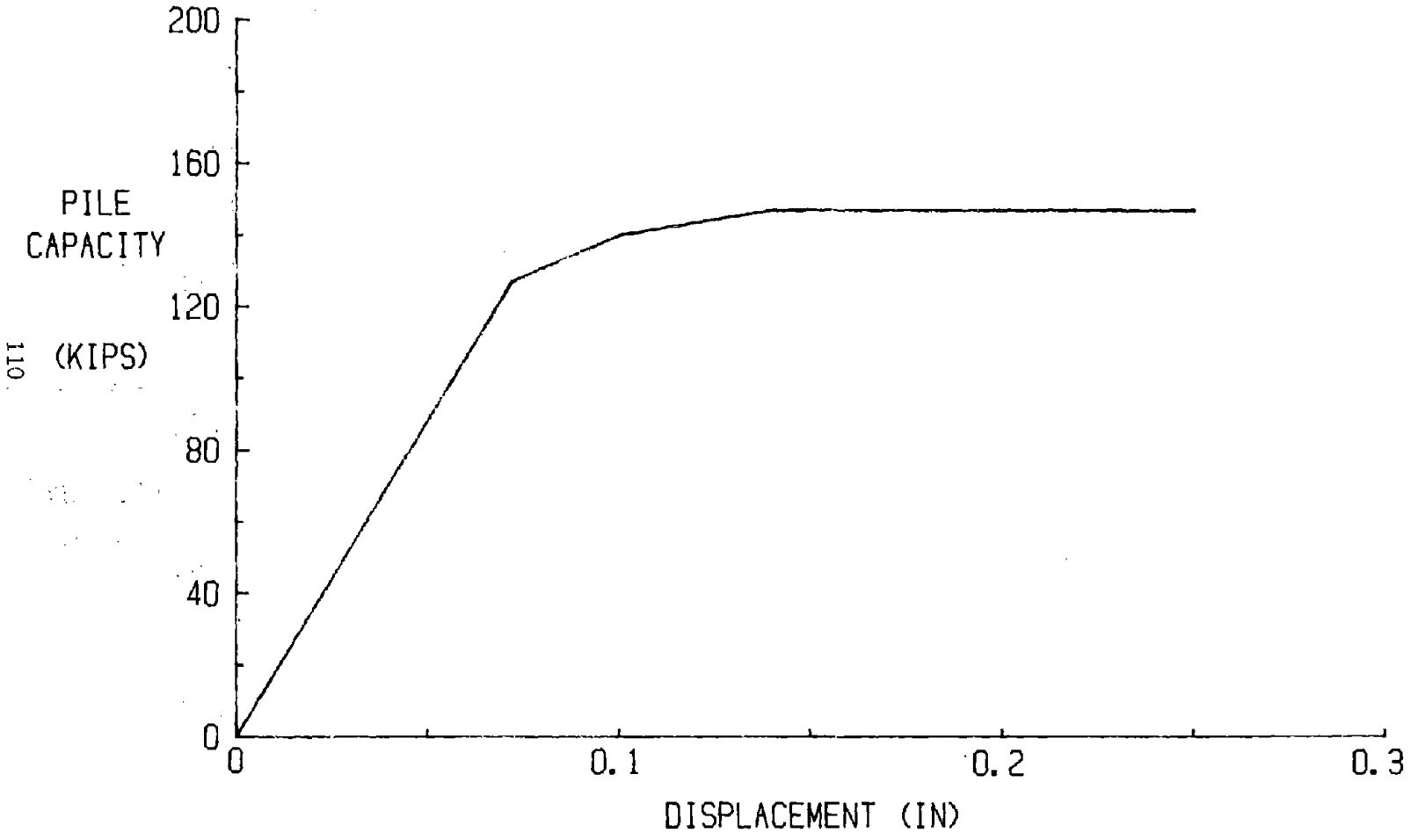

Figure 66. Test 5, load-displacement curve (1 kip = 4.45 KN; 1 in = 2.54 cm)

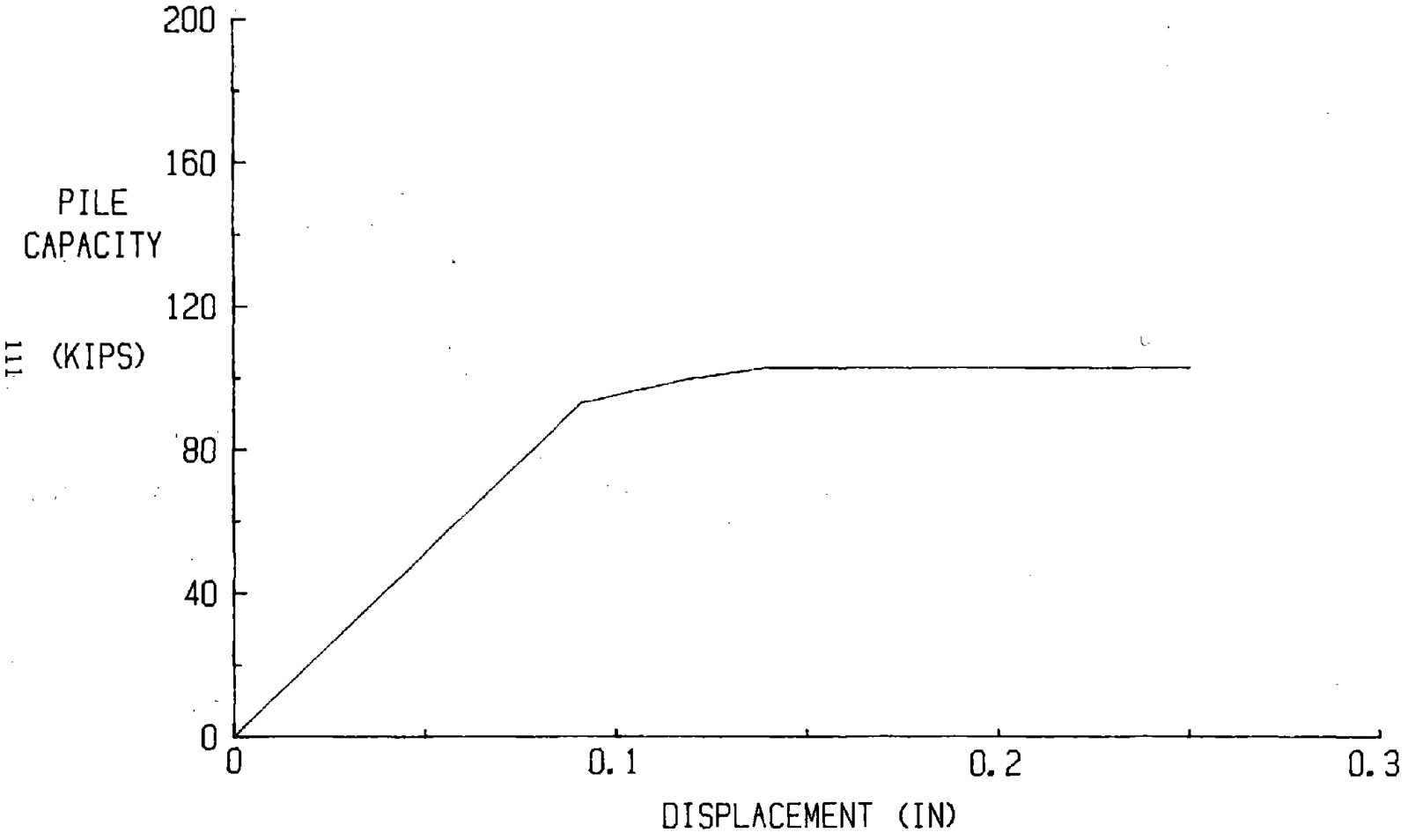

Figure 67. Test 6, load-displacement curve (1 kip = 4.45 KN; 1 in = 2.54 cm)

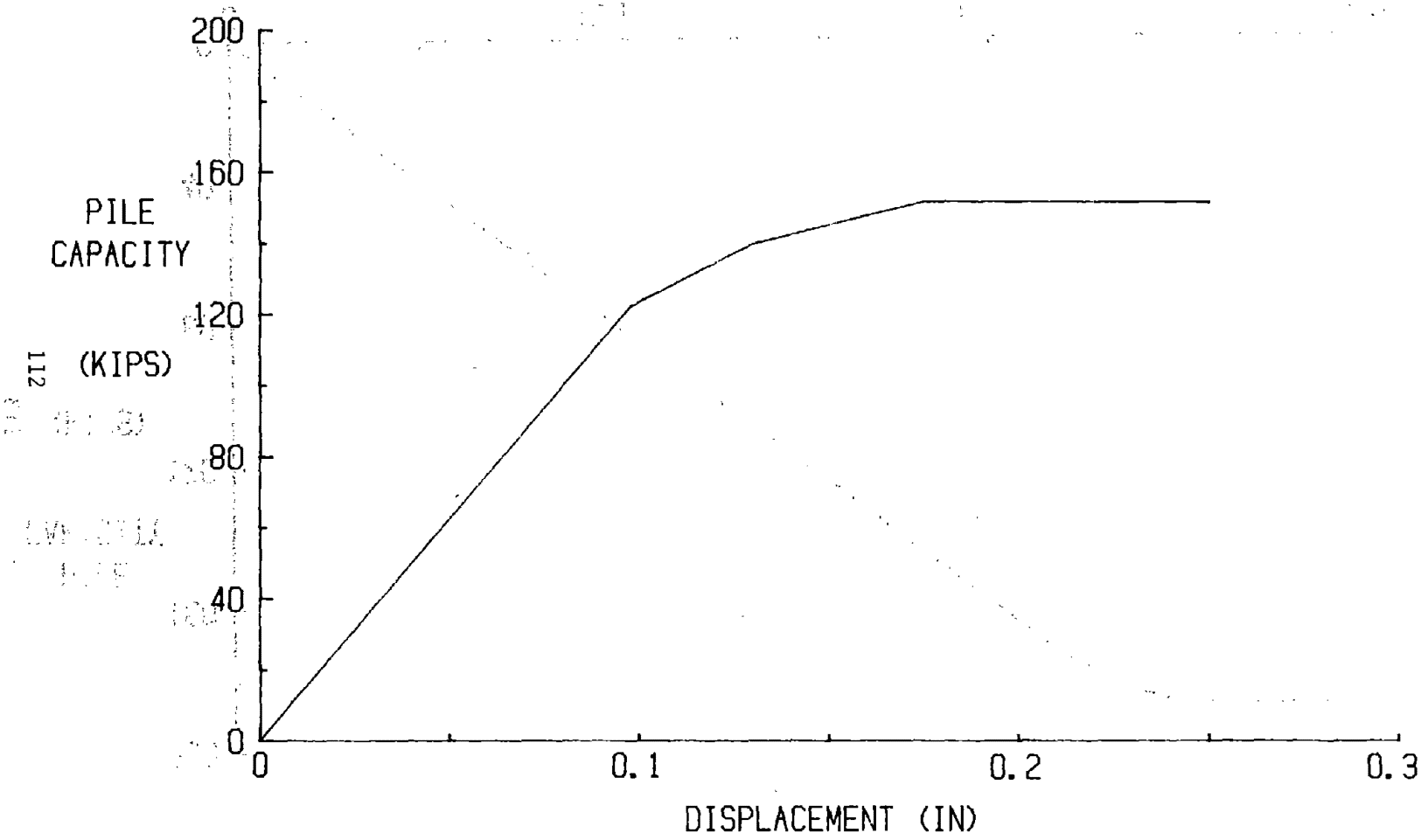

Figure 68. Test 15, load-displacement curve (1 kip = 4.45 KN; 1 in = 2.54 cm)

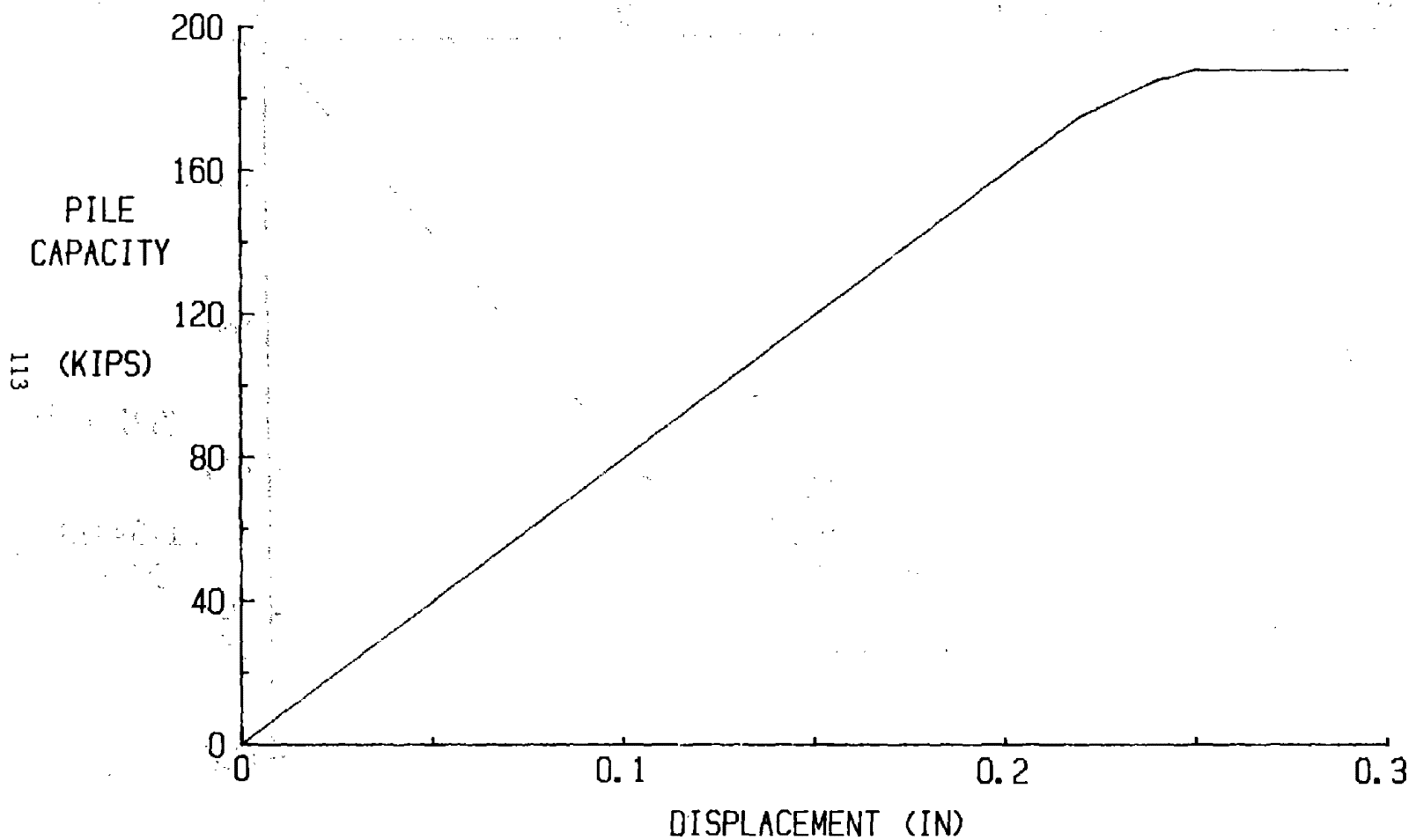

Figure 69. Test 16, load-displacement curve (1 kip = 4.45 KN; 1 in = 2.54 cm)

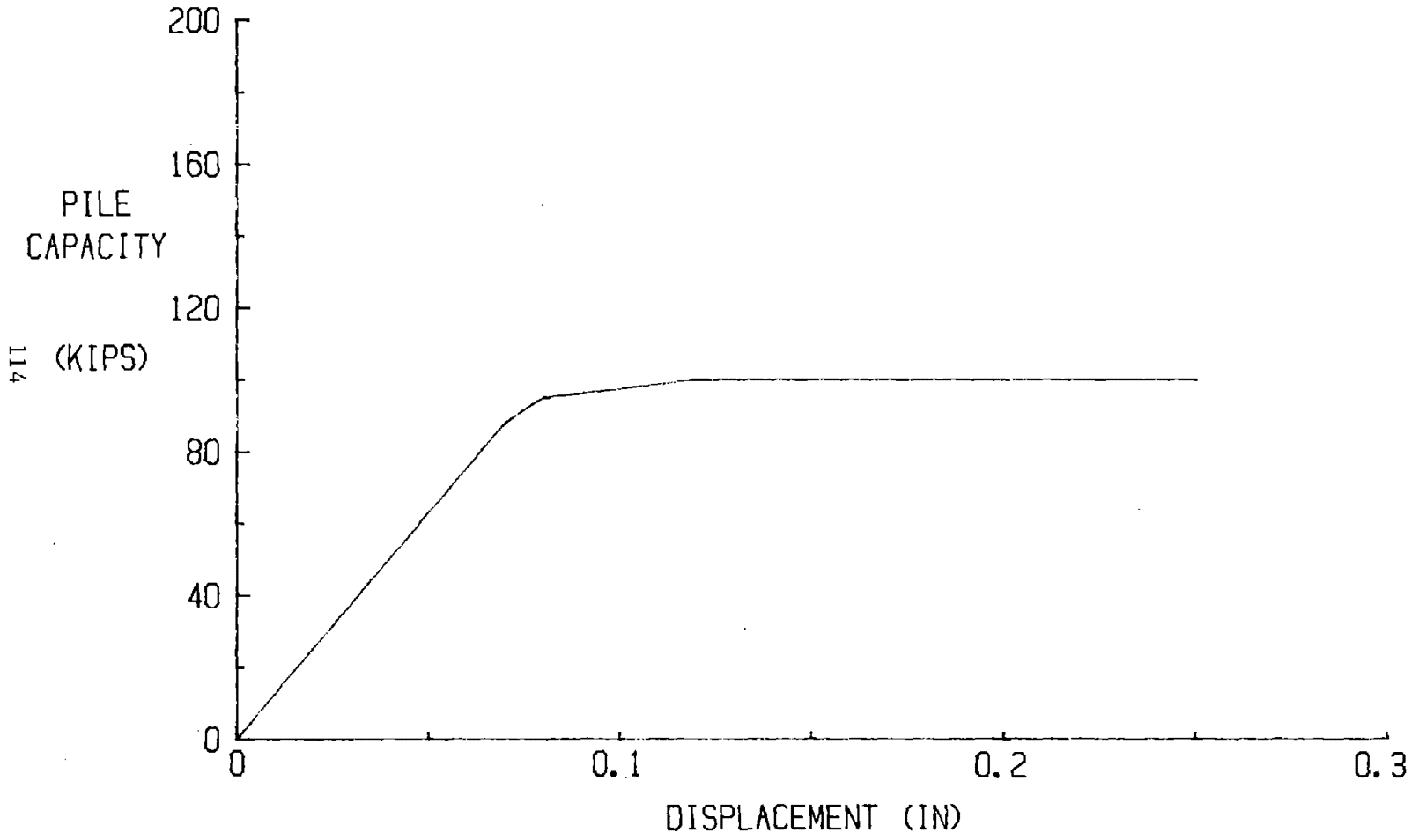

Figure 70. Test 18, load-displacement curve (1 kip = 4.45 KN; 1 in = 2.54 cm)

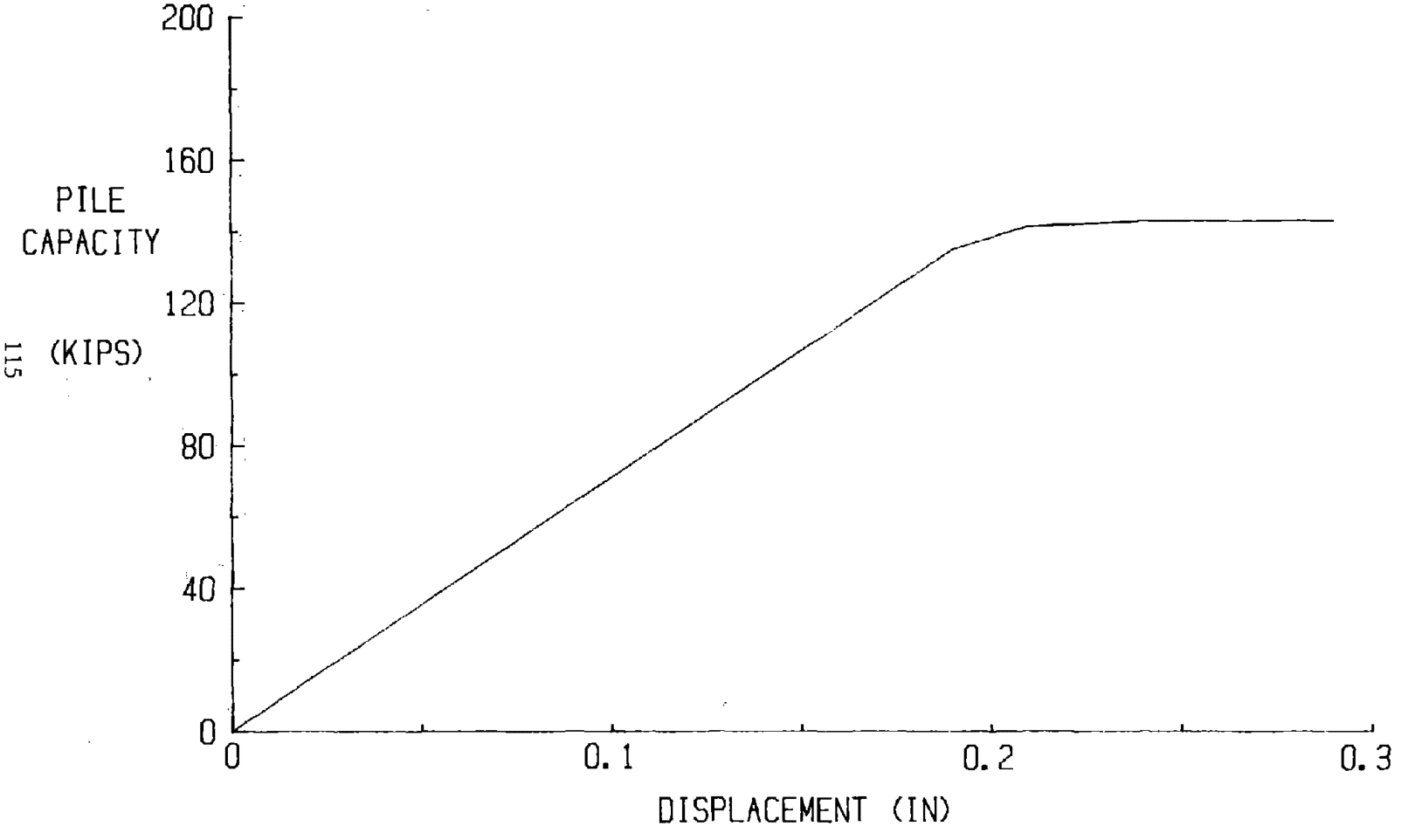

Figure 71. Test 20, load-displacement curve (1 kip = 4.45 KN; 1 in = 2.54 cm)

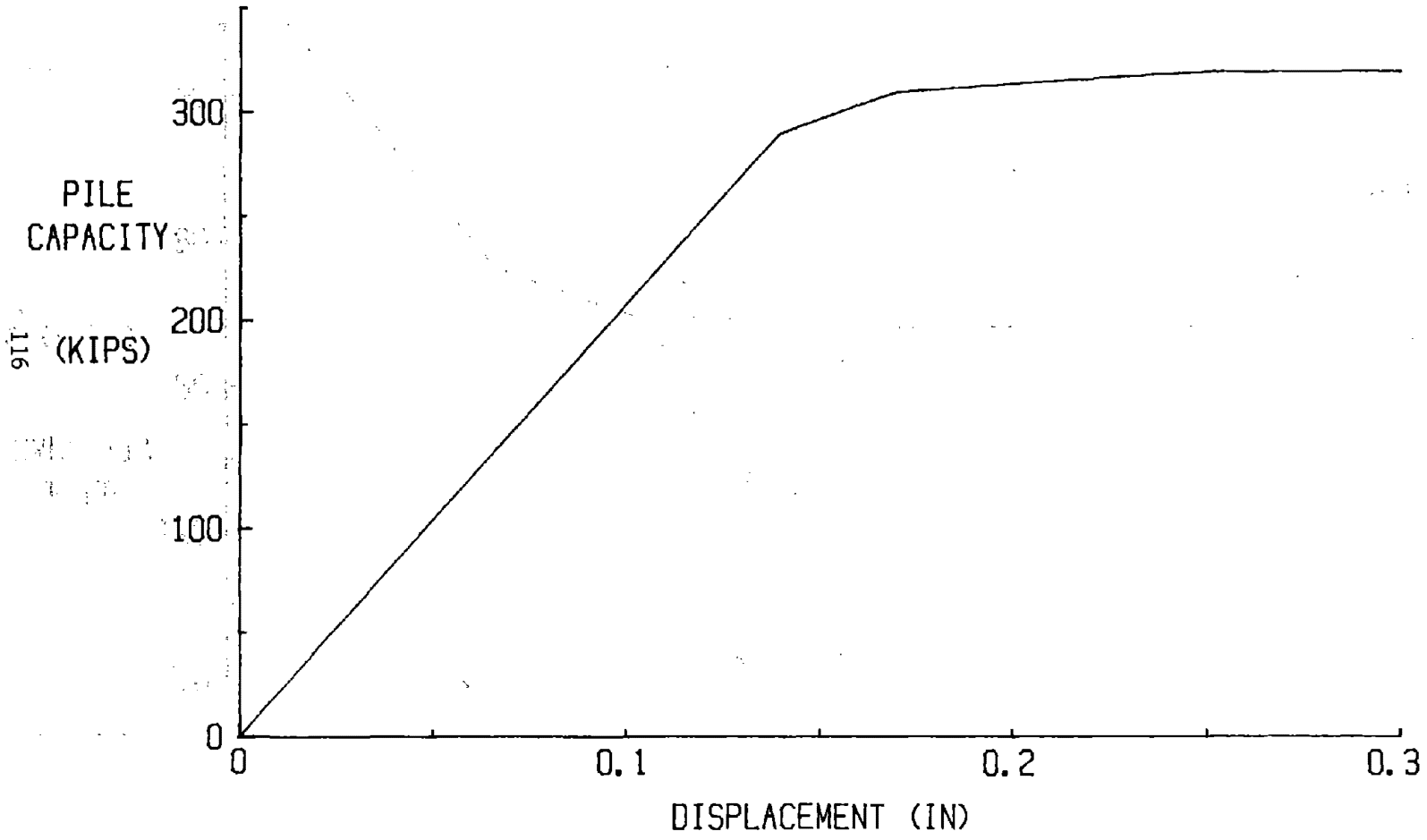

Figure 72. Test 21, load-displacement curve (1 kip = 4.45 KN; 1 in = 2.54 cm)

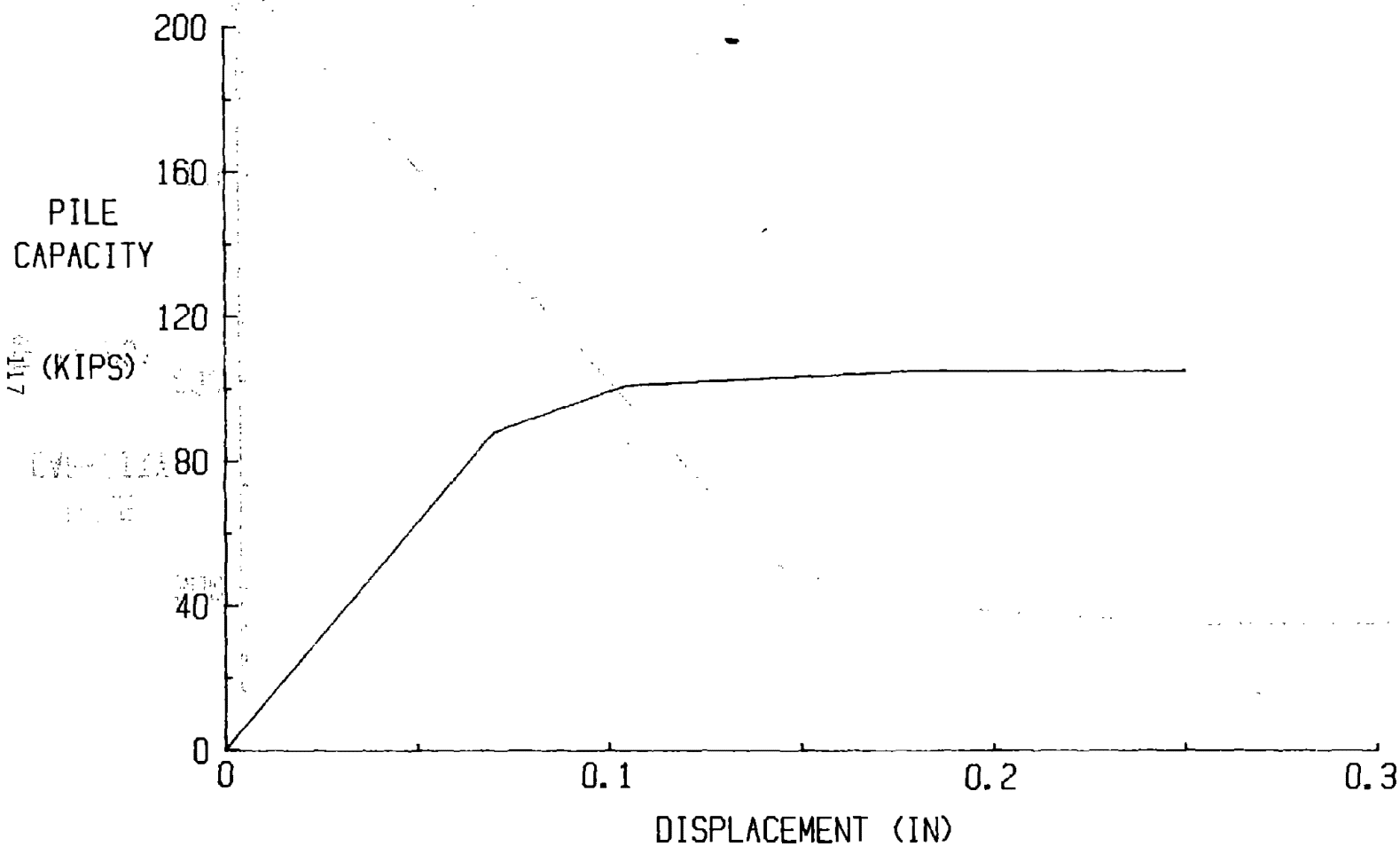

Figure 73. Test 22, load-displacement curve (1 kip = 4.45 KN; 1 in = 2.54 cm)

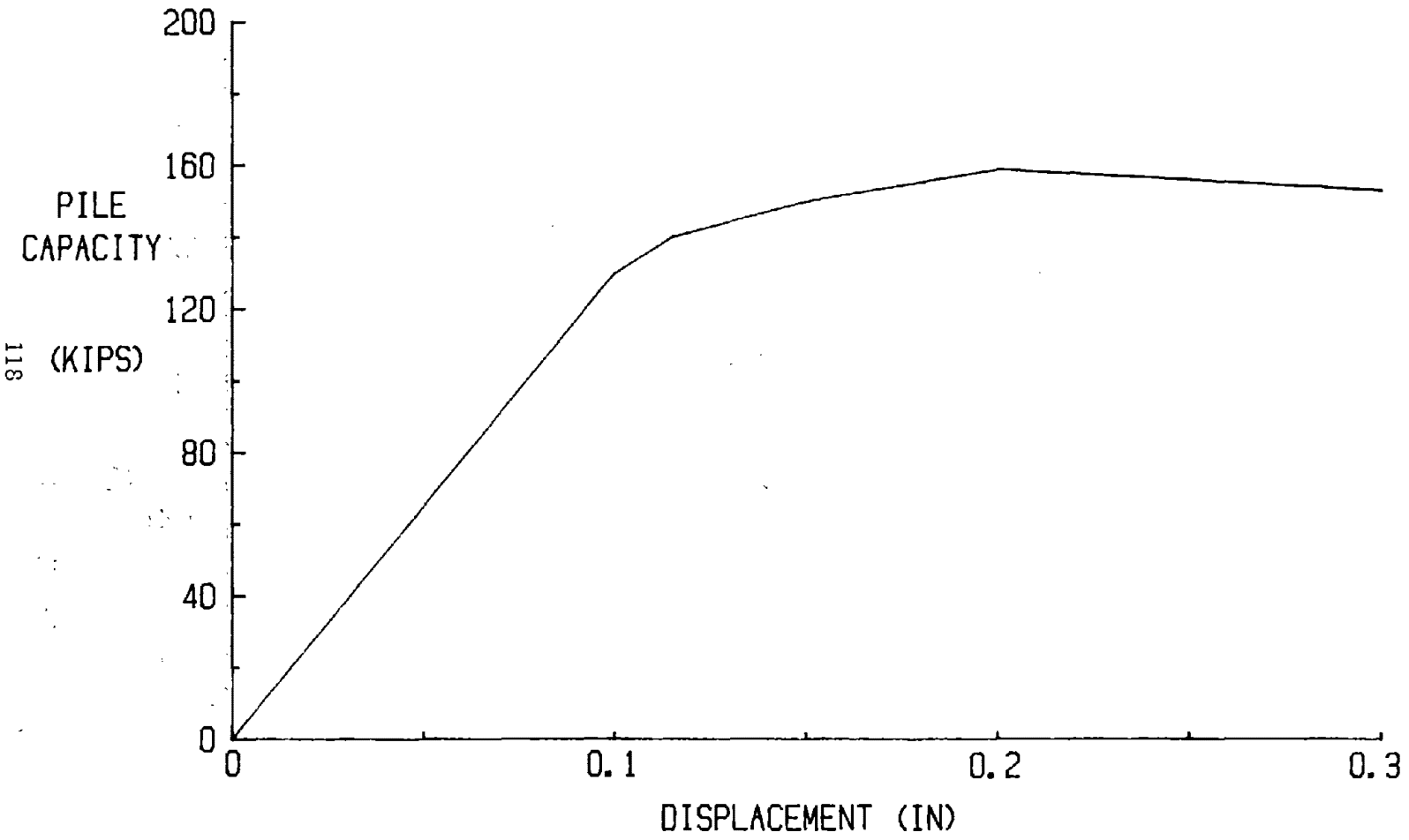

Figure 74. Prototype, load displacement curve (1 kip = 4.45 KN; 1 in = 2.54 cm)

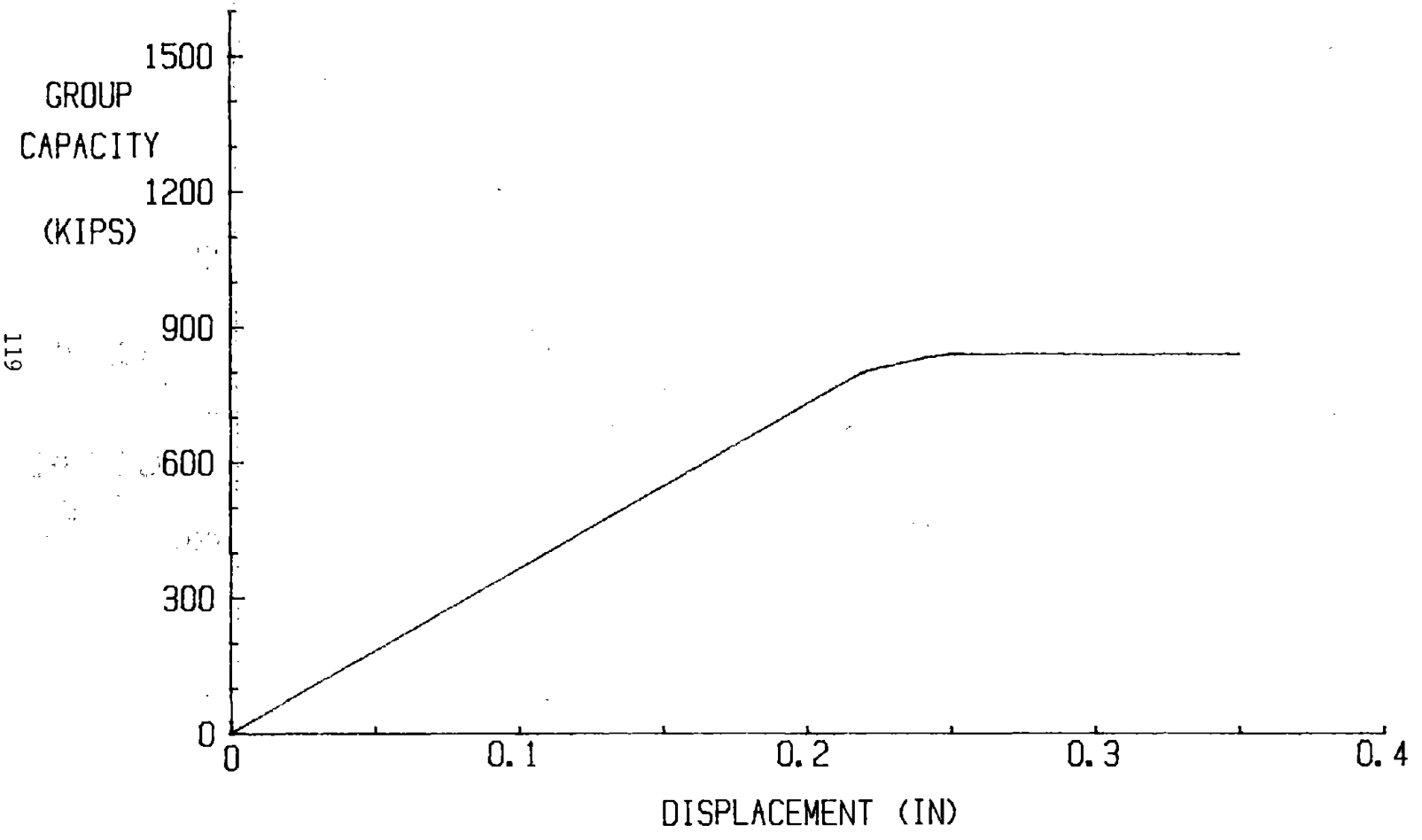

Figure 75. Test 18, group load-displacement curve (1 kip = 4.45 KN; 1 in = 2.54 cm)

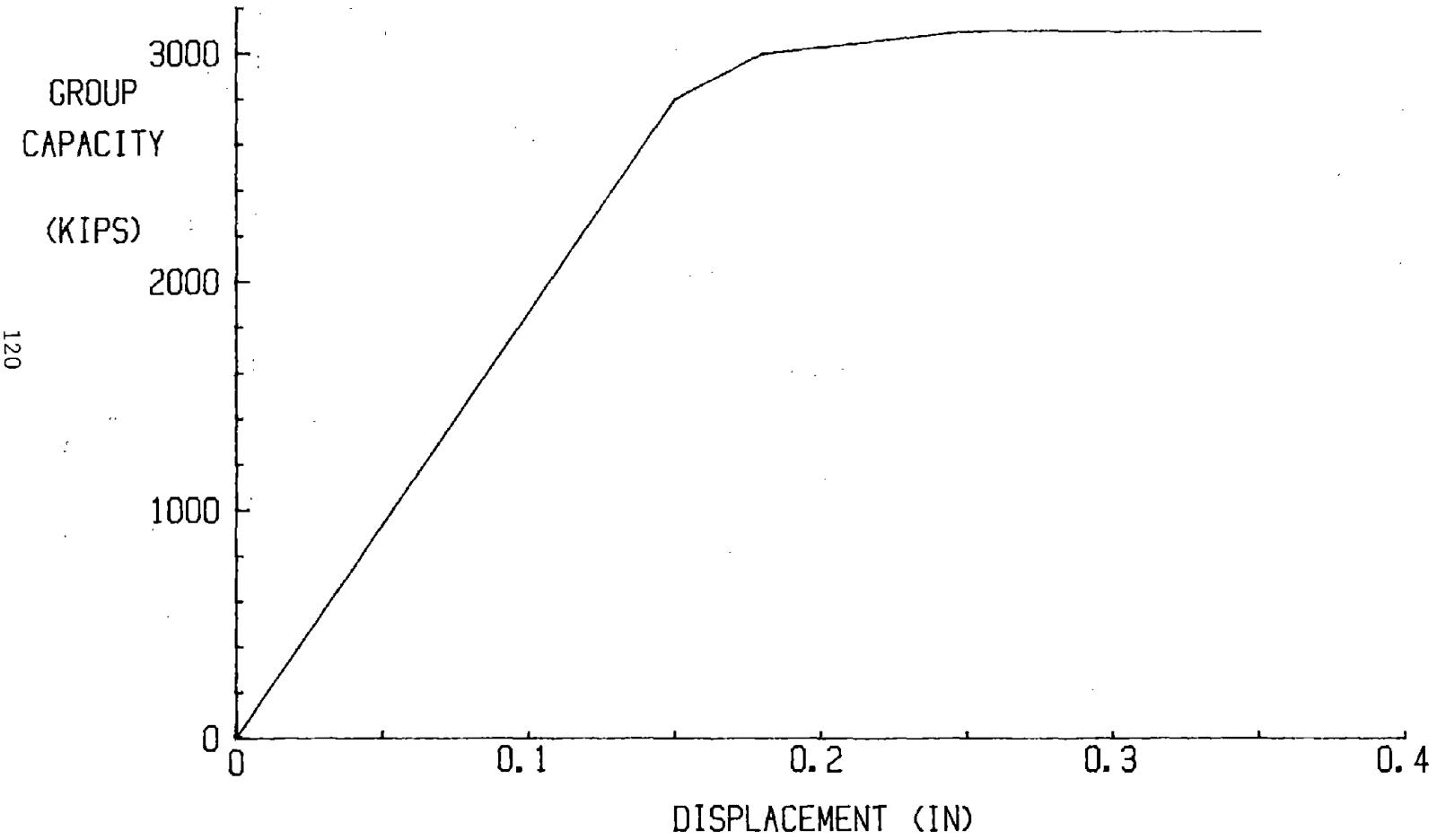

Figure 76. Test 21, group load-displacement curve (1 kip = 4.45 KN; 1 in = 2.54 cm)

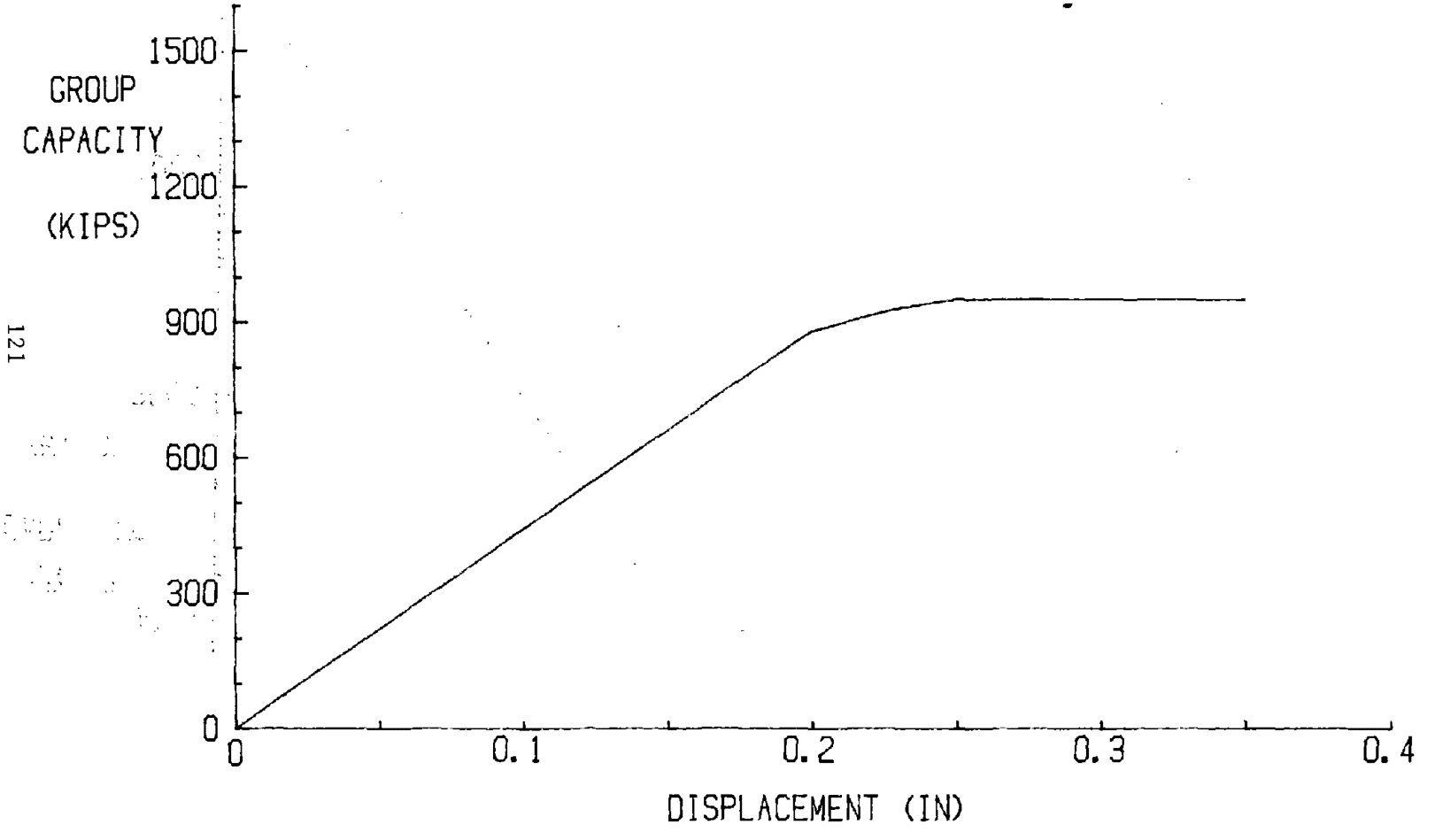

Figure 77. Test 22, group load-displacement curve (1 kip = 4.45 KN; 1 in = 2.54 cm)

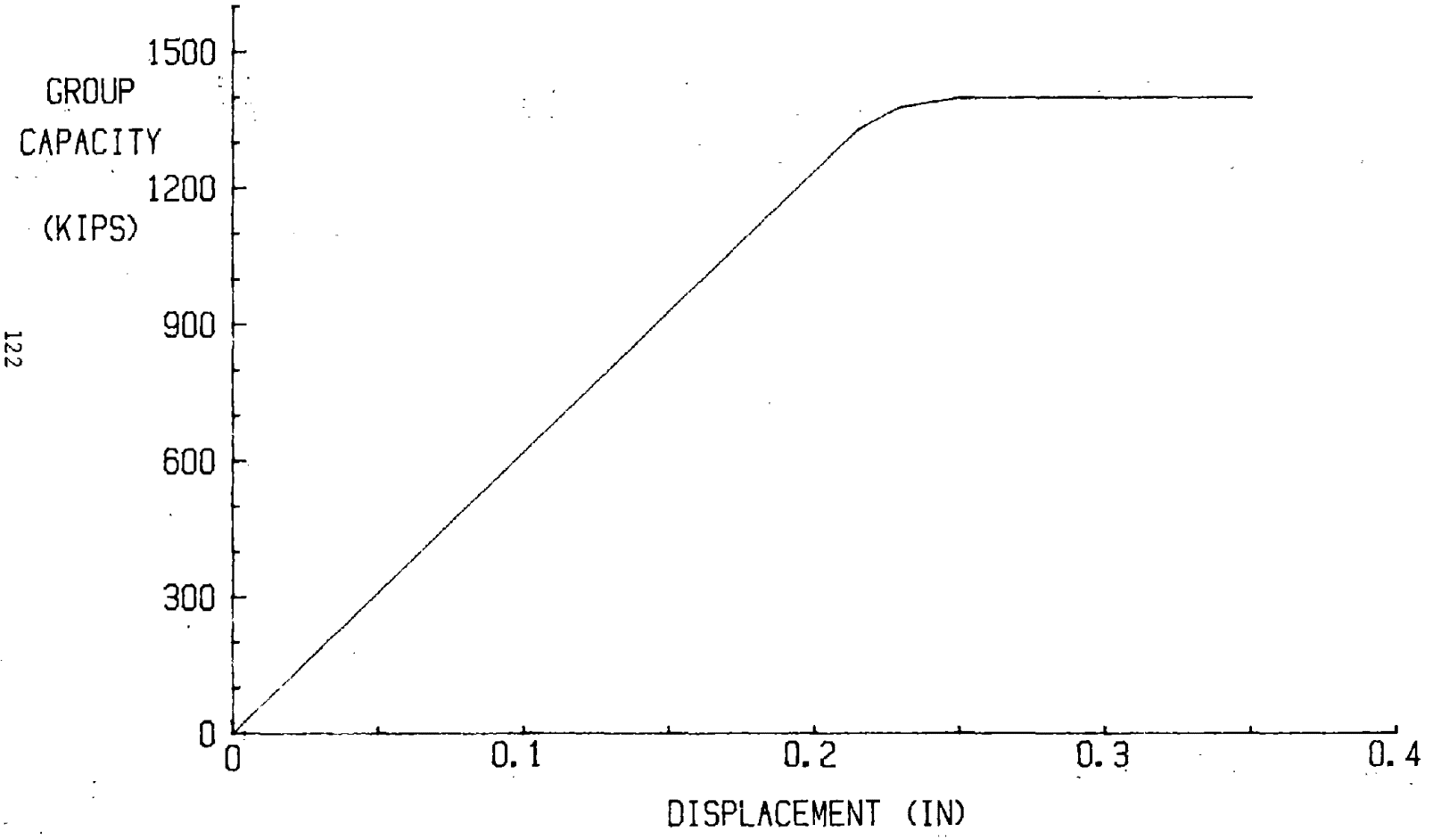

Figure 78. Prototype, group load-displacement curve (1 kip = 4.45 KN; 1 in = 2.54 cm)